ASME STANDARDS TECHNOLOGY, LLC

STP-PT-079

LOCAL HEATING OF PIPING: THERMAL ANALYSIS

STP-PT-079

LOCAL HEATING OF PIPING: THERMAL ANALYSIS

Prepared by:

Cole Davis, M.Sc.
Quest Integrity USA, LLC

ASME STANDARDS TECHNOLOGY, LLC

Date of Issuance: June 30, 2016

This report was prepared as an account of work sponsored by ASME Pressure Technology Codes & Standards and the ASME Standards Technology, LLC (ASME ST-LLC).

ASME Standards Technology, LLC
Two Park Avenue, New York, NY 10016-5990

ISBN No. 978-0-7918-7125-6

TABLE OF CONTENTS

LIST OF FIGURES

FOREWORD

The objective of this project is to perform thermal analysis of pipeline heating configurations, with the intention of creating guidelines for the sizing of heating bands.

The author acknowledges, with deep appreciation, the activities of ASME staff and volunteers who have provided valuable technical input, advice and assistance with review of, commenting on, and editing of, this document.

Established in 1880, the American Society of Mechanical Engineers (ASME) is a professional not-for-profit organization with more than 135,000 members and volunteers promoting the art, science and practice of mechanical and multidisciplinary engineering and allied sciences. ASME develops codes and standards that enhance public safety, and provides lifelong learning and technical exchange opportunities benefiting the engineering and technology community. Visit www.asme.org for more information.

The ASME Standards Technology, LLC (ASME ST-LLC) is a not-for-profit Limited Liability Company, with ASME as the sole member, formed in 2004 to carry out work related to new and developing technology. The ASME ST-LLC mission includes meeting the needs of industry and government by providing new standards-related products and services, which advance the application of emerging and newly commercialized science and technology, and providing the research and technology development needed to establish and maintain the technical relevance of codes and standards. Visit www.stllc.asme.org for more information.

EXECUTIVE SUMMARY

The initial phase of the project served to calibrate and verify the modeling assumptions used for the thermal analysis via comparison with experimental measurements taken for two post weld heat-treated pipes using multiple heating band configurations. The second phase analyzed five pipe diameters. The intent of the second phase was to determine appropriate sizing requirements for heating bands in order to minimize temperature variation around the weld location, for pipe diameters ranging from 6 to 30 inches.

The calibration cases were run to steady state while the thermal contact resistance was adjusted to match the centerline inside diameter (ID) temperature measurements from the experimental cases. The outside diameter (OD) temperature probes were set to adjust the power input such that their value matched the experimental measurements at the same locations.

The prediction model cases were run to steady state. Five different pipe diameters were investigated with three different pipe thicknesses per diameter. The heat band (HB) and gradient control band (GCB) were iteratively increased in length until the maximum temperature difference in the soak band (SB) was less than 15°F. This occurred with four to six iterations per geometry. The trend of these iterations followed roughly a power relation between temperature differences desired to HB lengths required.

The HB lengths required for a temperature difference in the SB of 15°F when plotted against OD and t/OD are nearly planar. These HB lengths were found to be much larger than is recommended in AWS D10.10 (American Welding Society, 1999), and this difference increases with pipe diameter due to increasing natural convection effects. The results of these analyses can be used to develop new HB sizing guidelines for AWS D10.10.

ABBREVIATIONS AND ACRONYMS

ASME	American Society of Mechanical Engineers
AWS	American Welding Society
BPVC	Boiler and Pressure Vessel Code
CHT	Conjugate Heat Transfer
CFD	Computational Fluid Dynamics
FEA	Finite Element Analysis
GCB	Gradient Control Band
HB	Heat Band
ID	Inside Diameter
OD	Outside Diameter
PWHT	Post Weld Heat Treatment
SB	Soak Band

1 INTRODUCTION

The objective of this project was to perform thermal analysis of pipeline heating configurations, with the intention of creating guidelines for the sizing of heating bands. The analysis consisted of two phases. The initial phase served to calibrate and verify the modeling assumptions used for the thermal analysis via comparison with experimental measurements taken for two post weld heat treated pipes using multiple heating band configurations. The second phase analyzed five pipe diameters. The intent of the second phase was to determine appropriate sizing requirements for heating bands in order to minimize temperature variation around the weld location, for pipe diameters ranging from 6 to 30 inches. The results of these analyses can provide refinement of the requirements found in AWS D10.10 [1] regarding the width of the soak band, heated band and gradient control band as a function of pipe diameter, thickness and heating rate/holding time to help ensure that the through-wall temperature difference does not exceed 15°F within the soak band region. Once these requirements are determined, they can be used to update the technical rules in the appropriate ASME BPVC construction and B31 piping codes.

2 ANALYSIS METHODOLOGY

The approach was to perform conjugate heat transfer (CHT) analysis using the Star CCM+ computational fluid dynamics (CFD) software [2]. This is a fully functional and validated commercial CFD solver. It has the capability of performing the CHT analysis and solving for temperature distributions in the piping and in the surrounding air. The advantage of using a CFD solver, as opposed to using a finite element analysis (FEA) code, is that the natural convection on the solid surfaces can be directly accounted for, rather than applying approximate boundary conditions.

The project was broken up into two phases, a calibration phase and a prediction phase. The calibration phase consisted of two pipe geometries with different heating band configurations. Experimental temperature data was collected and provided to Quest Integrity by ASME. This data was then used to calibrate the CFD models by tuning the contact resistance between the heating band and pipe.

The prediction phase expanded on the calibrated CFD models to examine post weld heat treatment (PWHT) in pipes of differing diameters and thicknesses. For the prediction phase, five different pipe diameters with three different schedule thicknesses were modeled, changing the heat band length iteratively until a maximum 15°F difference existed in the soak band. These results were then used to suggest new PWHT heat band sizing guidelines.

2.1 Geometry

The configuration modeled consists of the piping with a band of ceramic electrical resistance heating elements. This in turn is covered by two layers of insulation over the heating band and one layer of insulation extending a distance beyond the heating band. The entire assembly is contained in a domain representing the surrounding air.

Figure 2-1 and Figure 2-2 show the configuration of the half-symmetric model, with the ambient domain shown in blue, the piping shown in yellow, the heating layer in green, and the insulation layers in gray and purple. Heat flows from the heating band into the piping and to the insulation via conduction. Heat is lost to the surroundings via natural convection and radiation. Figure 2-2 shows the configuration of the soak band (SB), the heat band (HB), and the gradient control band (GCB). For all cases, the domain was assumed to be ten times the pipe length in the axial direction, and five times the pipe length in the transverse directions.

Figure 2-1: PWHT model heating configuration. Top right, full domain. Main, half-symmetric heating configuration

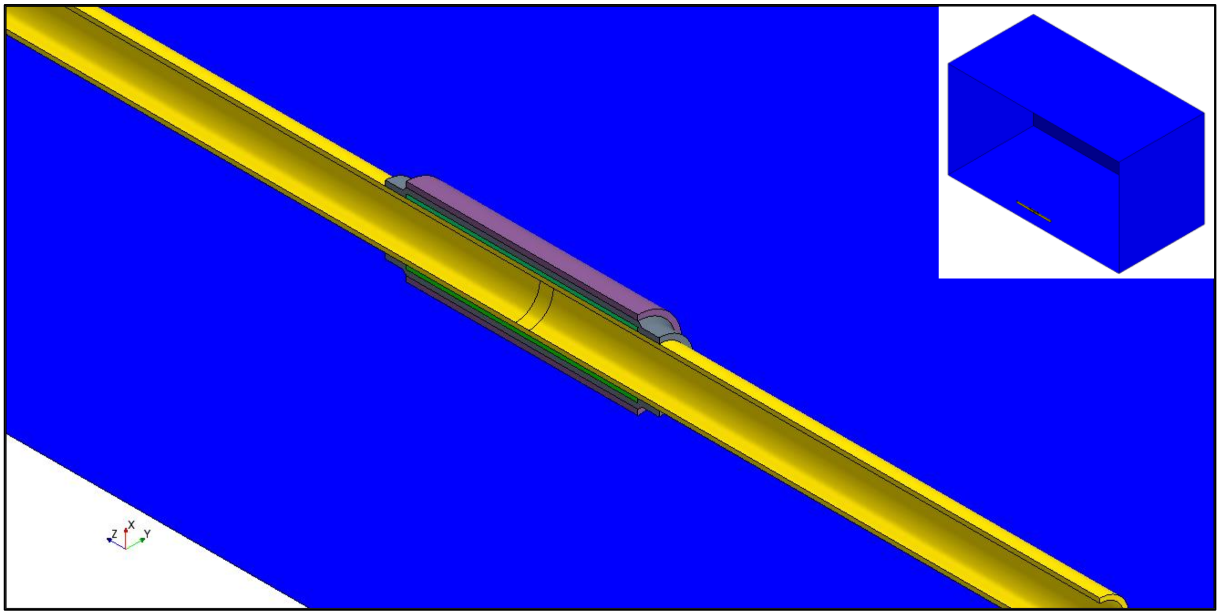

Figure 2-2: PWHT configuration.

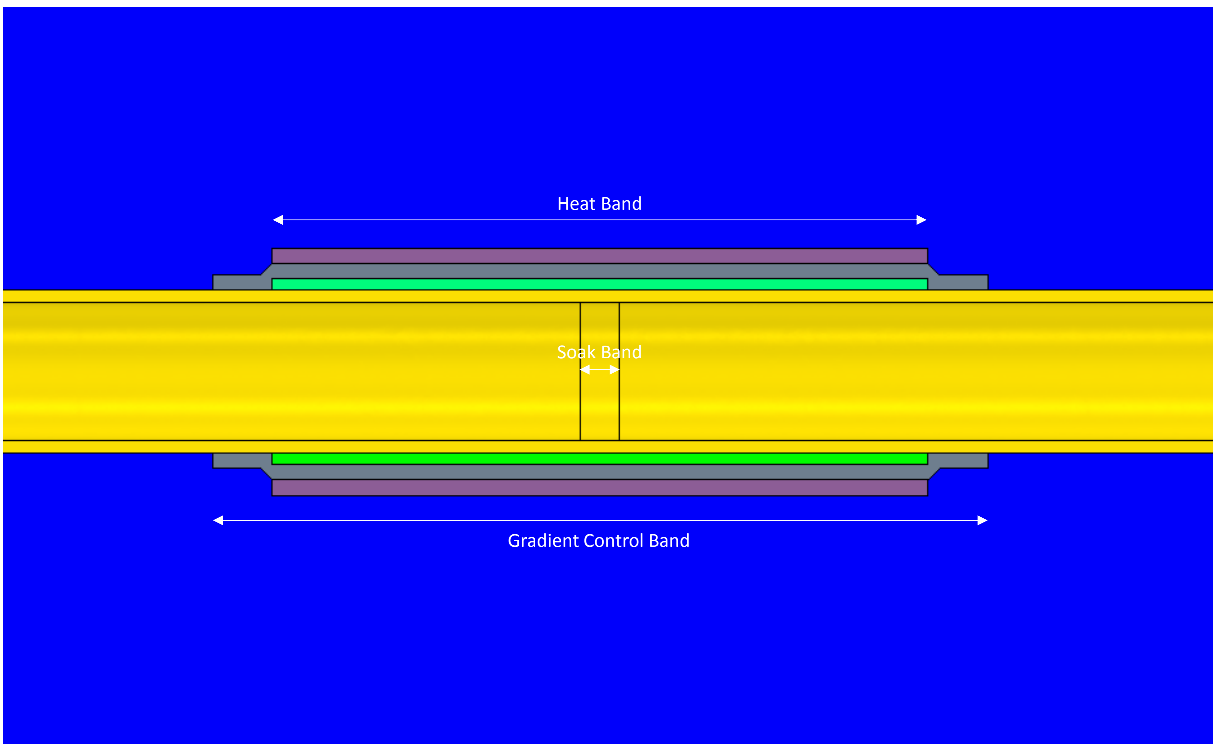

2.2 Physics

CFD is the analysis of fluid flow, heat transfer, and its accompanying phenomena [3]. CFD is structured around the Navier-Stokes equations, which describe all fluid motion and heat transfer. Exact solutions to the Navier-Stokes equations do not exist; it is therefore necessary to numerically approximate their solutions with computational modeling. As a part of the numeric solution, some assumptions are necessary; these assumptions frequently include the Reynolds decomposition that breaks the velocity field into components of its mean and fluctuation. Employing this assumption leads to an inequality between equations and variables, which requires the use of a turbulence model [4]. The k-ε turbulence model is formulated from the far field flow and therefore captures flow best in that region, however it often requires a wall function to capture turbulence near any boundary. The k-ω turbulence model is formulated in the near-wall region and therefore captures flow best in that region, however its accuracy is less in the far field flow. The k-ω SST turbulence model uses the k-ω turbulence model in the near-wall region and the k-ε turbulence model in far field flow. It combines the models using a blending function in the transition region to produce an accurate turbulence model for both far field flow and boundary layer flow [5]. Although these models are primarily concerned with pipe temperatures, natural convection plays a significant role in overall heat transfer, therefore the k-ω SST turbulence model was implemented for the steady state CHT CFD analyses.

Several other assumptions/physics were included in these models. Natural convection in the domain was modeled as an ideal gas, with temperature-dependent dynamic viscosity accounted for using Sutherland's Law. Temperature-dependent thermal conductivity was included in the material properties of air [6], pipe metal [7], and insulation [8]. Gravitational effects were included to capture buoyancy effects for natural convection. Conduction, convection, and surface-to-surface radiation effects were modeled to capture all applicable heat transfer mechanisms.

An important factor in the analysis is the appropriate handling of the thermal contact between the layers. Heat flow between two contacting solid bodies depends on thermal contact conductance, h_c. The inverse of this quantity $1/h_c$ is referred to as thermal contact resistance.

Heat flow, q, in a solid body is governed by Fourier's Law:

$$q = -kA\frac{dT}{dX}$$

where k is the thermal conductivity, A is the cross sectional area, and the thermal gradient is given by $\frac{dT}{dX}$. However, the heat flow through two contacting bodies is given by

$$q = \frac{T_A - T_B}{\left({}^{a}/_{k_a A}\right) + \left({}^{1}/_{h_c A}\right) + \left({}^{b}/_{k_b A}\right)}$$

where the two bodies in contact are defined in Figure 2-3.

Figure 2-3: Two body thermal contact

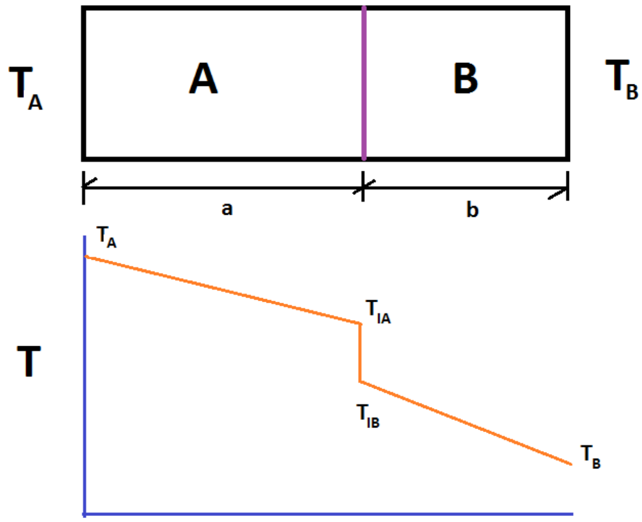

Note that the contact between bodies create a discontinuity in the temperature distribution. The heat flow across a contact boundary can be written as

$$q = h_c A \Delta T$$

The effect of contact resistance must be included to obtain the proper temperature distribution. In the case of the piping heating system, the contact resistance must be included between the heating layer and piping to obtain the physical temperature distribution.

Contact resistance (or conductance) is a function of the contact area between two bodies on a microscopic scale. For the piping system, this contact resistance is a function of the heating element size, element geometry, element layout (pattern), contact pressure ("tightness" of the wrap), pipe size, and pipe surface condition (including roughness and cleanliness). Unlike the pipe, the insulation blanket can conform easier to the heating elements, resulting in a different contact resistance.

When solving the CHT problem using CFD, the thermal contact resistance can be directly specified at a contact interface. Values of thermal contact resistance are difficult (or impossible) to determine analytically, and therefore are typically determined through experimental measurement. For this analysis, the thermal contact resistance value was the "tuning" parameter used to match the computational solution to experimental measurements. Using thermal contact resistance as a tuning parameter allows the heating layer to be treated as uniform, rather than having to include detailed element layouts in the models.

Note that since the actual temperature distribution is a function of the thermal contact resistance, which is a function of the particular heating elements used, the results are strictly valid only for the exact equipment used for the heat treating experiments. Other heat treating providers, alternative equipment, or alternative designs could impact the thermal resistance, and thus the resulting thermal distribution. It is suggested that the heat treating experiments be repeated using alternate equipment or an alternate provider.

Heat flows from the heating element into the piping and to the insulation via conduction. Heat is then lost to the surroundings via natural convection and radiation. Heat is applied to the system through a prescribed power input governed by a series of temperature probes. These temperature probes correspond to thermocouples used for control zones during PWHT. The power input is then adjusted such that the temperature probes achieve the prescribed PWHT temperature. The boundary conditions for the system are shown below. The top boundary of the ambient domain was modeled as a pressure outlet so that air could circulate in and out of the model as needed without adding convection in the area of interest.

Figure 2-4: Piping Heating Configuration. Full-symmetry shown, half-symmetry modelled

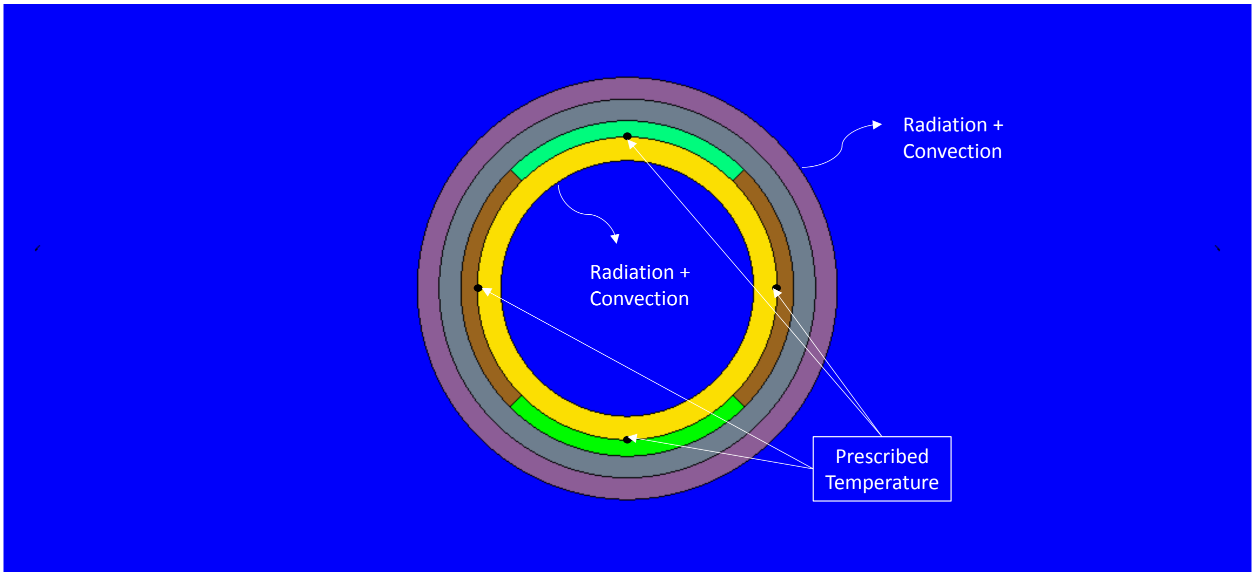

The use of the CFD solver allows the buoyancy-driven flow pattern throughout the system to determine the film coefficients. This is advantageous as the natural convection heat flow can be directly computed, rather than estimated. In addition, this allows 3D effects (top vs. bottom vs. sides of piping) to be included. This is important to determine an accurate temperature distribution around the weld. During the heat treatment, the surrounding air (especially inside) the pipe will be expected to heat locally, resulting in spatially varying sink temperatures for a steady state analysis. Using CFD-based analysis allows the air temperature to be directly computed, rather than using an estimated (likely uniform) sink temperature. Note that sufficient mesh refinement is required to accurately capture boundary layer convective effects. The y+ value provides a measure of mesh refinement in the boundary layer. It is defined as the distance from the wall normalized by the viscous length scale [4]. A value of 50 or less is recommended and a value of 5 or less is highly preferred to ensure boundary layer accuracy. In all cases the y+ value was significantly less than 50 and only exceeded one at a limited number of points remote from the area of interest.

2.3 Calibration Model Cases

Experimental PWHT simulation measurements were taken for two different nominal pipe diameters, eight inch and 14 inch pipes, in four HB configurations for the former and three HB configurations for the later. For every case the weld was not placed rather the joined pipes were placed with ends abutting. Temperature readings were taken at the 3, 6, 9, and 12 o'clock locations at or near the centerlines on the outside diameter (OD) and inside diameter (ID) and at the 6 and 12 o'clock locations axially along the OD of the pipe at the edge of the SB, HB, and GCB for every configuration. These configurations can be seen in Appendix A: and a summary of the cases can be found in Figure 2-5. Temperature measurements were taken as the pipes were heated to a nearly steady state condition and then allowed to cool. For the purposes of the steady state CFD calibration models, the temperature profiles at steady state were extracted and used exclusively. The extracted profiles can be seen in Figure 2-6.

Figure 2-5: Calibration case summary

Description	Case ID	OD (in)	Wall thickness (in)	HB length (in)	GCB length (in)
14 inch narrow band	1	14	1.25	20	30.5
14 inch medium band	2	14	1.25	36.75	47.5
14 inch wide band	3	14	1.25	48	59.72
8 inch narrow band	4	8.63	1.375	15	23
8 inch medium band	5	8.63	1.375	30.5	38.5
8 inch wide band	6	8.63	1.375	45.5	53.3
8 inch medium band with second layer of insulation extending the length of GCB	7	8.63	1.375	30.5	50.5

Figure 2-6: Circumferential ID and OD temperature profiles at centerline.

Case	O'clock	ID Temp (°F)	OD Temp (°F)
Case 1	12	1214	1250
	3	1202	1249
	6	1199	1249
	9	1198	1249
Case 2	12	1226	1250
	3	1227	1250
	6	1221	1250
	9	1217	1250
Case 3	12	1237	1252
	3	1238	1248
	6	1235	1250
	9	1233	1249

Case	O'clock	ID Temp (°F)	OD Temp (°F)
Case 4	12	1230	1255
	3	1224	1257
	6	1225	1258
	9	1224	1253
Case 5	12	1240	1250
	3	1238	1250
	6	1234	1250
	9	1241	1250
Case 6	12	1241	1250
	3	1236	1250
	6	1236	1250
	9	1239	1250
Case 7	12	1242	1250
	3	1240	1250
	6	1236	1250
	9	1243	1251

The CFD models were calibrated by setting the temperature probe control points mentioned in section 2.2 to the measured OD centerline temperatures measured in the data and listed in Figure 2-6. The contact resistance between the pipe and the heating band was adjusted until ID temperature probes matched the measured ID experimental data listed in Figure 2-6. Weight was given to matching the wide band data more closely than the narrow band data while erring on the conservative or greater temperature difference between OD and ID surfaces. Matching was achieved using four control zones similarly to the four control zones used in the experimental cases.

Temperature dependent thermal conductivity for the pipes was taken from ASME BPV Part 2 Section D [7]. The 14 inch diameter experiment and CFD modeling were performed using 1Cr-1/2Mo material and the eight inch diameter experiment and CFD modeling was performed using carbon steel. The CFD model interpolated between the table values for exact temperature thermal conductivity values.

2.4 Prediction Model Cases

The prediction models used the same models developed for the calibration cases with a few parameter changes. For all of the prediction cases, material properties for P91 steel were used. The temperature-dependent thermal conductivity values were extracted from ASME BPV Part 2 Section D [7]. Five different diameters with three thicknesses each were modeled. The SB was assumed to be three times the pipe thickness as given in ASME B36.10M [9]. The GCB was calculated using the equation $GCB = HB + 4\sqrt{Rt}$, where R is the inside radius and t is the pipe thickness. This equation is found in AWS D10.10 [1]. The HB was iteratively changed until the maximum temperature difference in the soak band was no more than 15°F. A summary of the pipe dimensions for each case can be seen in Figure 2-7.

Figure 2-7: Prediction model geometry parameters

Nominal diameter	OD (in)	Pipe schedule	Thickness (in)	SB (in)	Pipe length (in)
6	6.625	80	0.432	1.296	132.5
		120	0.562	1.686	132.5
		160	0.719	2.157	132.5
10	10.75	80	0.594	1.782	215
		120	0.844	2.532	215
		160	1.125	3.375	215
14	14	80	0.75	2.25	280
		120	1.094	3.282	280
		160	1.406	4.218	280
24	24	80	1.219	3.657	480
		120	1.812	5.436	480
		160	2.344	7.032	480
30	30	80	1.356*	4.068	600
		120	2.015*	6.045	600
		160	2.607*	7.821	600

Note: ASME B36.10M [9] does not specify a thickness for 30 inch diameter schedule 80, 120, 160 pipes so the proportional thicknesses were scaled from the 24 inch diameter pipe and the 30 inch diameter schedule 30 pipe.

3 RESULTS

3.1 Calibration Model Cases

The calibration cases were run to steady state while the thermal contact resistance was adjusted to match the centerline ID temperature measurements from the experimental cases. The OD temperature probes were set to adjust the power input such that their value matched the experimental measurements at the same locations. The calibrated resistance value was found to be 0.0037 m^2K/W. the calibrated centerline temperature profiles can be seen in Figure 3-1. The optimum value of resistance varied with each experimental case. Note that the most conservative value of resistance was used (Case 6) for subsequent analyses.

Figure 3-1: Calibration centerline ID temperatures for thermal contact resistance of 0.0037 m2K/W

Case	o-clock	ID – CFD (°F)	ID – Experimental (°F)
Case 1	12	1195.754	1214
	3	1189.911	1202
	6	1187.924	1199
Case 2	12		
	3		
	6		
Case 3	12	1232.28	1237
	3	1227.191	1238
	6	1224.968	1235
Case 4	12	1199.439	1230
	3	1195.749	1224
	6	1193.333	1225
Case 5	12		
	3		
	6		
Case 6	12	1240.318	1241
	3	1238.18	1236
	6	1236.866	1236
Case 7	12		
	3		
	6		

As discussed with ASME, note that in the final calibration, run cases 2, 5, and 7 were omitted because of non-standard geometry irregularities.

3.2 Prediction Model Cases

The prediction model cases were run to nearly steady state. There did exist some minor transient flow in the models, however its nature is relatively small and should not affect the overall results of the models. Five different pipe diameters were investigated with three different pipe thicknesses per diameter. The temperature desired for proper PWHT in P91 steel is between 1350 and 1400°F, therefore the temperature control probes were set to 1390°F such that the minimum temperature in the SB exceeded 1350°F. For 14 inch diameter and larger pipes, four control zones were used so that the temperature could be controlled at the 12, 3, and 6 o'clock locations. For the six and ten-inch diameter pipes, two control zones were used so that temperature could be controlled at the 12 and 6 o'clock locations. The HB and GCB were iteratively increased in length until the maximum temperature difference in the SB was less than 15°F. This occurred with four to six iterations per geometry. For all final HB lengths the minimum SB temperature exceeded the desired 1350°F.

The trend followed roughly a power relation between temperature differences desired to HB length required. To calculate the HB required for a 15°F temperature difference (delta 15 points), for each case a linear interpolation was performed between the bounding iterations. This can be seen in Figure 3-2 through Figure 3-6.

Figure 3-2: CFD SB delta T results for 6 inch schedule 80, 120, 160 P91 pipes

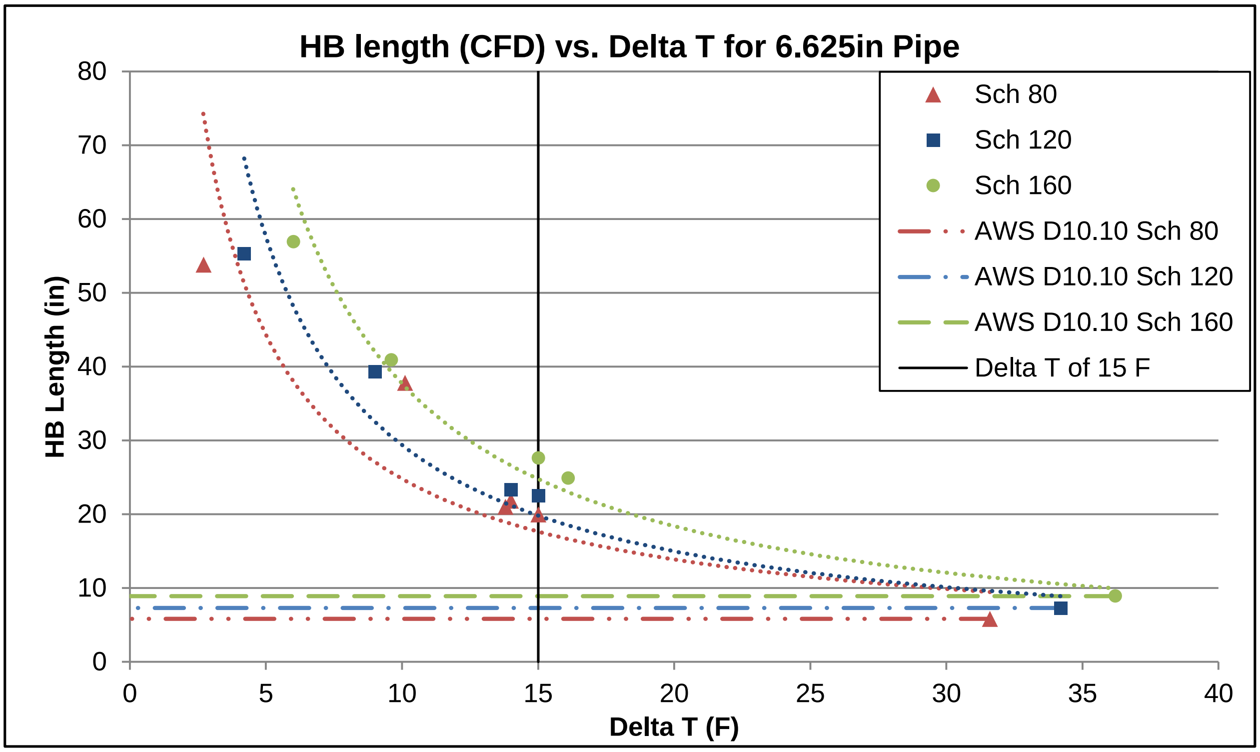

Figure 3-3: CFD SB delta T results for 10 inch schedule 80, 120, 160 P91 pipes

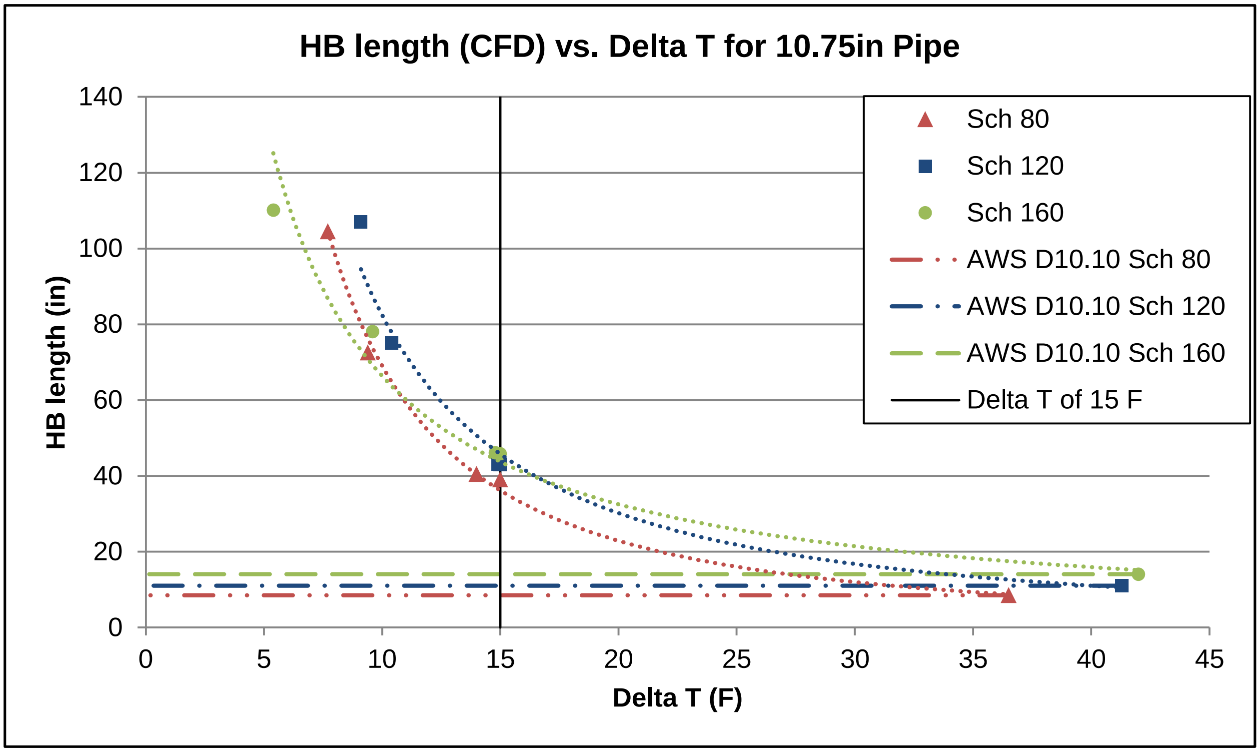

Figure 3-4: CFD SB delta T results for 14 inch schedule 80, 120, 160 P91 pipes

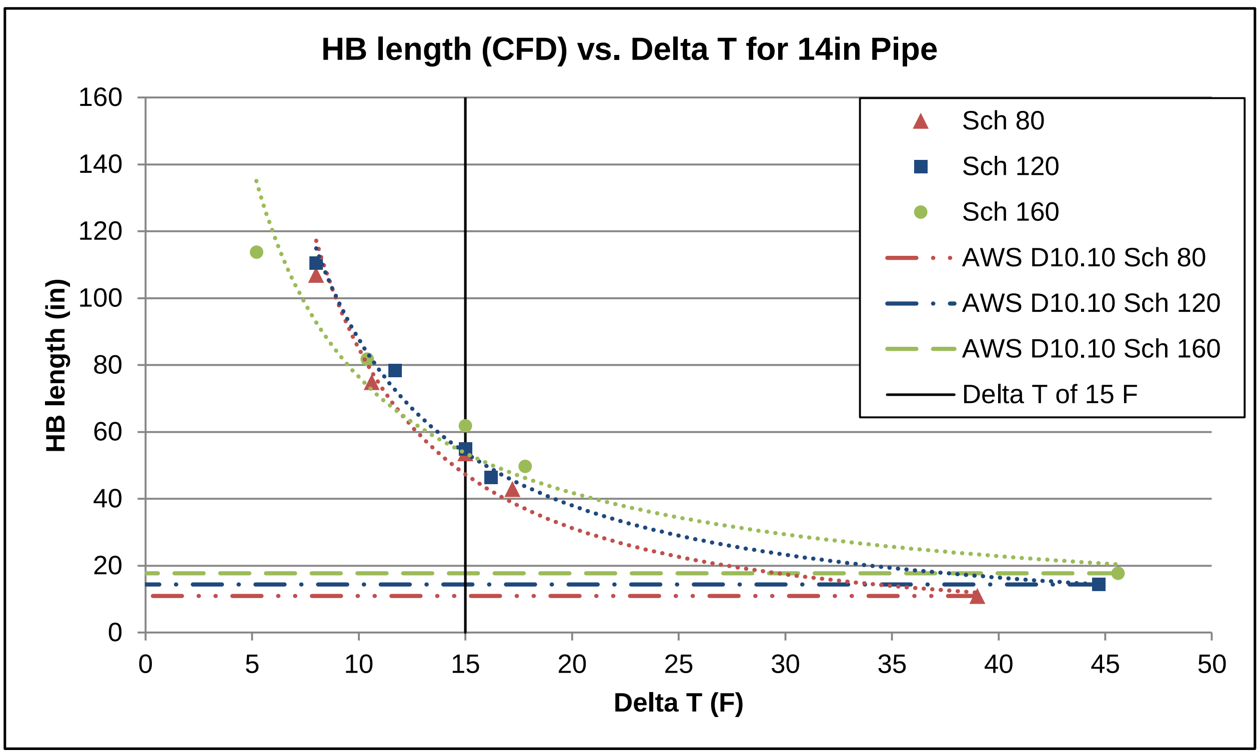

Figure 3-5: CFD SB delta T results for 24 inch schedule 80, 120, 160 P91 pipes

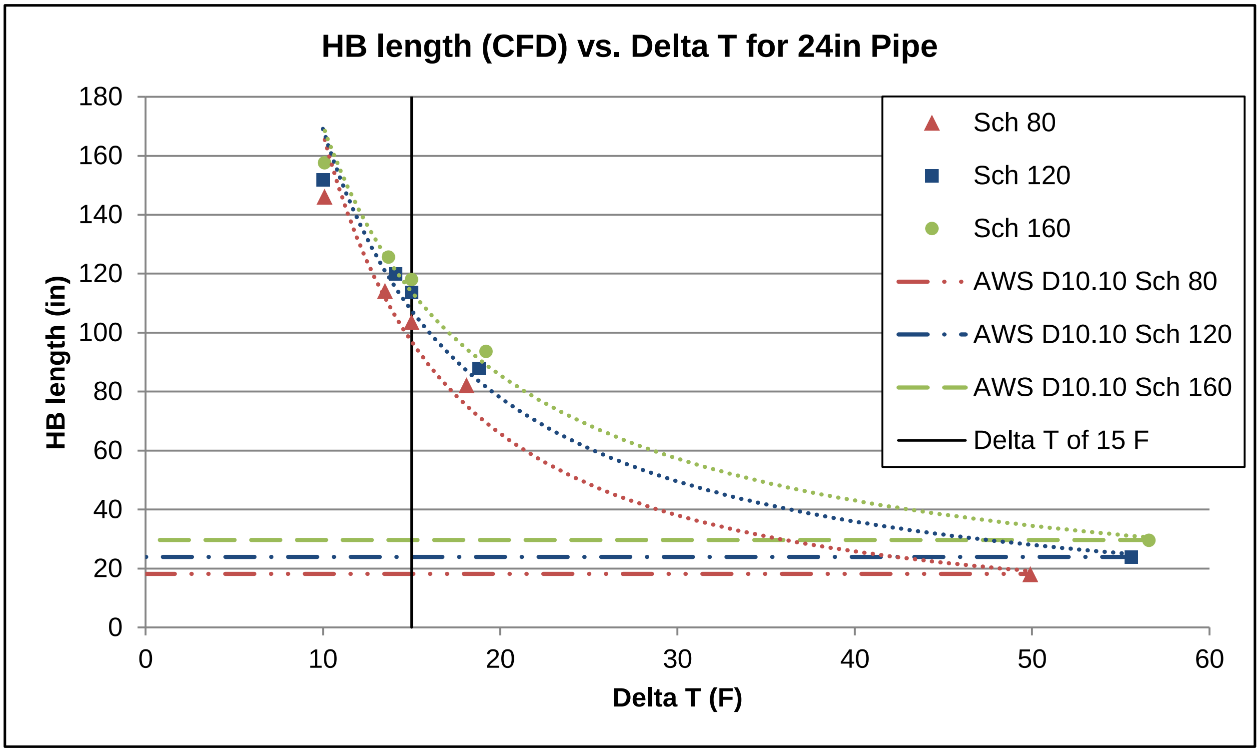

Figure 3-6: CFD SB delta T results for 30 inch schedule 80, 120, 160 P91 pipes

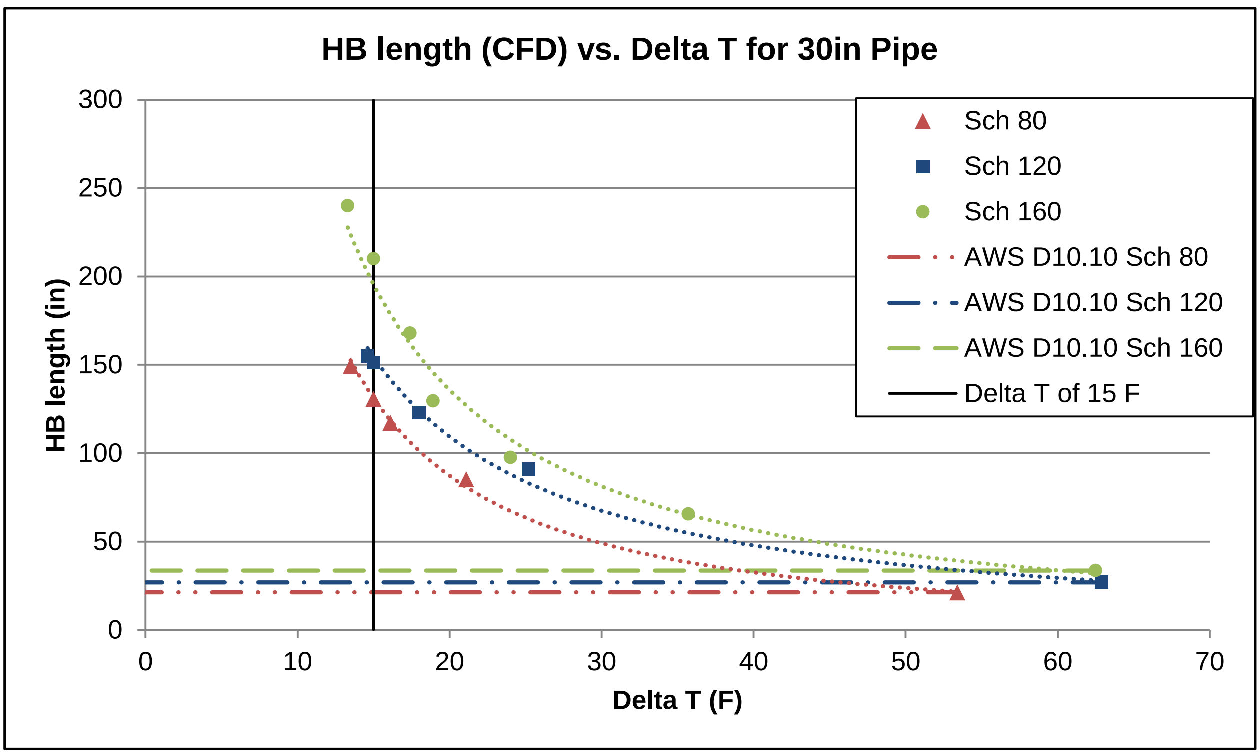

If a larger temperature gradient than 15°F is deemed acceptable, the required HB length can be interpolated using the power fit curves. The coefficients for those curves are in Figure 3-7 and take the form of Equation 1.

$$HB = C\Delta T^{m} \qquad \textbf{Equation 1}$$

Figure 3-7: Power curve-fit coefficients

Nominal diameter	OD (in)	Pipe schedule	m	C
6	6.625	80	-0.84962	171.3196
		120	-0.98545	275.7616
		160	-1.04276	405.7331
10	10.75	80	-1.59879	2693.57
		120	-1.45099	2368.222
		160	-1.03184	706.5476
14	14	80	-1.43952	2263.167
		120	-1.20669	1404.228
		160	-0.87259	550.5781
24	24	80	-1.3397	3580.331
		120	-1.10806	2125.196
		160	-0.98549	1624.449
30	30	80	-1.42265	6196.065
		120	-1.20315	4053.562
		160	-1.24303	5529.964

For each geometry, the first analysis represents the prescribed HB length according to AWS D10.10 [1]. As seen in Figure 3-8, the prescribed heat band lengths according to AWS D10.10 resulted in temperature variations around the weld significantly greater than 15°F. The predicted temperature variation ranged from 31-63°F, with the variation increasing for larger diameter pipes.

Figure 3-8: Delta T in SB for AWS D10.10 HB

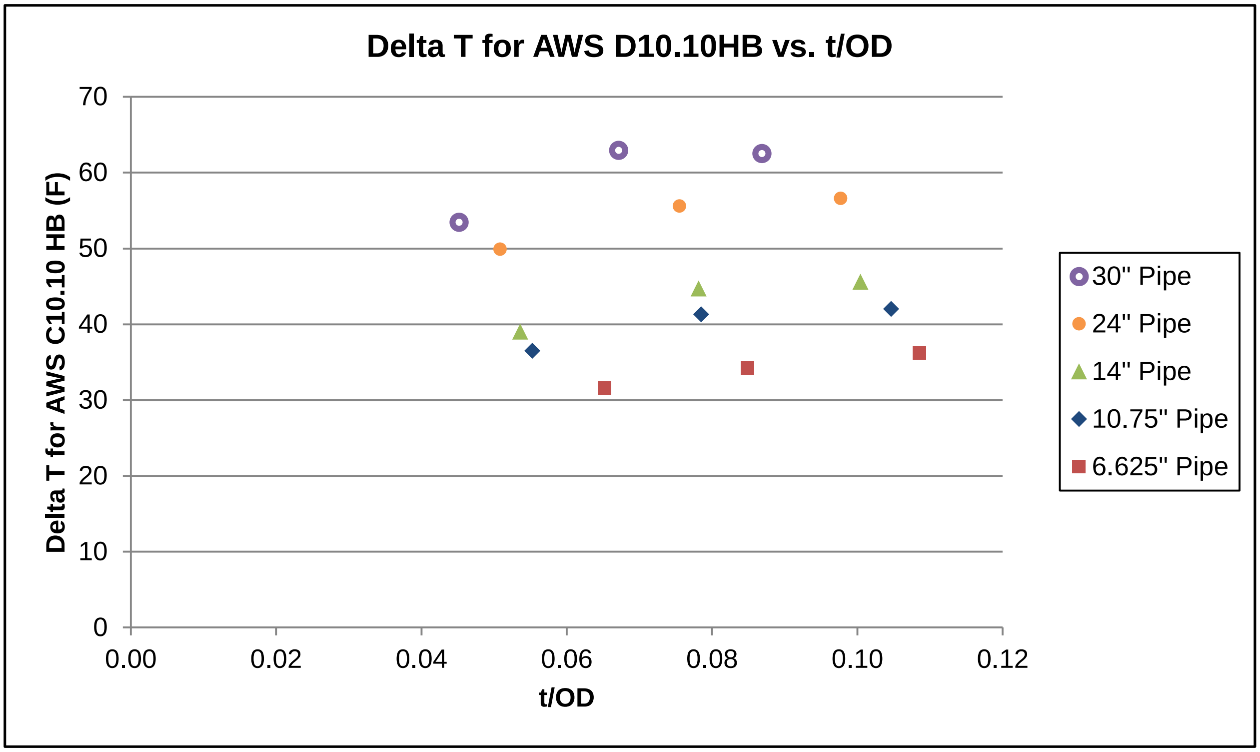

When the delta 15°F points for all prediction cases are plotted against OD and t/OD, it can be seen in Figure 3-9 and Figure 3-10 that they are nearly planar. This is with the exception of the 30 inch OD schedule 160 point. This is likely because this pipe size is well beyond the realm of validity of the calibration cases. When examining the results from the calibration cases it can be seen that the ID SB temperatures more closely match the 8 inch wide band case and are a few degrees conservative for the 14 inch wide band case. This conservatism is likely increased as the pipe diameter increases. When this is coupled with the thicker walled pipe, the HB length starts to show asymptotic behavior as it approaches the delta 15°F point. It is recommended that further testing be performed on a 30 inch OD pipe such that the models can be better calibrated for these large diameters. This would allow the models to be better tuned to handle a larger variety of pipe sizes without excess conservatism.

Figure 3-9: CFD HB results for SB temperature difference of 15°F plotted against OD and t/OD

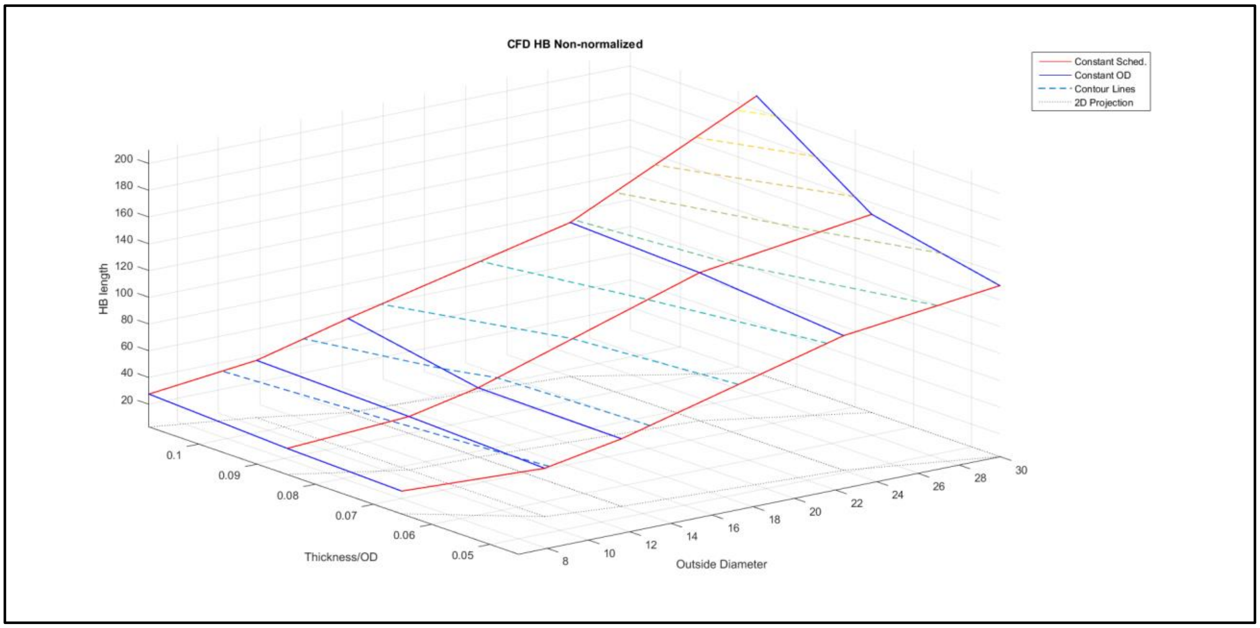

Figure 3-10: CFD HB results for SB temperature difference of 15°F plotted against OD and t/OD. Viewed from in-plane direction

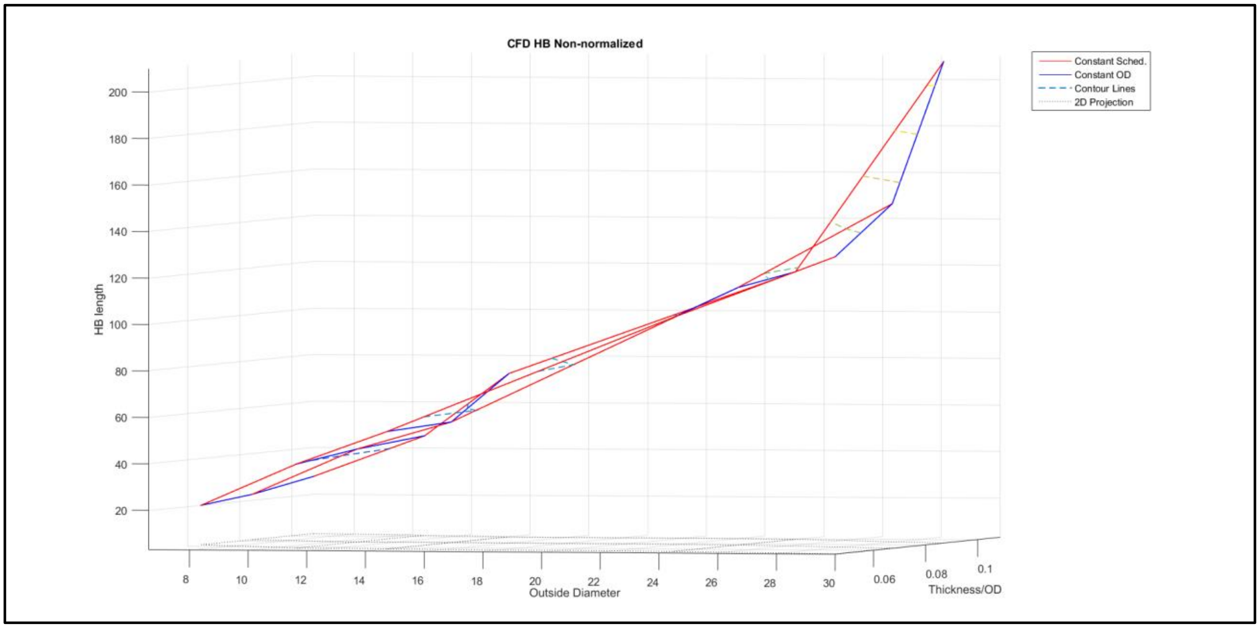

The ratio between the prescribed HB length given in AWS D10.10 [1] and the HB length calculated in this study shows an increasing disparity as the pipe diameter increases. This is due to the increased presence of natural convection on the ID surface of the larger diameter pipes. This disparity can be seen in Figure 3-11 and Figure 3-12. In all cases, a much larger HB length is likely required to obtain the target temperature distribution as compared to AWS guidelines.

Plots showing the temperature distribution of the domain, pipe, and SB as well as plots showing the velocity distributions of natural convection in the domain can be found in Appendix B:.

Figure 3-11: Required HB lengths for a SB delta T=15°F from CFD and HB length from AWS D10.10

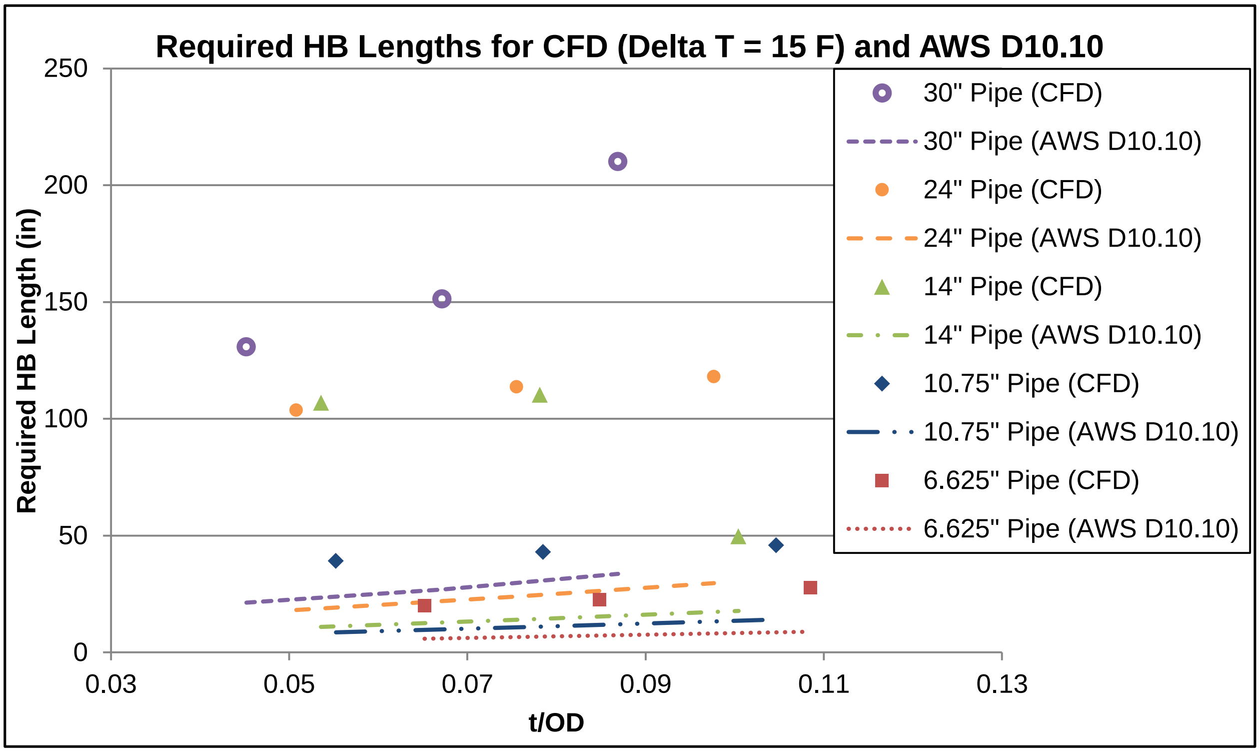

Figure 3-12: Ratio of CFD HB length for SB delta T=15°F over HB length from AWS D10.10

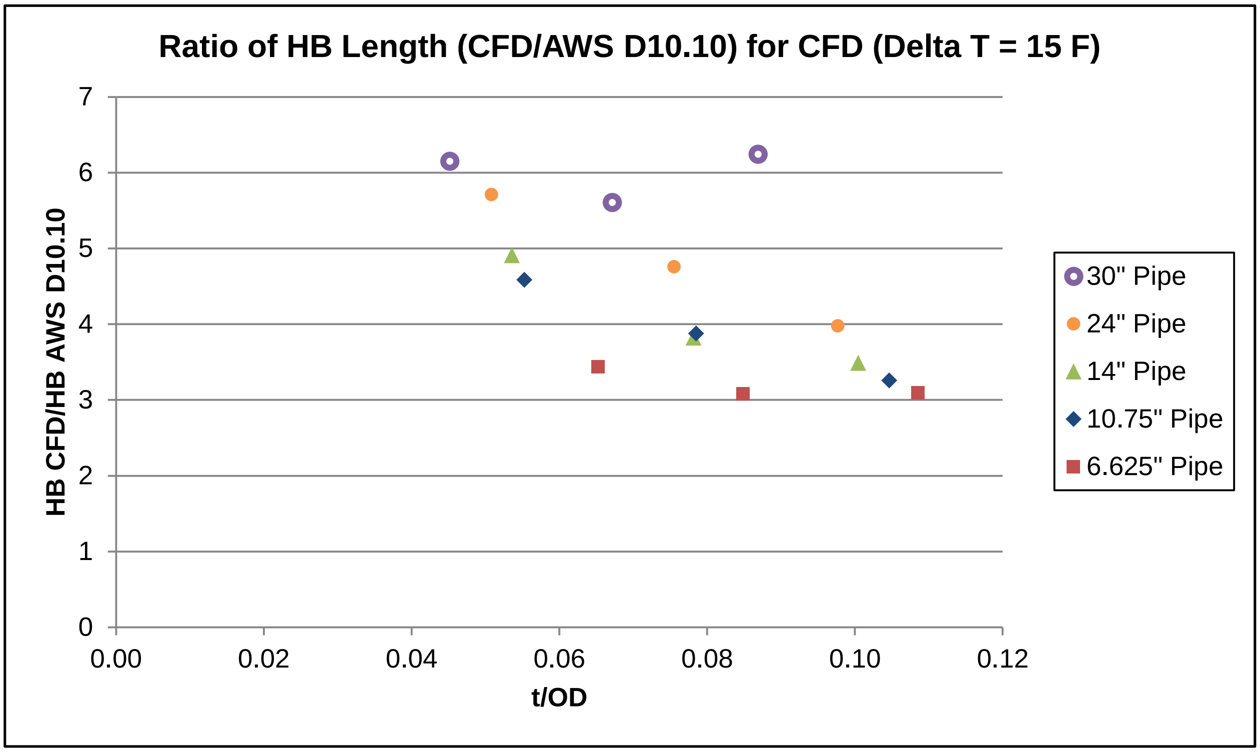

ASME requested guidance regarding the measuring of the ID SB temperature; a correlation function was developed that provides the axial distance on the pipe from centerline where the OD temperature matches the minimum ID SB temperature. Using the multiple cases conducted for each pipe OD, pipe schedule, and varying HB lengths, plots and linear functions were developed relating the HB to the axial distance X from the weld centerline. Due to natural convection the 6 o'clock location always recorded the minimum SB temperature and thus was considered for these relations. Figure 3-13 through Figure 3-17 show the relation between HB length and X both normalized by OD. Figure 3-18 gives the coefficients of the linear relations. It should be noted that since the 30-inch schedule 160 pipe, as previously explained, demonstrated a deviation from the trend, a separate linear representation was developed for this pipe size. The error bars in these figures represent the plus or minus distance X corresponding to a plus or minus ID SB temperature variance equal to 5°F. This temperature variance is less than the limits that can typically be expected for thermocouple measurements.

Figure 3-13: Axial distance where OD temperature equals min ID SB temperature for 6 in pipe

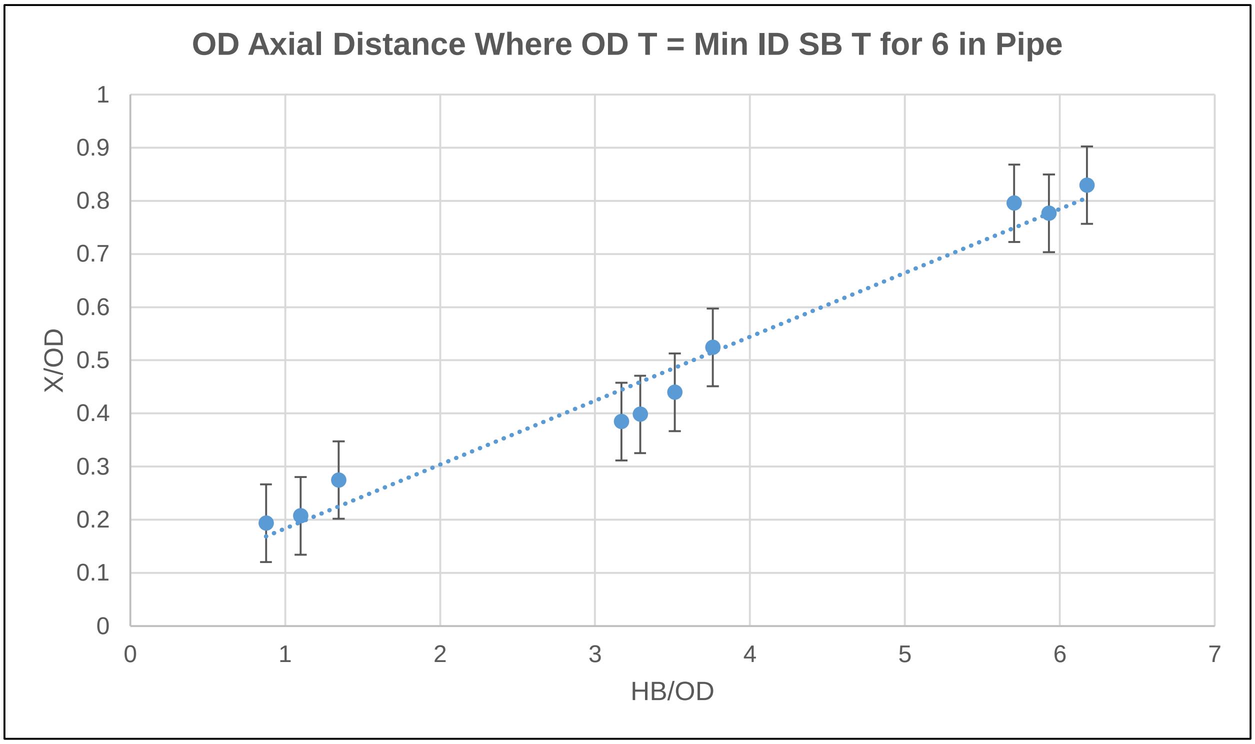

Figure 3-14: Axial distance where OD temperature equals min ID SB temperature for 10 in pipe

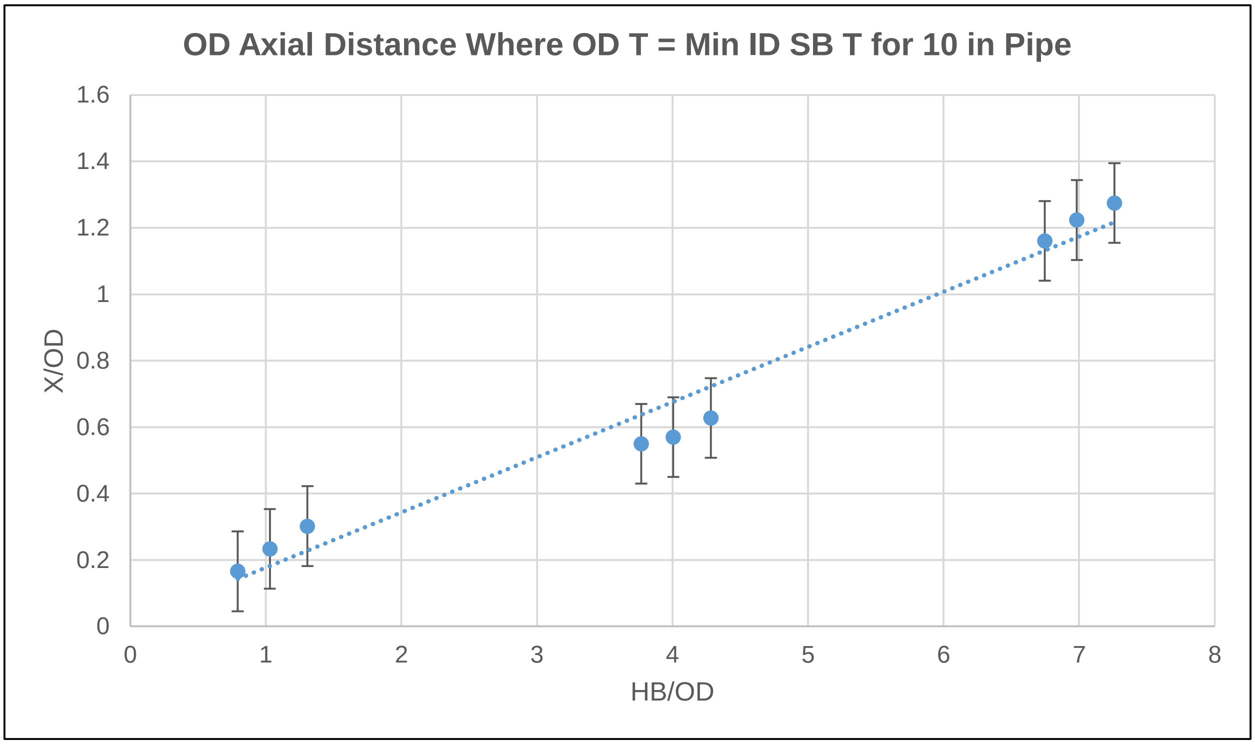

Figure 3-15: Axial distance where OD temperature equals min ID SB temperature for 14 in pipe

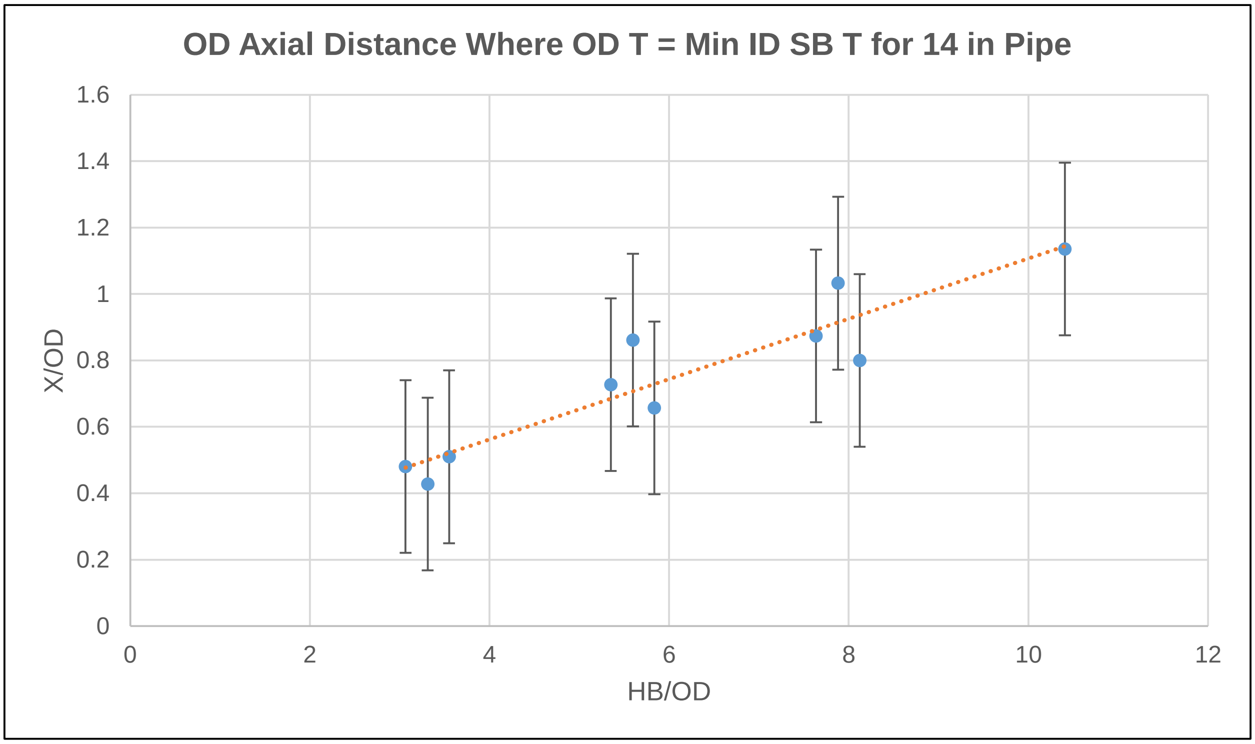

Figure 3-16: Axial distance where OD temperature equals min ID SB temperature for 24 in pipe

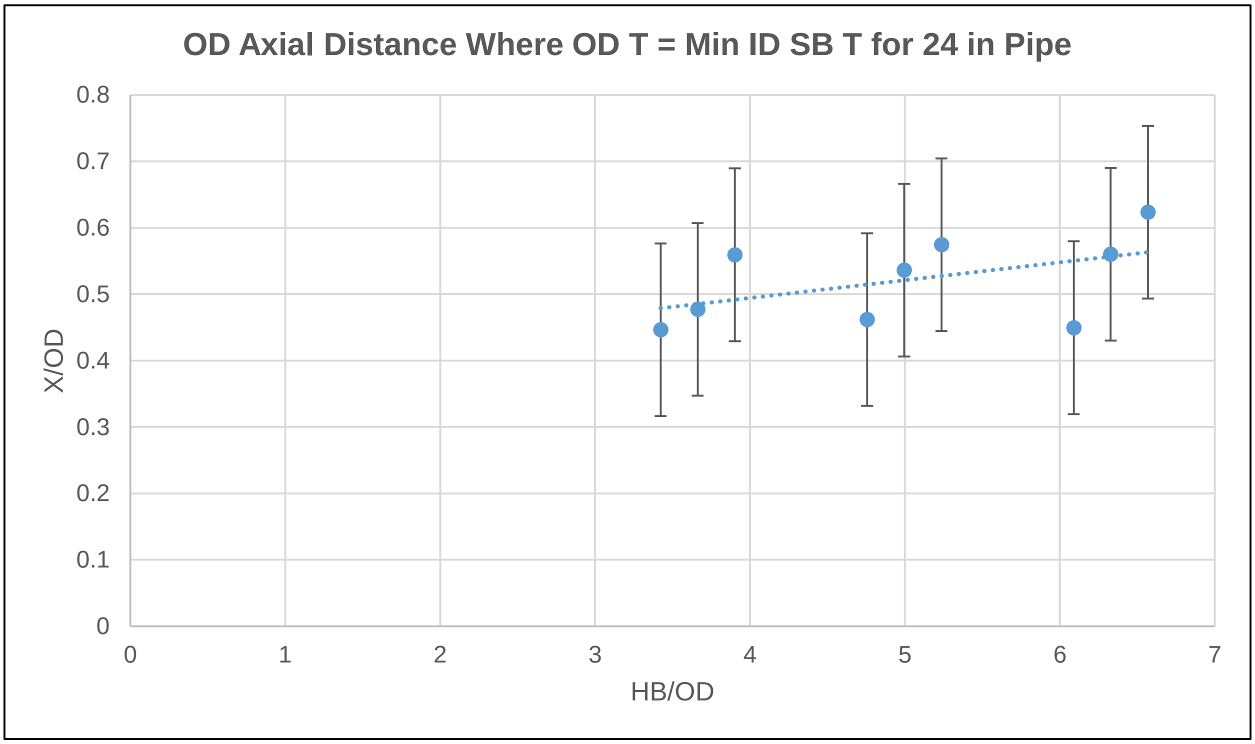

Figure 3-17: Axial distance where OD temperature equals min ID SB temperature for 30 in pipe

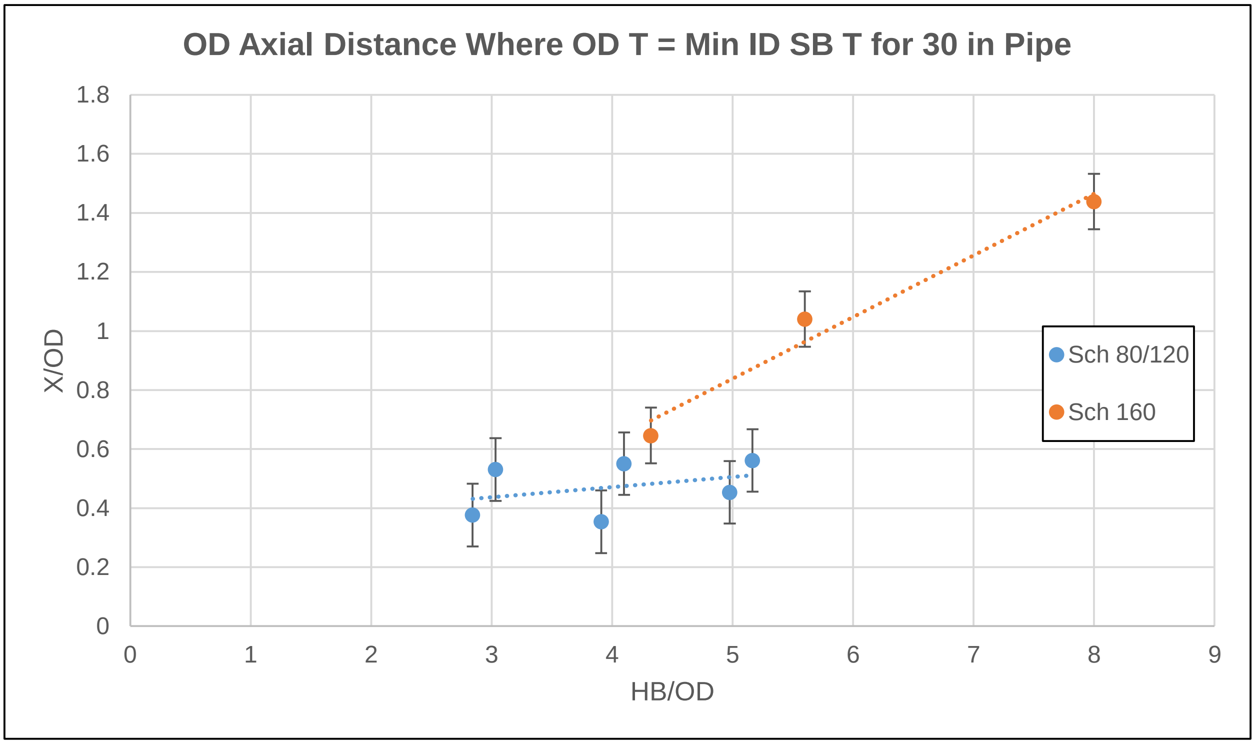

Figure 3-18: Curve-fit coefficients for OD/ID temperature correlation

Nominal diameter	OD (in)	Pipe schedule	slope	y-intercept	Error bar length
6	6.625	80	0.1203	0.0629	0.073
		120			
		160			
10	10.75	80	0.166	0.0112	0.12
		120			
		160			
14	14	80	0.0908	0.199	0.26
		120			
		160			
24	24	80	0.0268	0.3868	0.13
		120			
		160			
30	30	80	0.0344	0.3333	0.106
		120			
		160	0.209	-0.2069	0.09

4 RECOMMENDED FUTURE WORK

The prediction cases carry significant conservatism due to the information available. The temperature control algorithm and thermal contact resistance used in the model were tuned to match the most conservative experimental results. Without this calibration, the CFD analyses would predict higher ID surface temperatures than were observed during experiment. The experimental results were used to estimate steady-state conditions for the CFD analyses. In reality, the heat input (power) of the heating band likely varied during the experiment due to the thermocouple temperature control. Additional information regarding the transient power consumption could be used to refine the analysis. Because of the noted behavior of the 30 inch OD schedule 160 case, it would be recommended to follow this study up with a further empirical study so that the present CFD models can be updated and rerun with better large diameter pipe calibration data. Additional information regarding the calibration test set-up, including ambient temperature, pipe end conditions, thermo-couple type and installation procedure could also be used to refine the analyses.

It is speculated that additional research into adding multiple axial control zones in addition to the circumferential control zones could significantly reduce the necessary length of the HB to achieve the desired OD to ID temperature difference. By adding axial control zones on either side of the central control zones, more heat could be added to the system while maintaining the desired centerline temperature. This could effectively flatten the axial temperature gradient near the SB and reduce the required width of the HB. Further CFD modeling would be required to confirm and develop new HB requirements. Quest Integrity could modify its existing models at an additional charge.

5 CONCLUSION

The objective of this project was to perform thermal analysis of pipeline heating configurations, with the intention of creating guidelines for the sizing of heating bands. The analysis consisted of two phases. The initial phase served to calibrate and verify the modeling assumptions used for the thermal analysis via comparison with experimental measurements taken for two post weld heat treated pipes using multiple heating band configurations. The second phase analyzed five pipe diameters. The intent of the second phase was to determine appropriate sizing requirements for heating bands to minimize temperature variation around the weld location, for pipe diameters ranging from 6 to 30 inches.

The calibration cases were run to steady state while the thermal contact resistance was adjusted to match the centerline ID temperature measurements from the experimental cases. The OD temperature probes were set to adjust the power input such that their value matched the experimental measurements at the same locations.

The prediction model cases were run to steady state. Five different pipe diameters were investigated with three different pipe thicknesses per diameter. The HB and GCB were iteratively increased in length until the maximum temperature difference in the SB was less than 15°F. This occurred with four to six iterations per geometry. The trend of these iterations followed roughly a power relation between temperature differences desired to HB lengths required.

The HB lengths required for a temperature difference in the SB of 15°F when plotted against OD and t/OD are nearly planar. These HB lengths were found to be much larger than is recommended in AWS D10.10 [1], and this difference increases with pipe diameter due to increasing natural convection effects. The results of these analyses can be used to develop new HB sizing guidelines for AWS D10.10.

Appendix A: Experimental Design Drawings

Figure A-1: Case 1

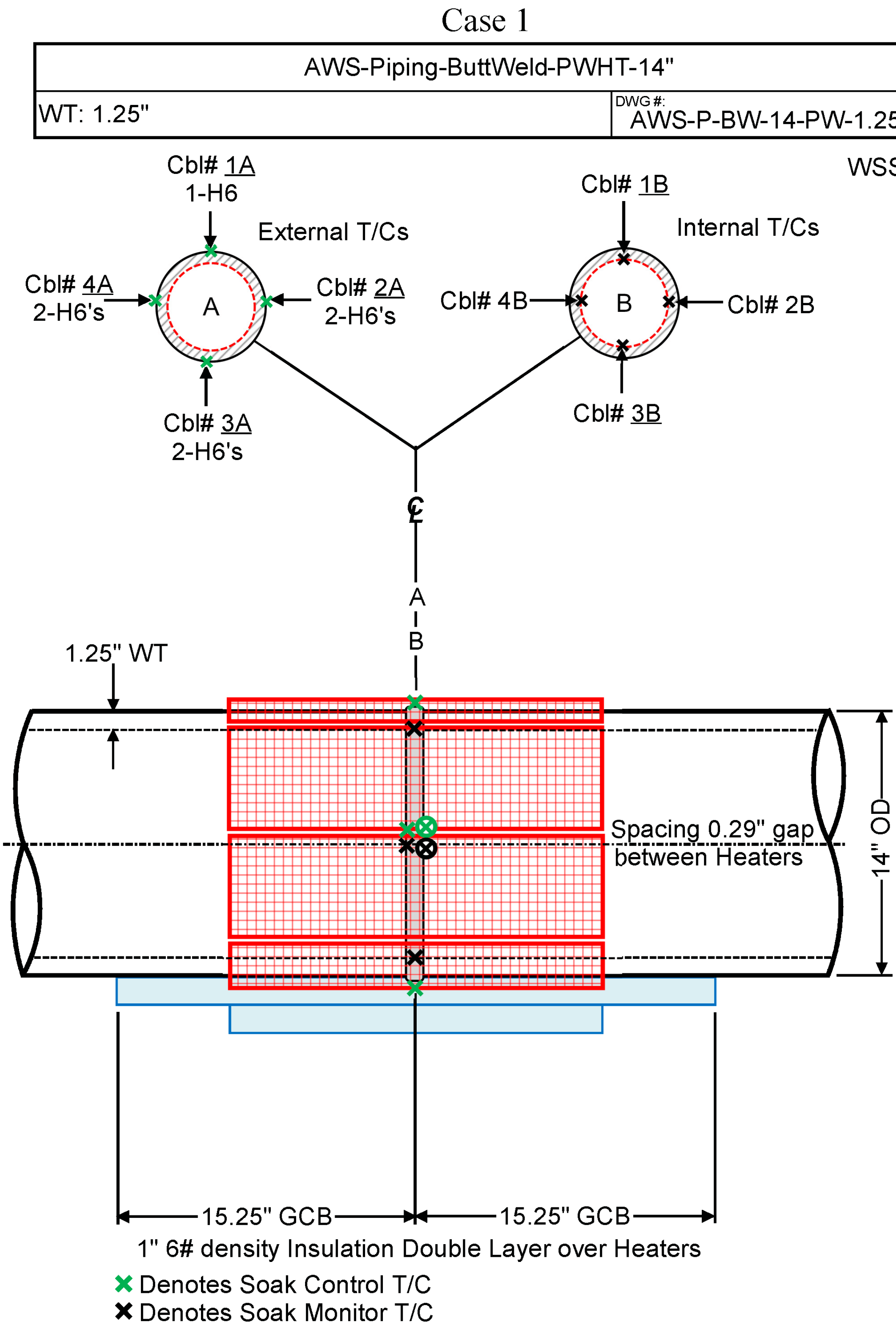

Case 1

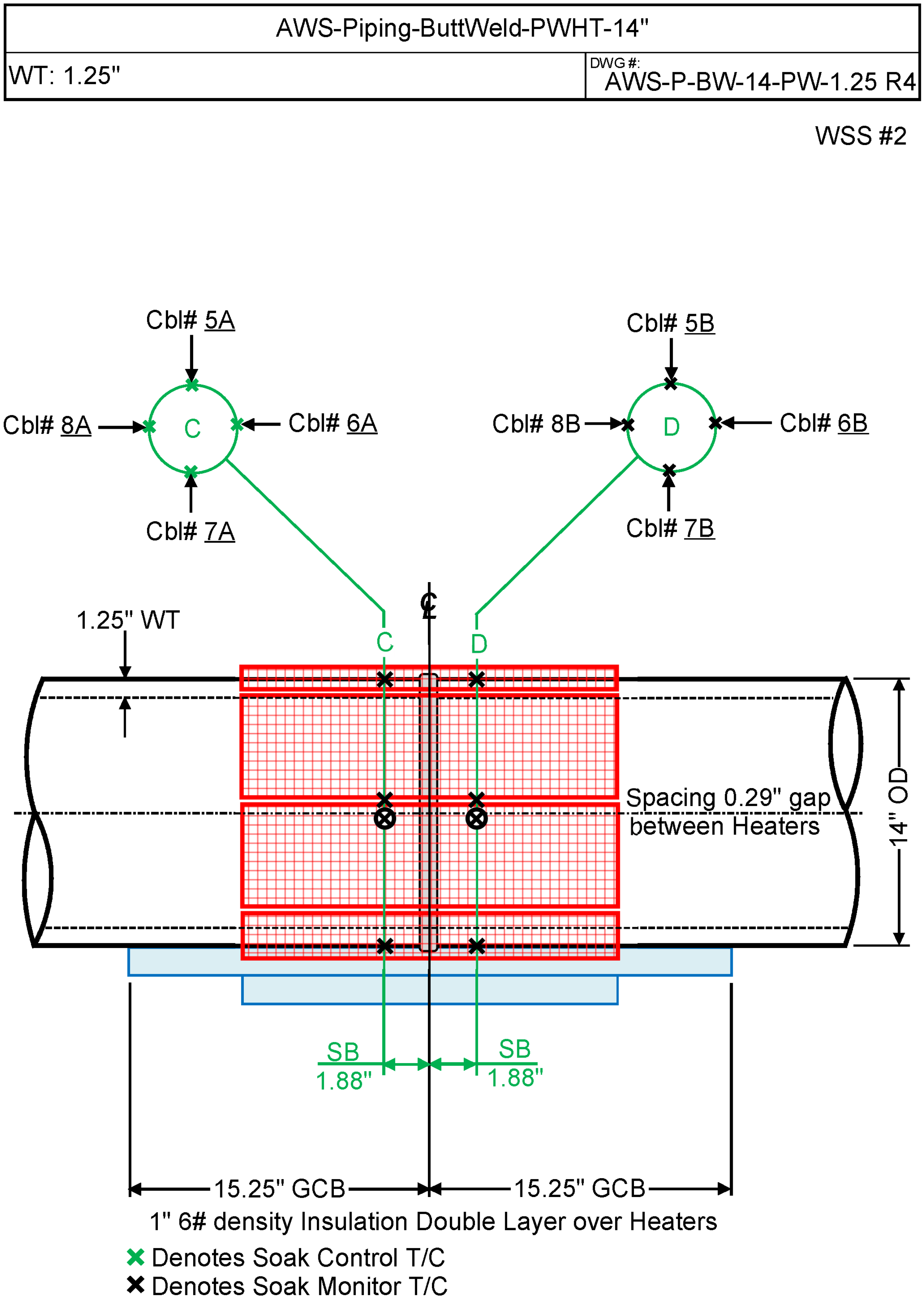
AWS-Piping-ButtWeld-PWHT-14"
WT: 1.25"
DWG #:
AWS-P-BW-14-PW-1.25 R4
WSS #2
Cbl# 5A
Cbl# 8A
C
Cbl# 6A
Cbl# 7A
Cbl# 5B
Cbl# 8B
D
Cbl# 6B
Cbl# 7B
1.25" WT
C
D
Spacing 0.29" gap
between Heaters
14" OD
SB
1.88"
SB
1.88"
15.25" GCB
15.25" GCB
1" 6# density Insulation Double Layer over Heaters
Denotes Soak Control T/C
Denotes Soak Monitor T/C

Case 1

AWS-Piping-ButtWeld-PWHT-14"	
WT: 1.25"	DWG #: AWS-P-BW-14-PW-1.25 R4

WSS #3

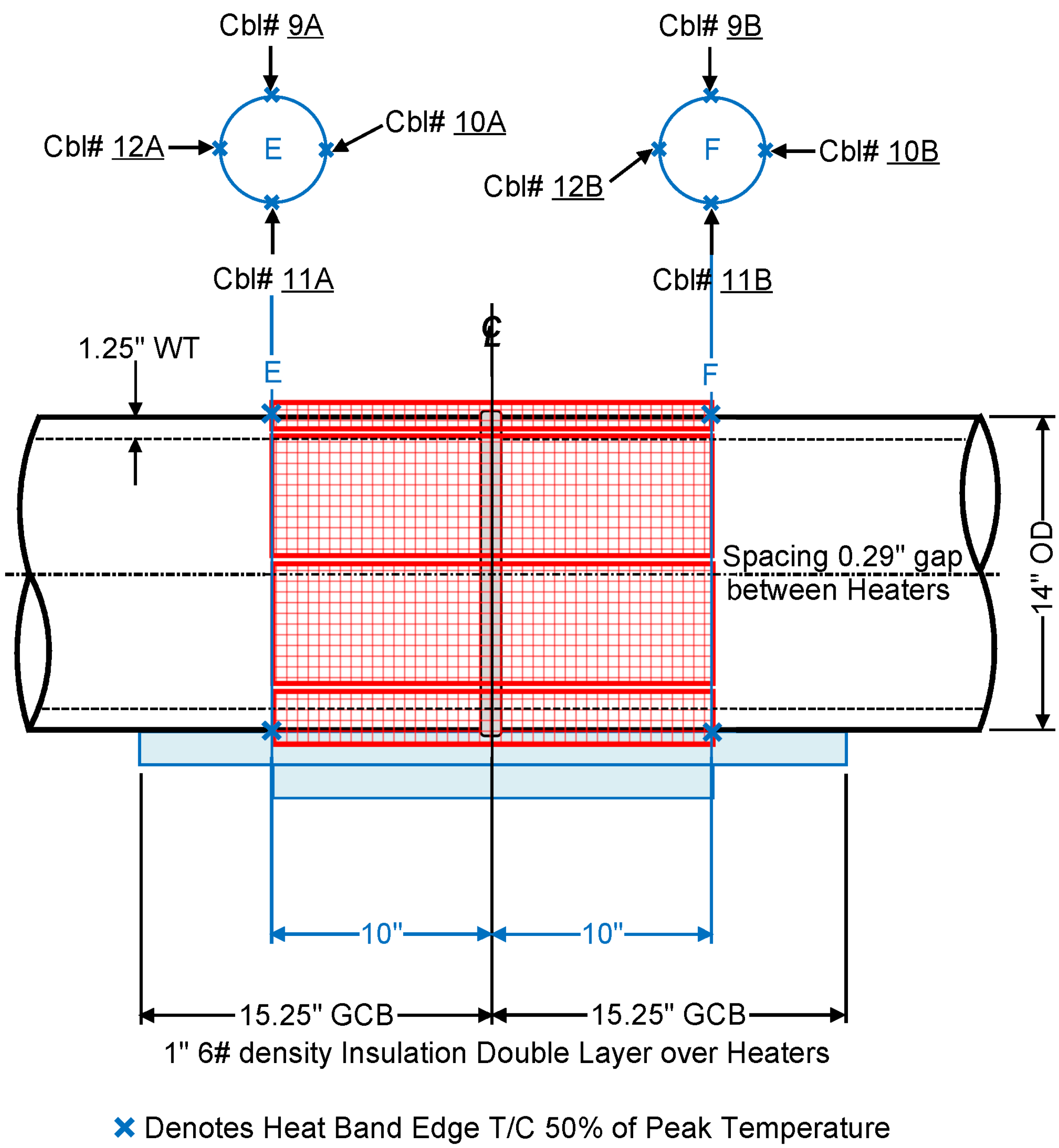

Case 1

AWS-Piping-ButtWeld-PWHT-14"	
WT: 1.25"	DWG #: AWS-P-BW-14-PW-1.25 R4

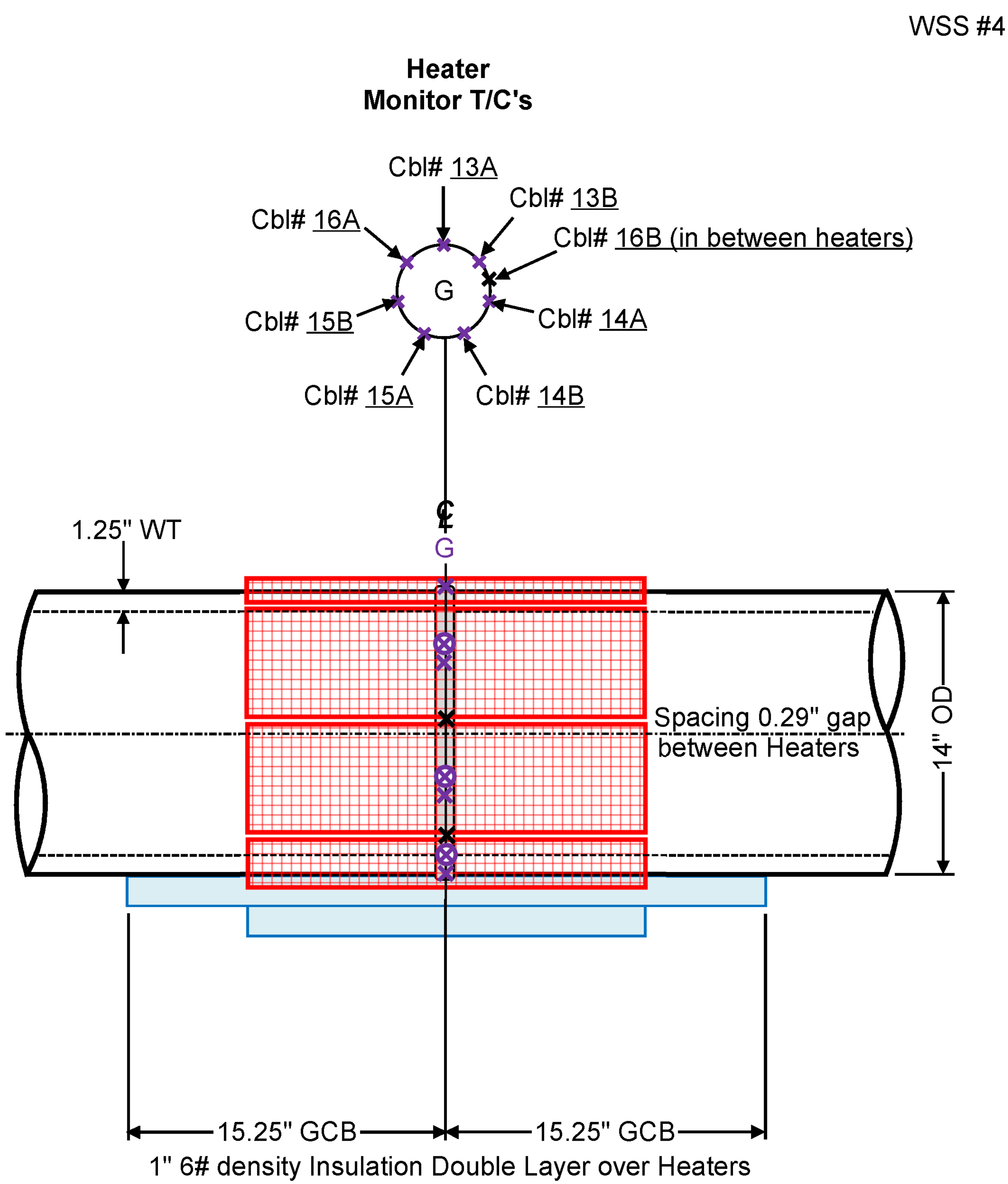

Case 1

AWS-Piping-ButtWeld-PWHT-14"	
WT: 1.25"	DWG #: AWS-P-BW-14-PW-1.25 R4

WSS #5

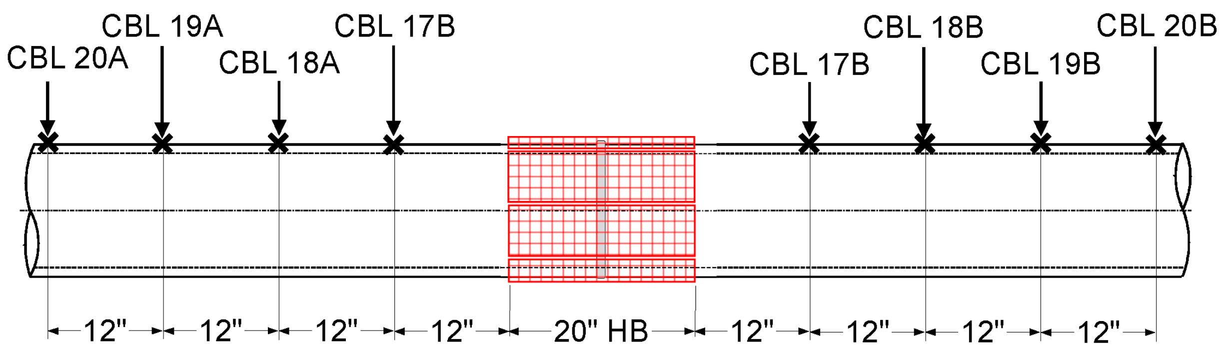

Figure A-2: Case 2

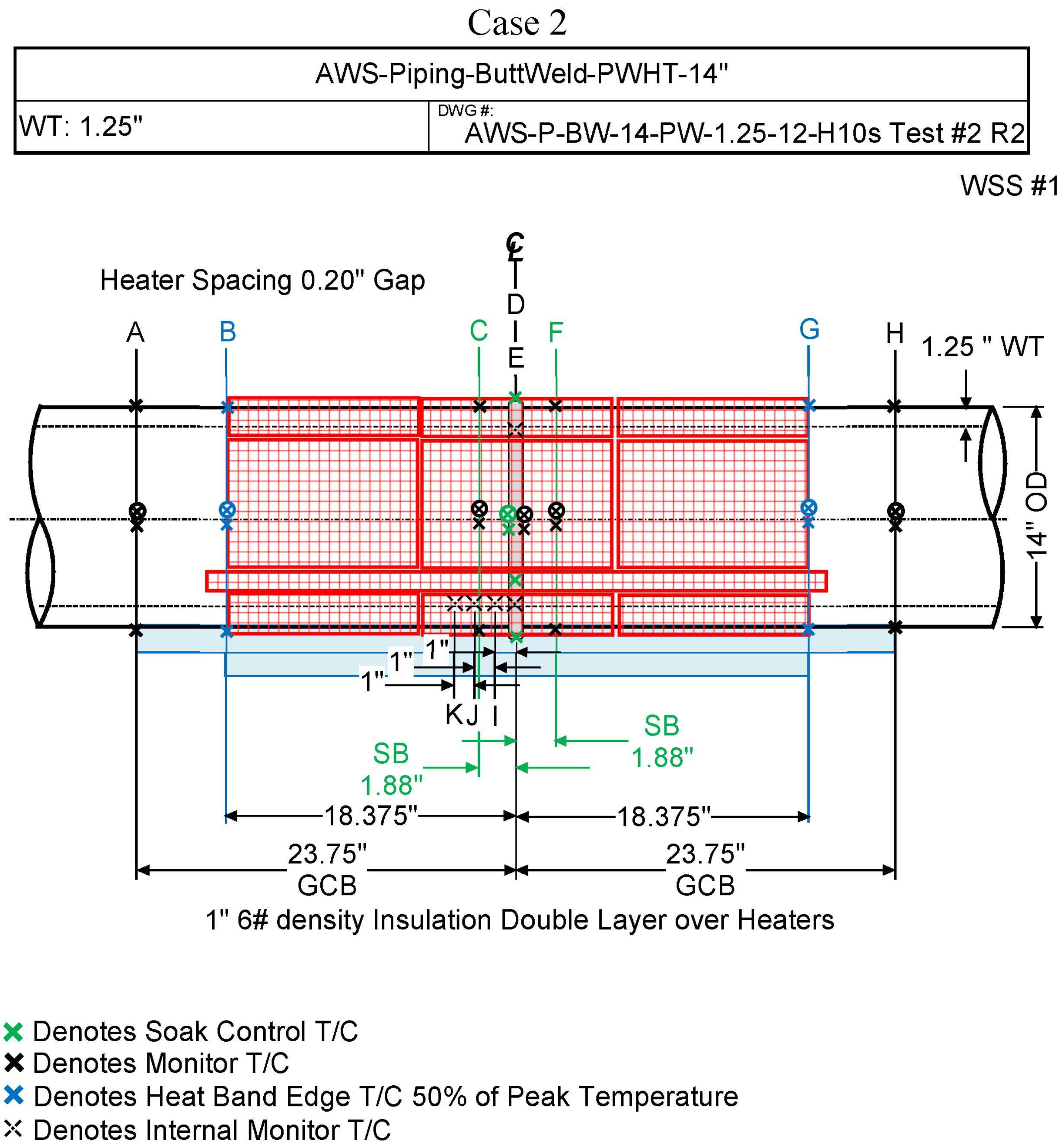

Case 2

AWS-Piping-ButtWeld-PWHT-14"	
WT: 1.25"	DWG #: AWS-P-BW-14-PW-1.25-12-H10s Test #2 R2

WSS #2

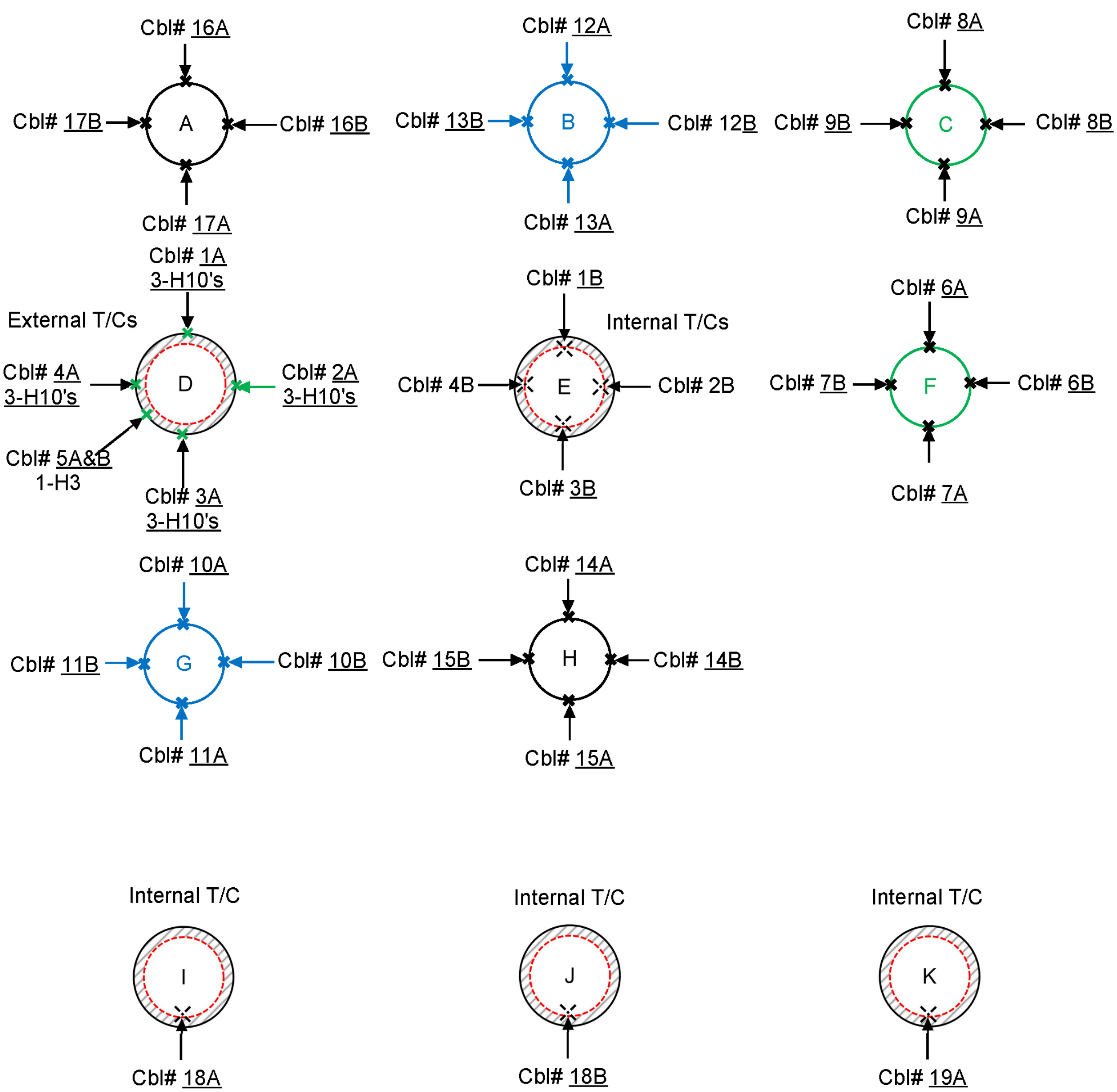

Figure A-3: Case 3

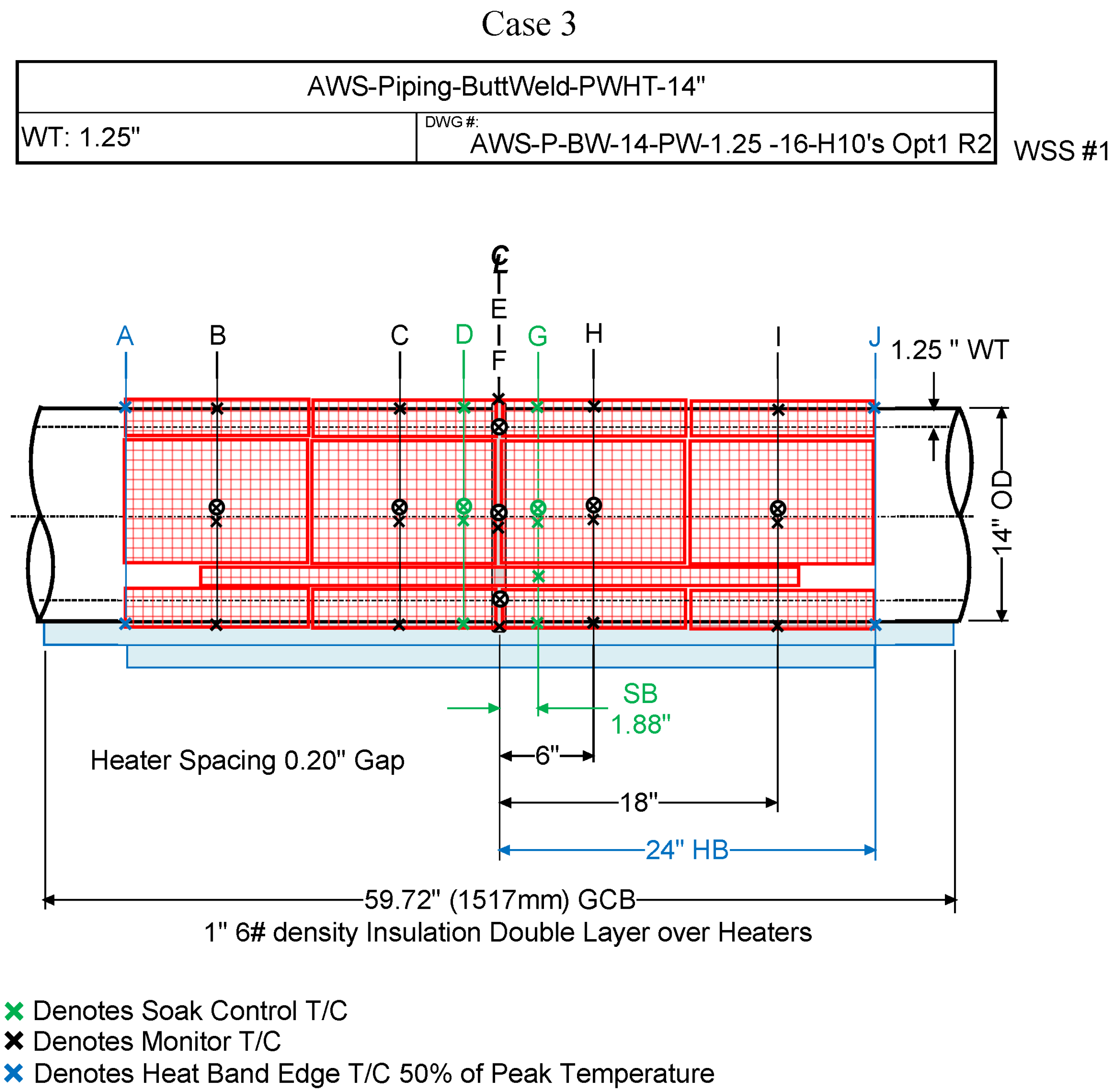

Case 3

AWS-Piping-ButtWeld-PWHT-14"	
WT: 1.25"	DWG #: AWS-P-BW-14-PW-1.25 -16-H10's Opt1 R2

WSS #2

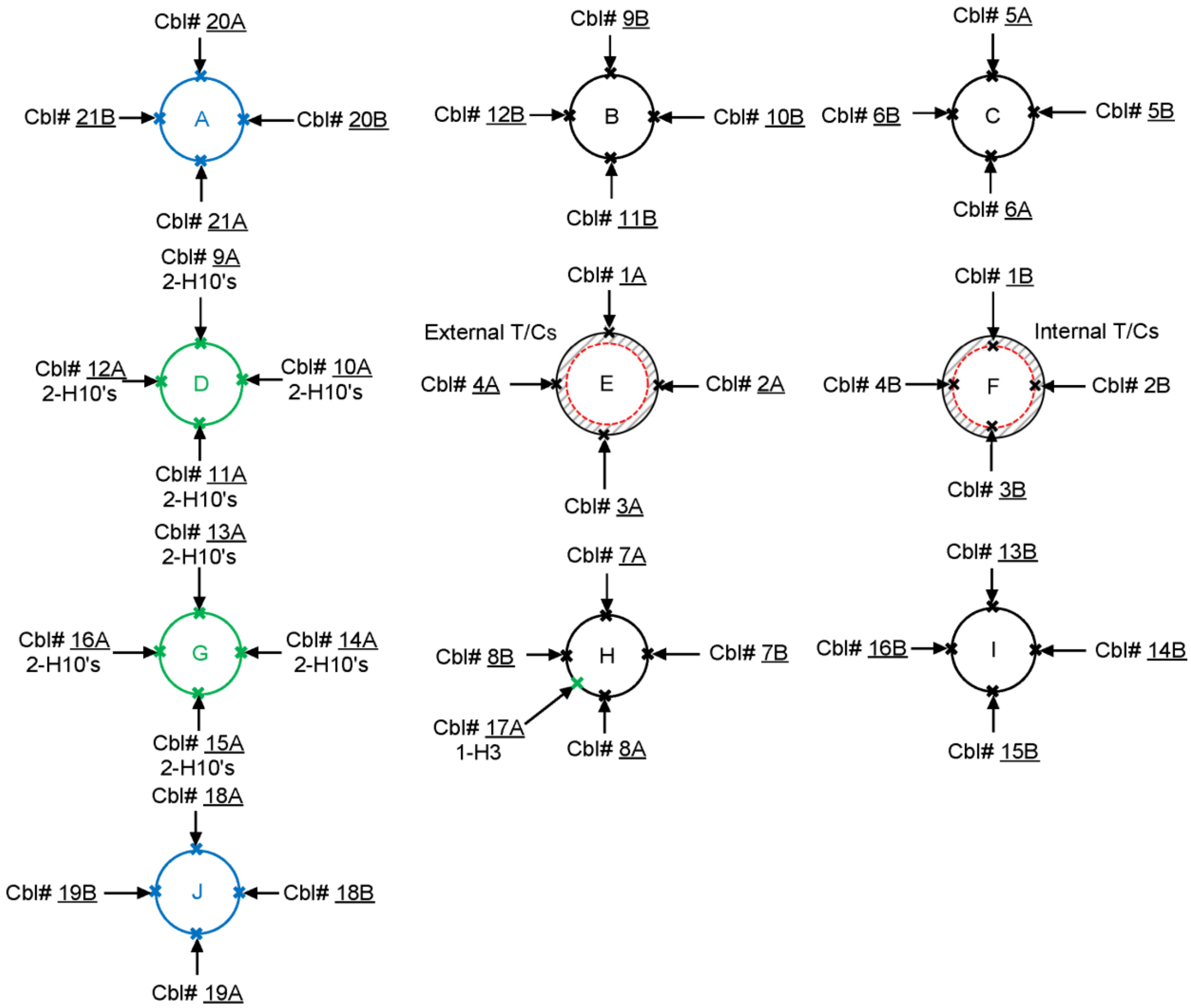

Figure A-4: Case 4

Case 4

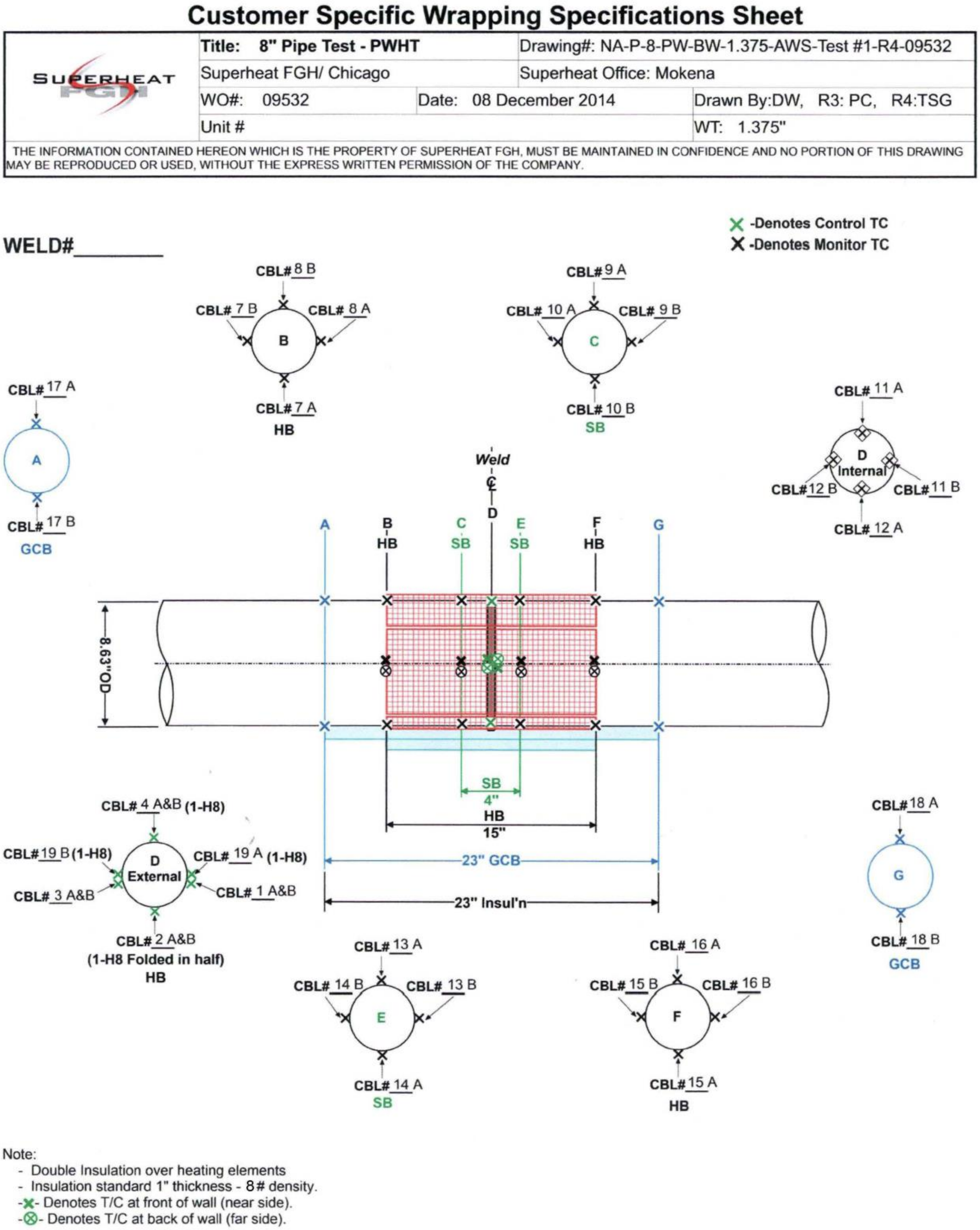

Figure A-5: Case 5

Case 5

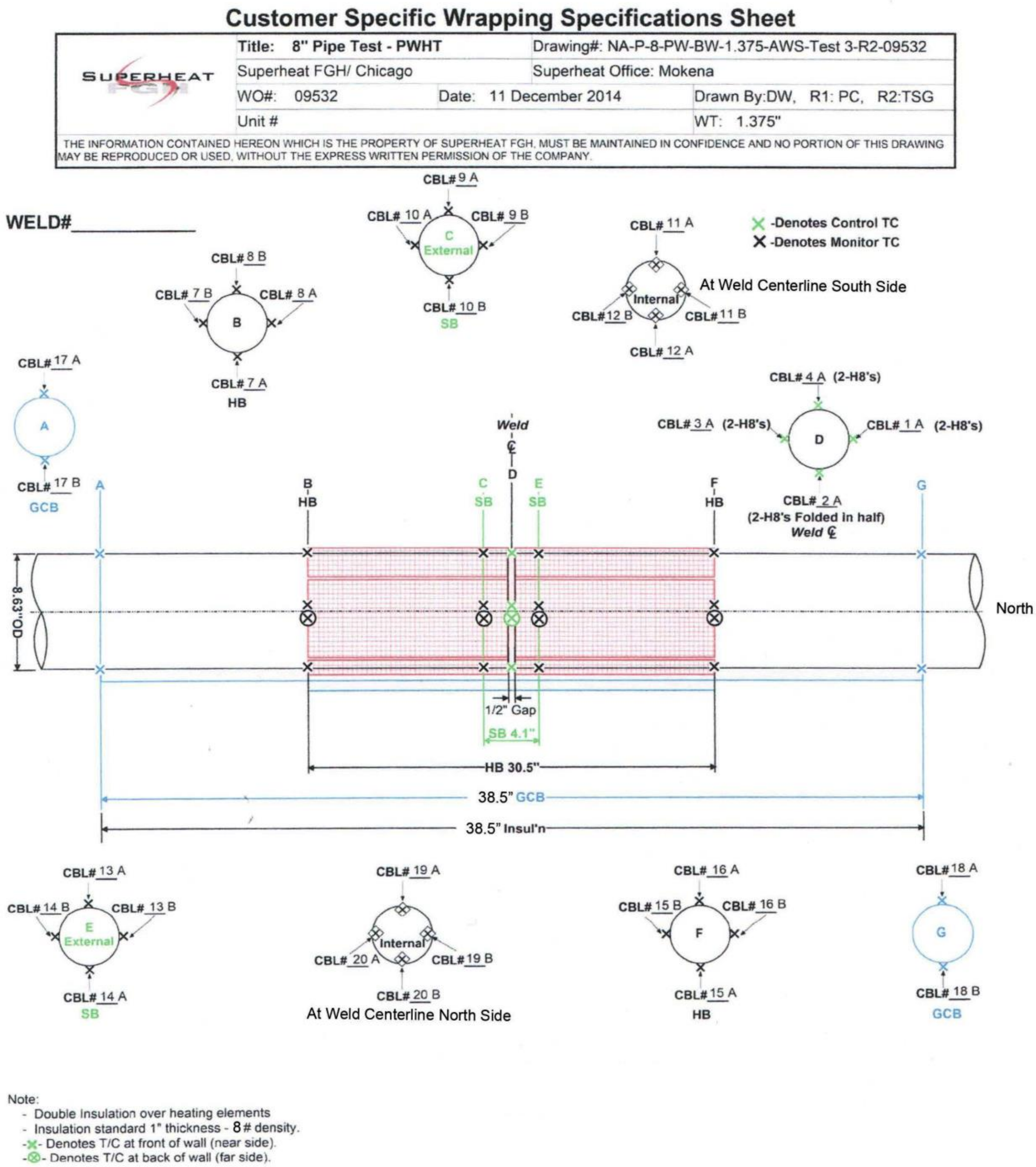

Figure A-6: Case 6

Case 6

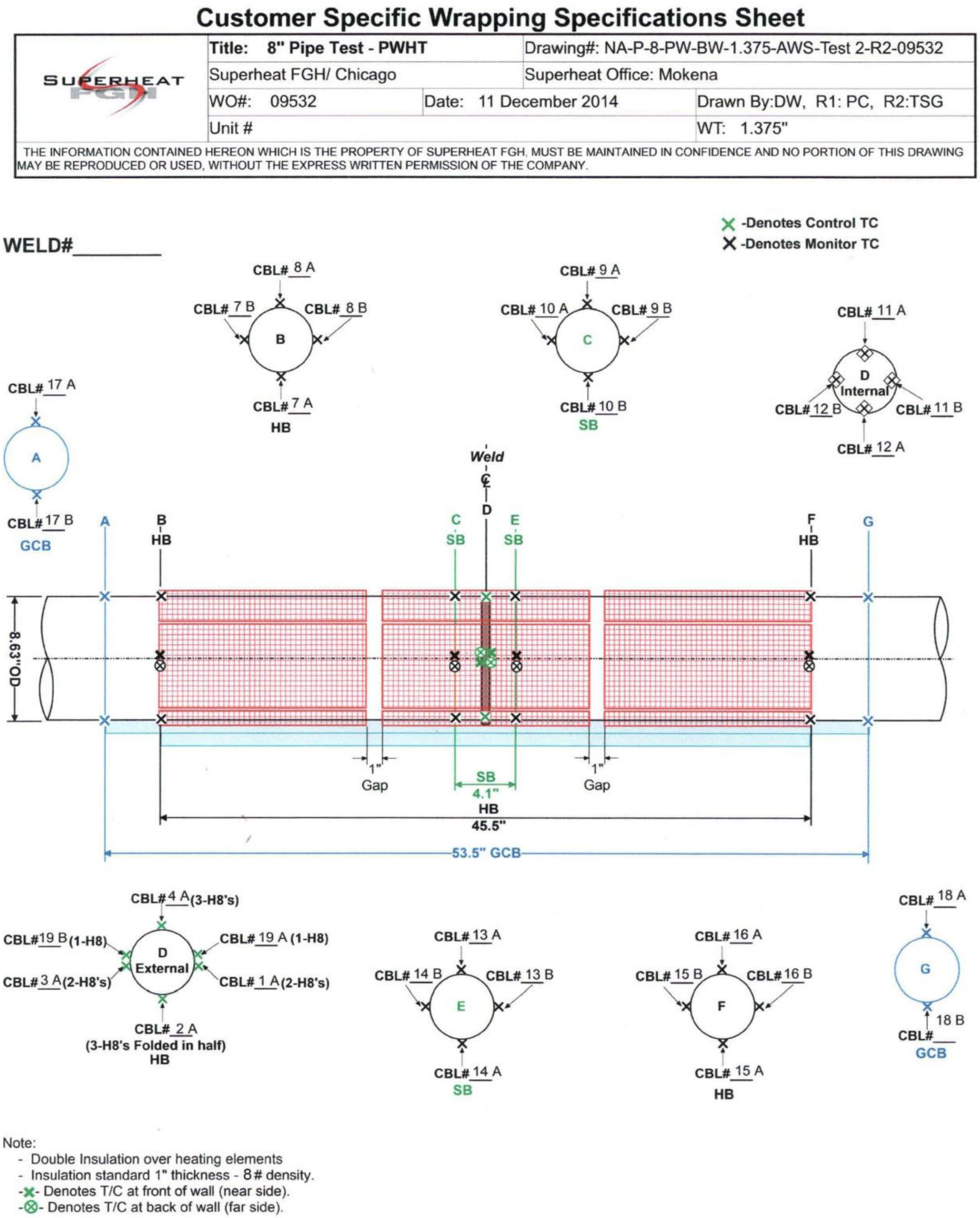

Figure A-7: Case 7

Case 7

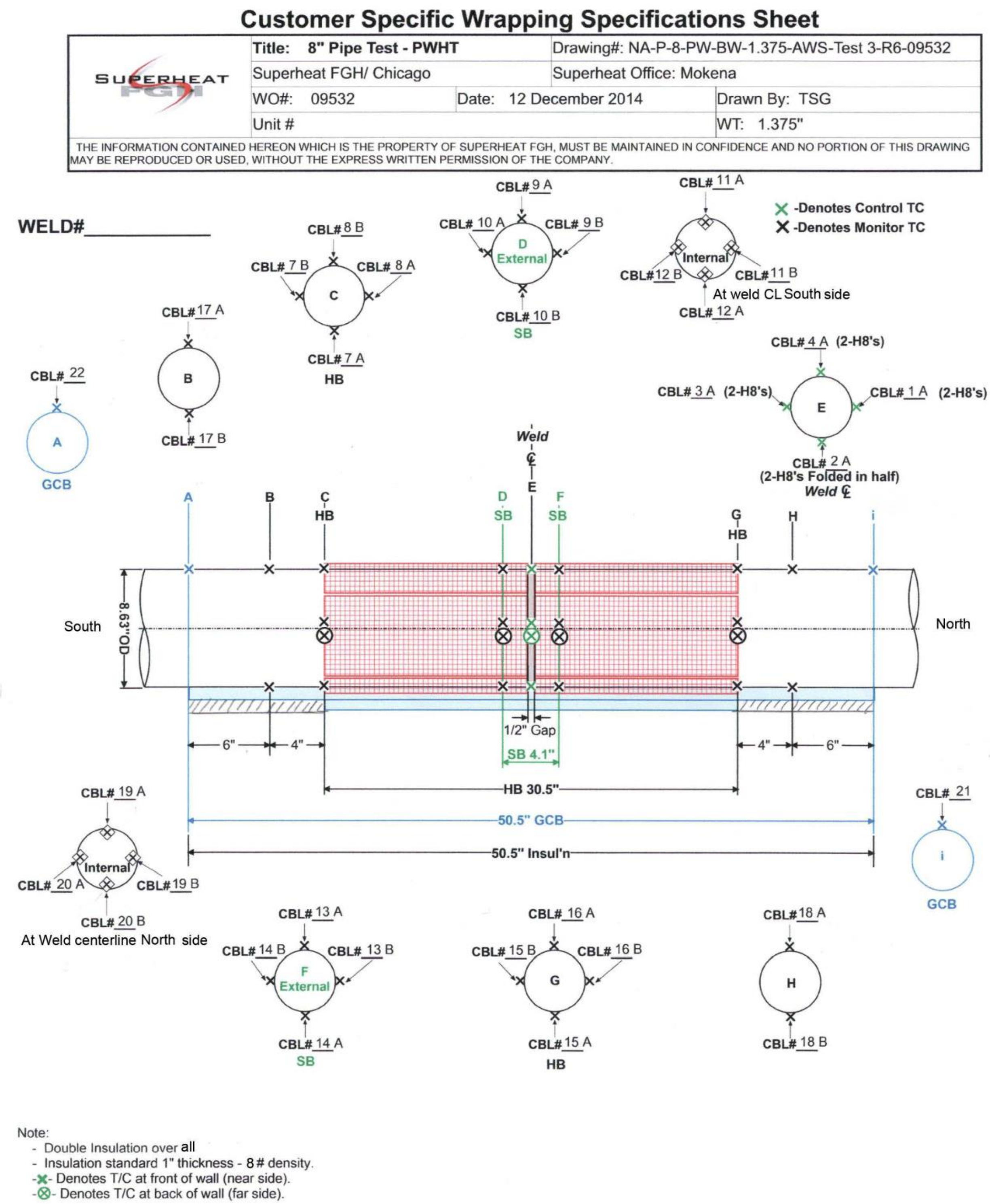

Appendix B: Prediction Cases Images

Figure B-1: Temperature contours, cross section of all regions (°F). 6 inch schedule 80

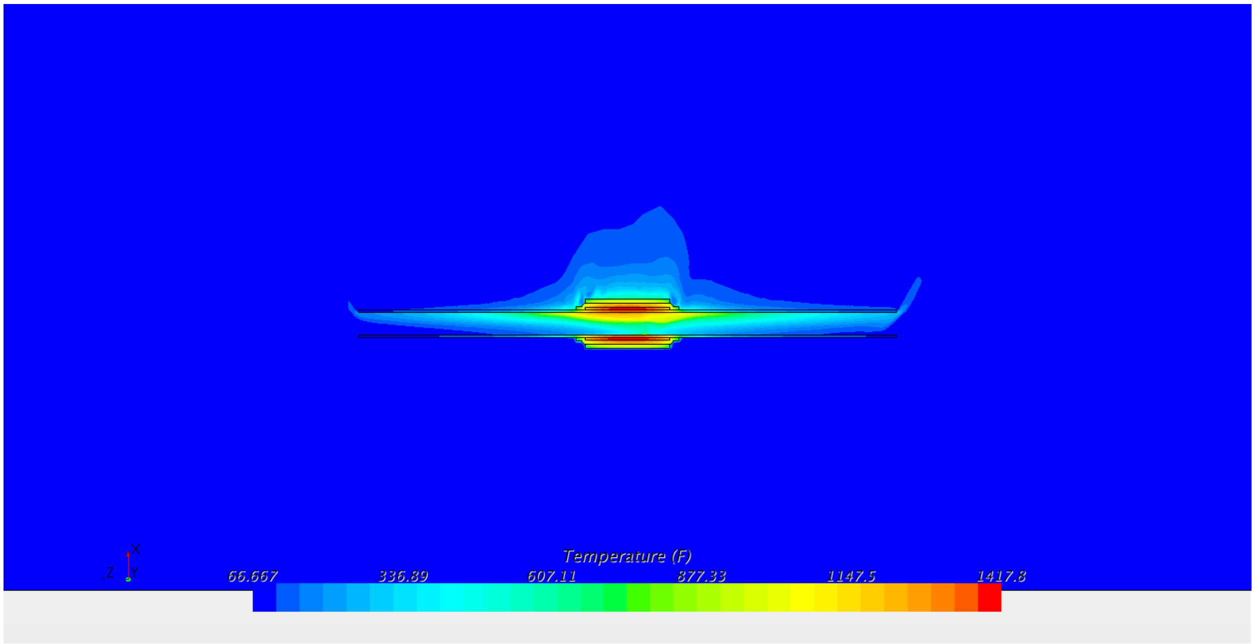

Figure B-2: Temperature contours, cross section of all regions, close-up (°F). 6 inch schedule 80

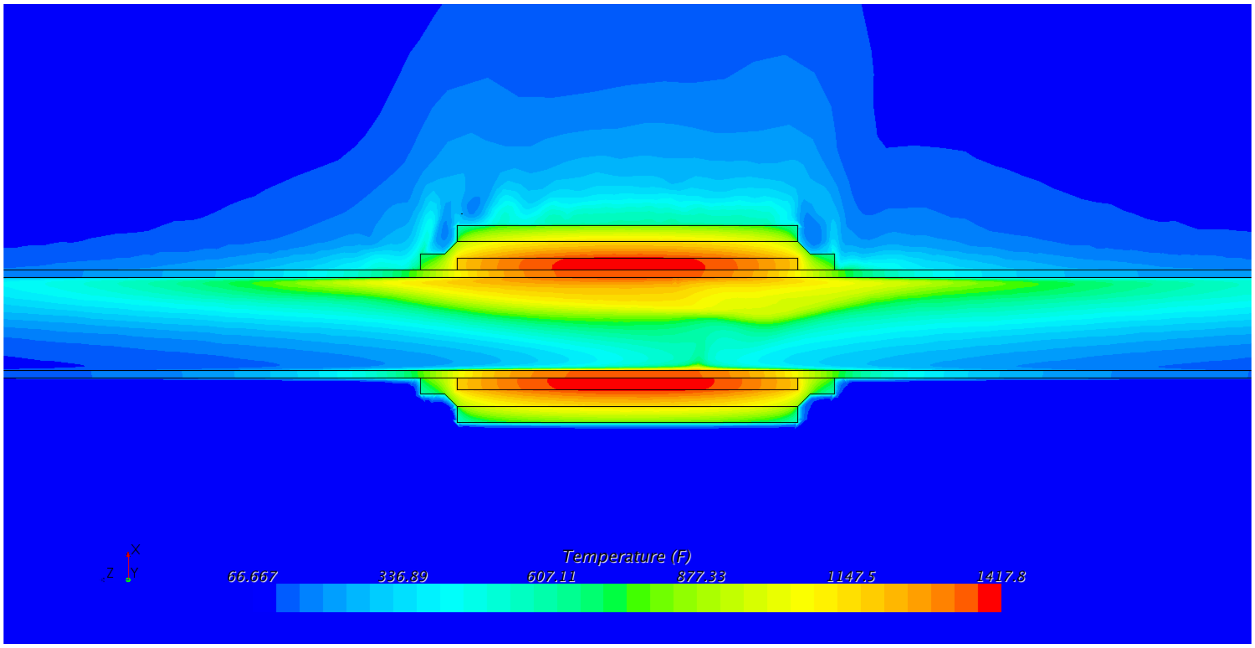

Figure B-3: Temperature contours in pipe wall (°F). 6 inch schedule 80

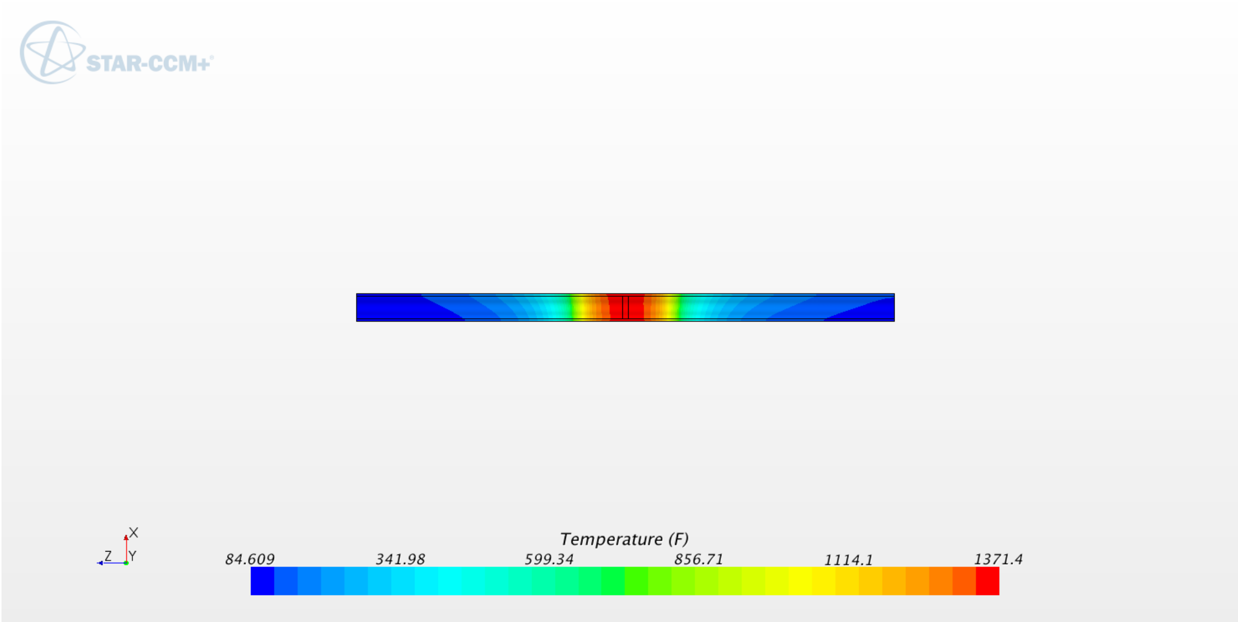

Figure B-4: Temperature contours in pipe wall, close-up (°F). 6 inch schedule 80

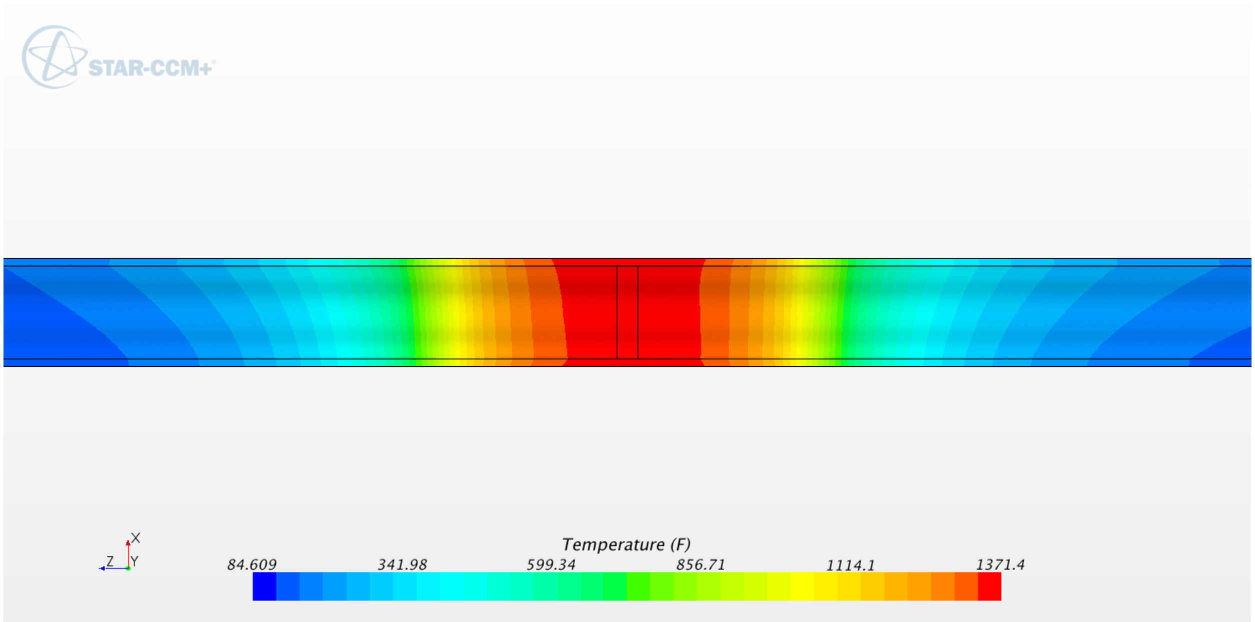

Figure B-5: Temperature contours in SB (°F). 6 inch schedule 80

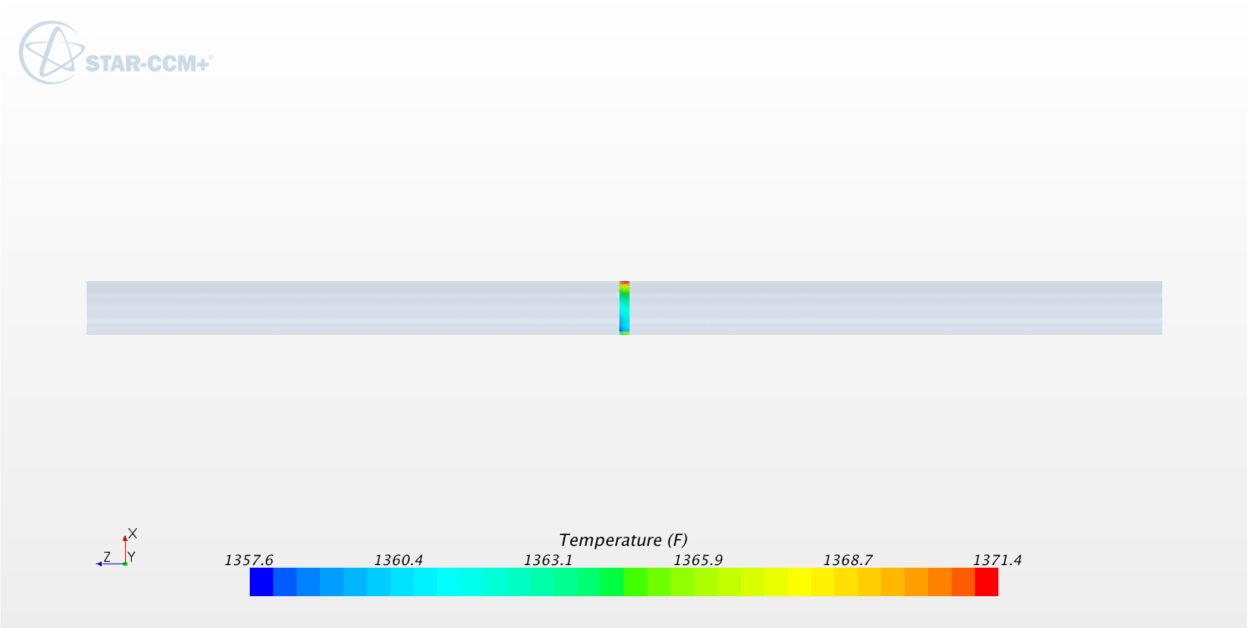

Figure B-6: Temperature contours in SB, isometric view (°F). 6 inch schedule 80

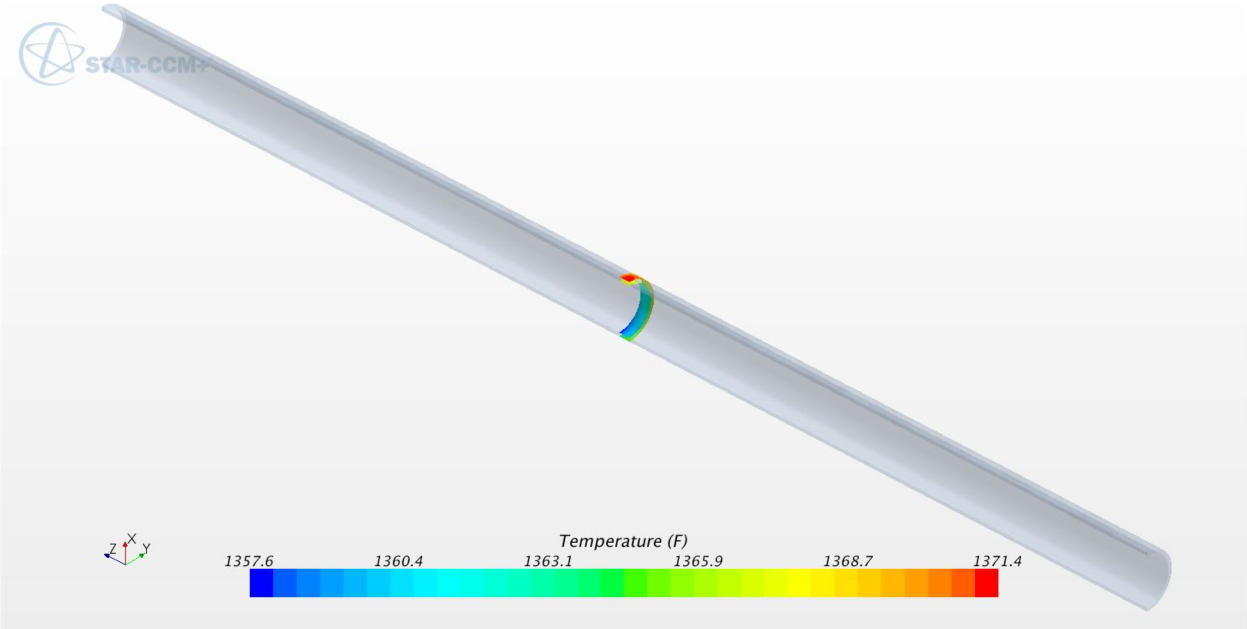

Figure B-7: Velocity contours, cross section of all regions (ft/s). 6 inch schedule 80

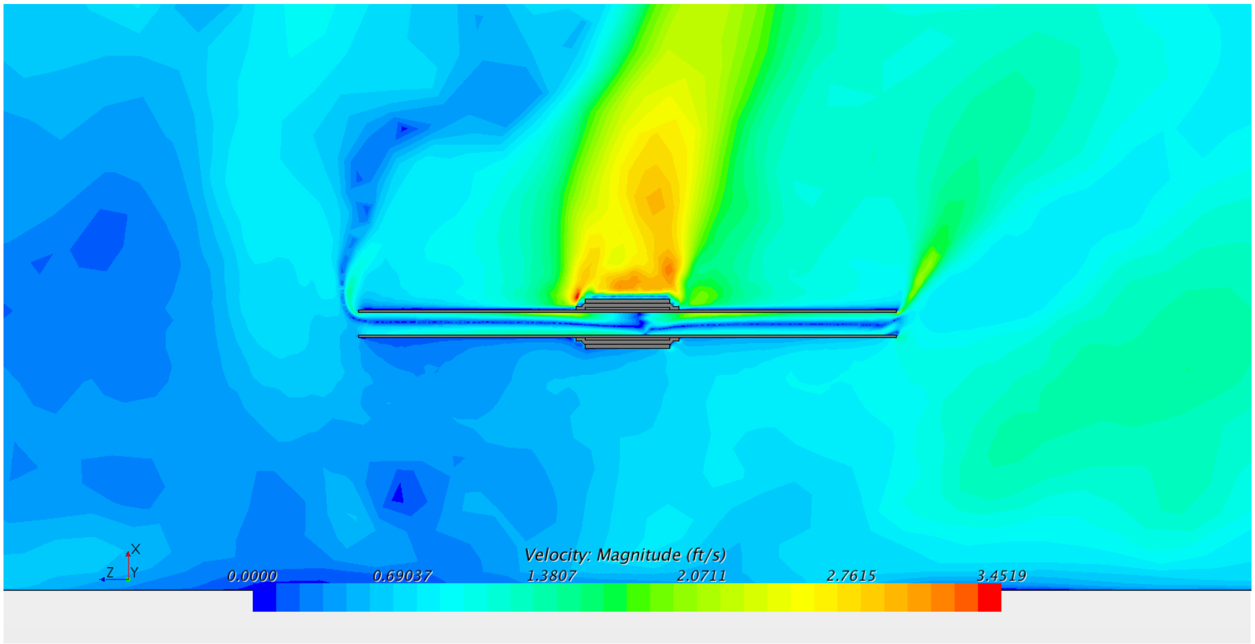

Figure B-8: Velocity contours, cross section of all regions, isometric view (ft/s). 6 inch schedule 80

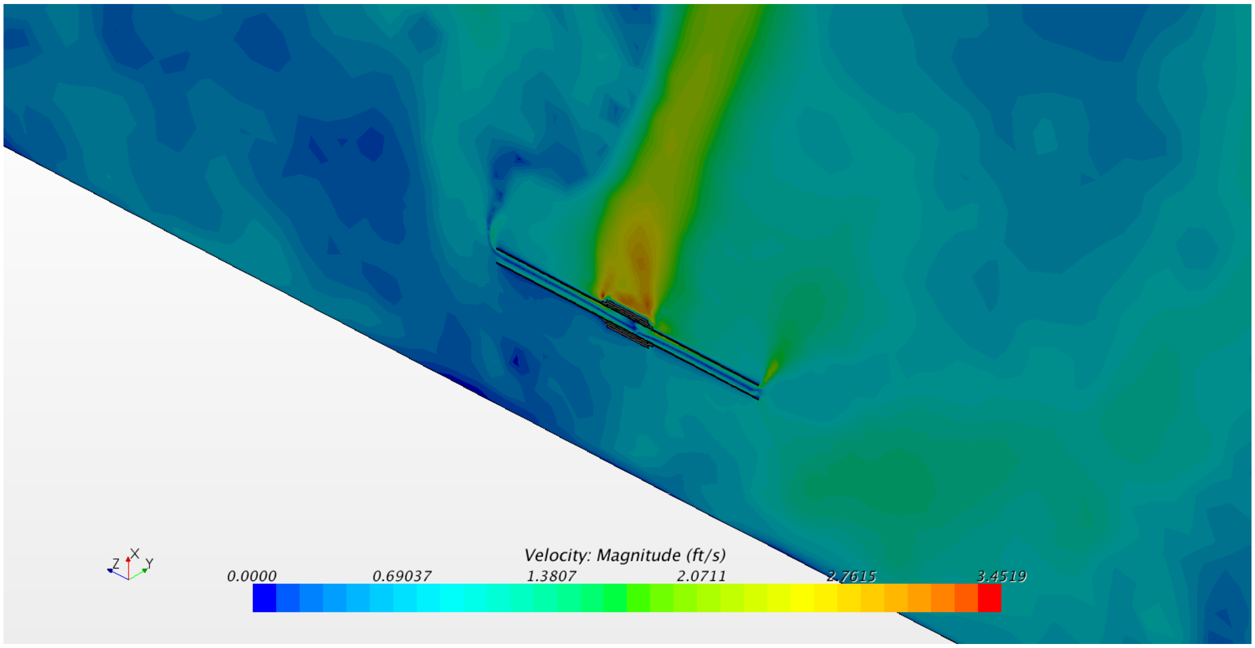

Figure B-9: Temperature contours, cross section of all regions (°F). 6 inch schedule 120

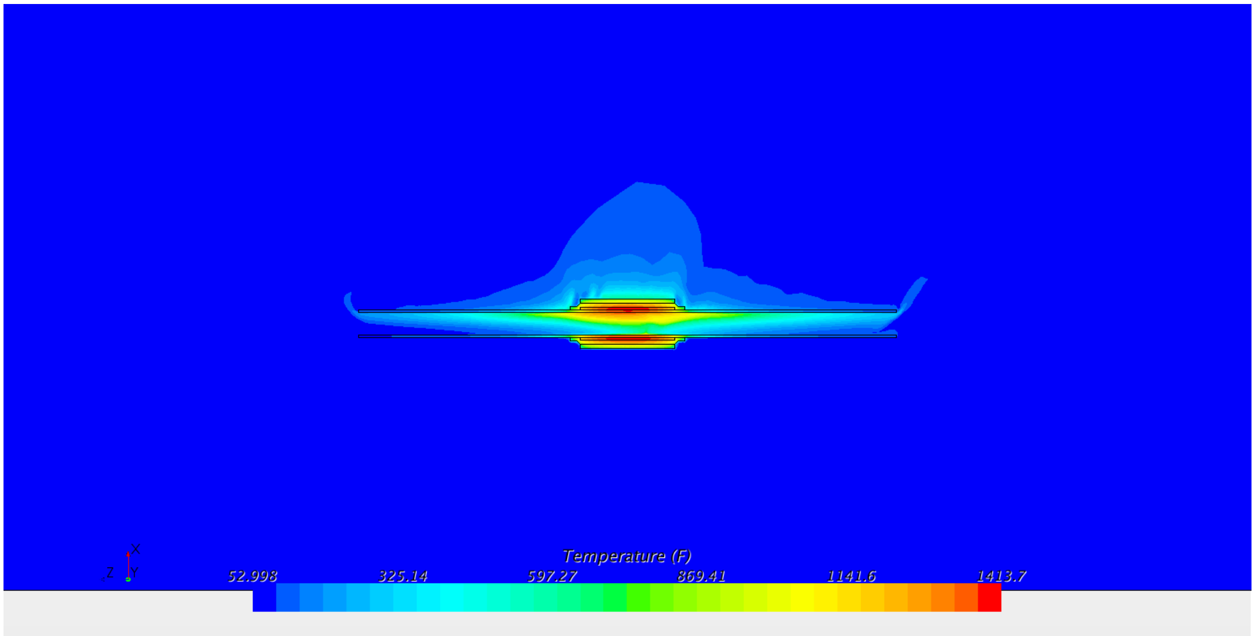

Figure B-10: Temperature contours, cross section of all regions, close-up (°F). 6 inch schedule 120

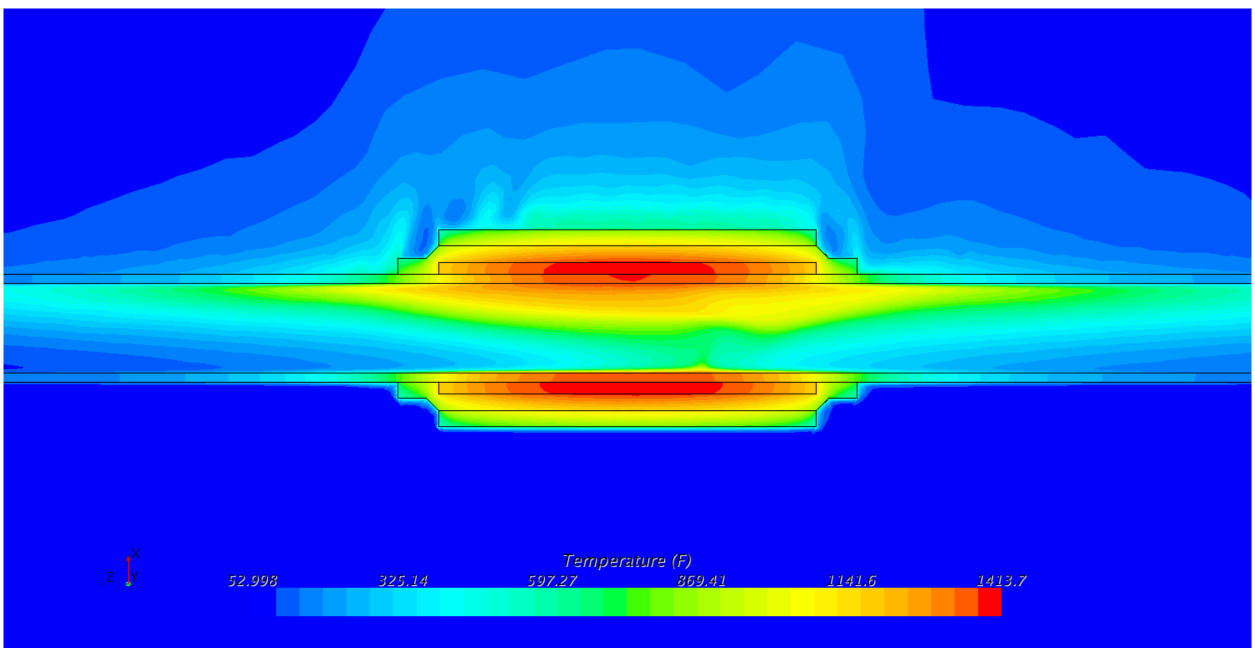

Figure B-11: Temperature contours in pipe wall (°F). 6 inch schedule 120

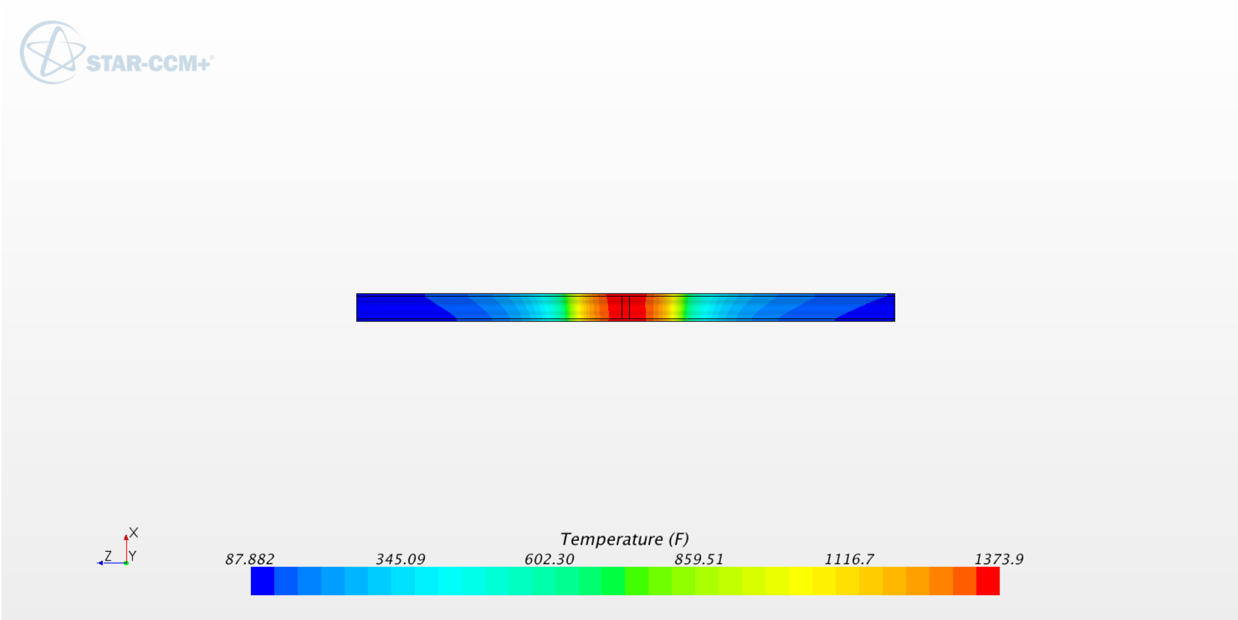

Figure B-12: Temperature contours in pipe wall, close-up (°F). 6 inch schedule 120

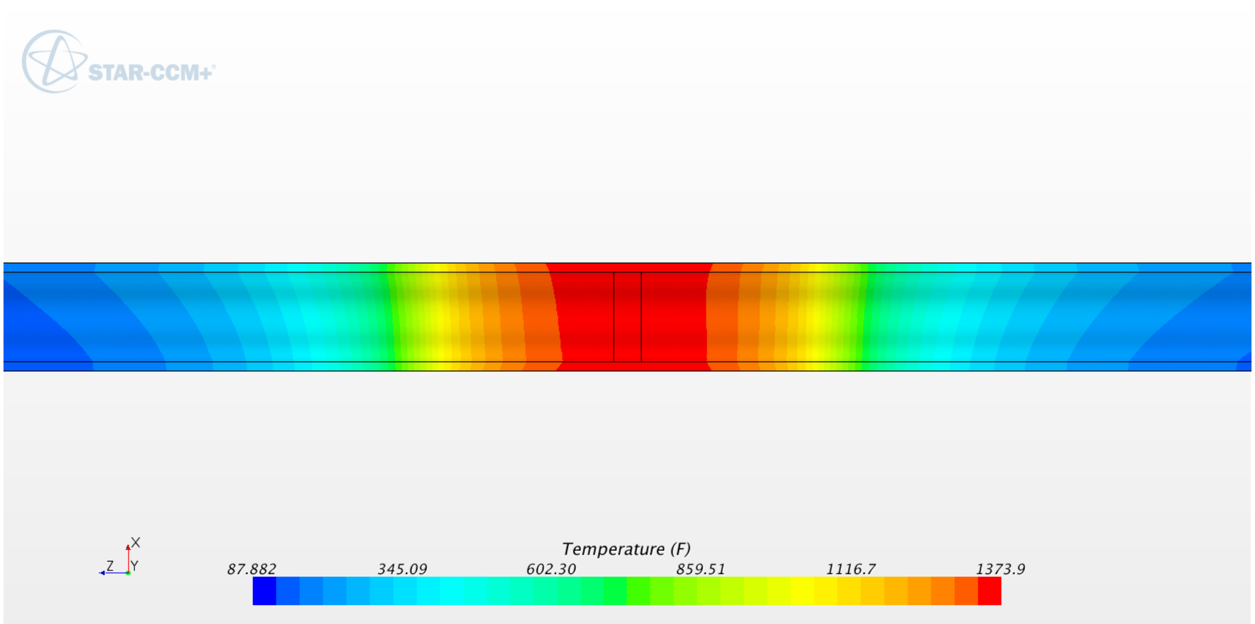

Figure B-13: Temperature contours in SB (°F). 6 inch schedule 120

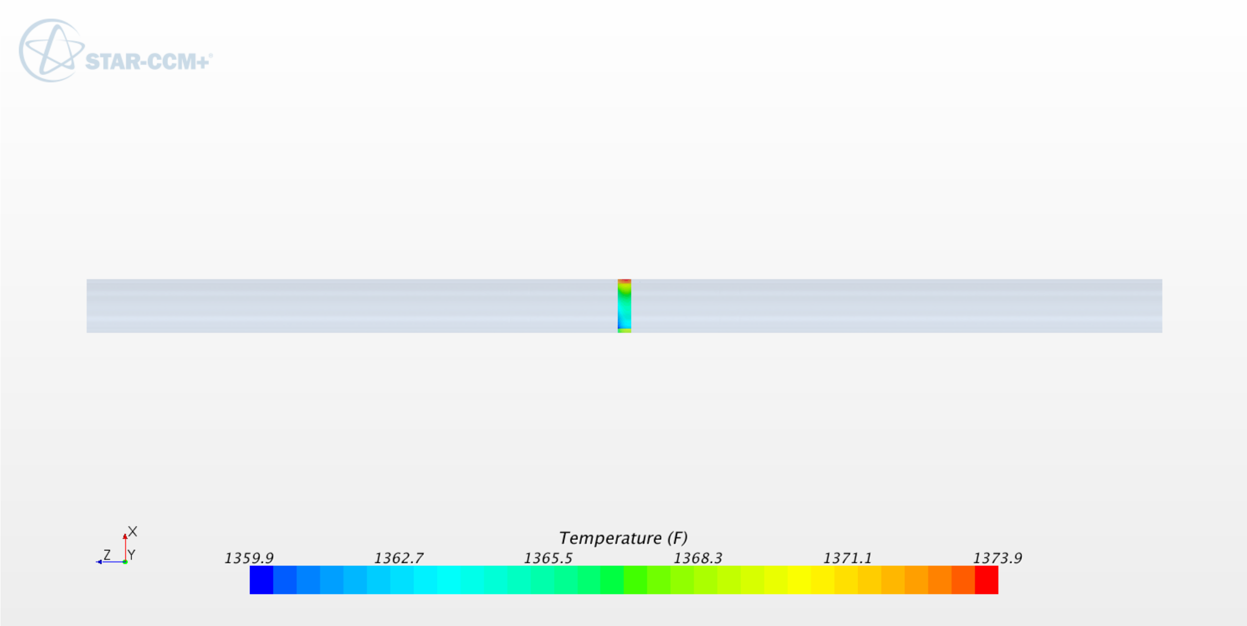

Figure B-14: Temperature contours in SB, isometric view (°F). 6 inch schedule 120

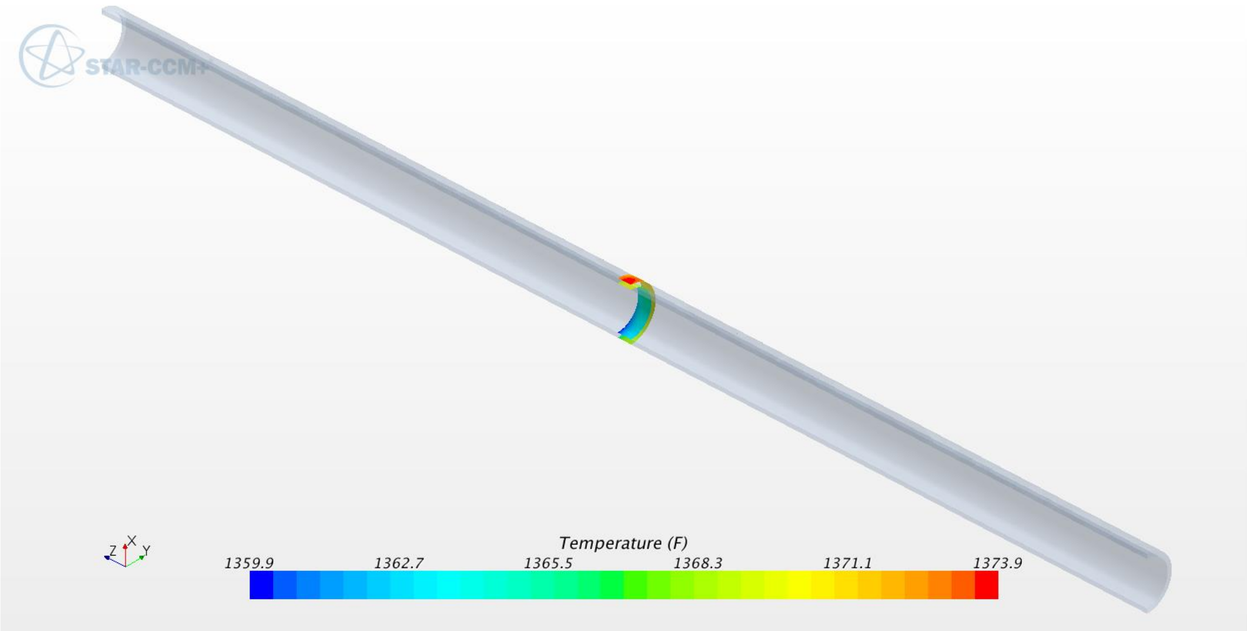

Figure B-15: Velocity contours, cross section of all regions (ft/s). 6 inch schedule 120

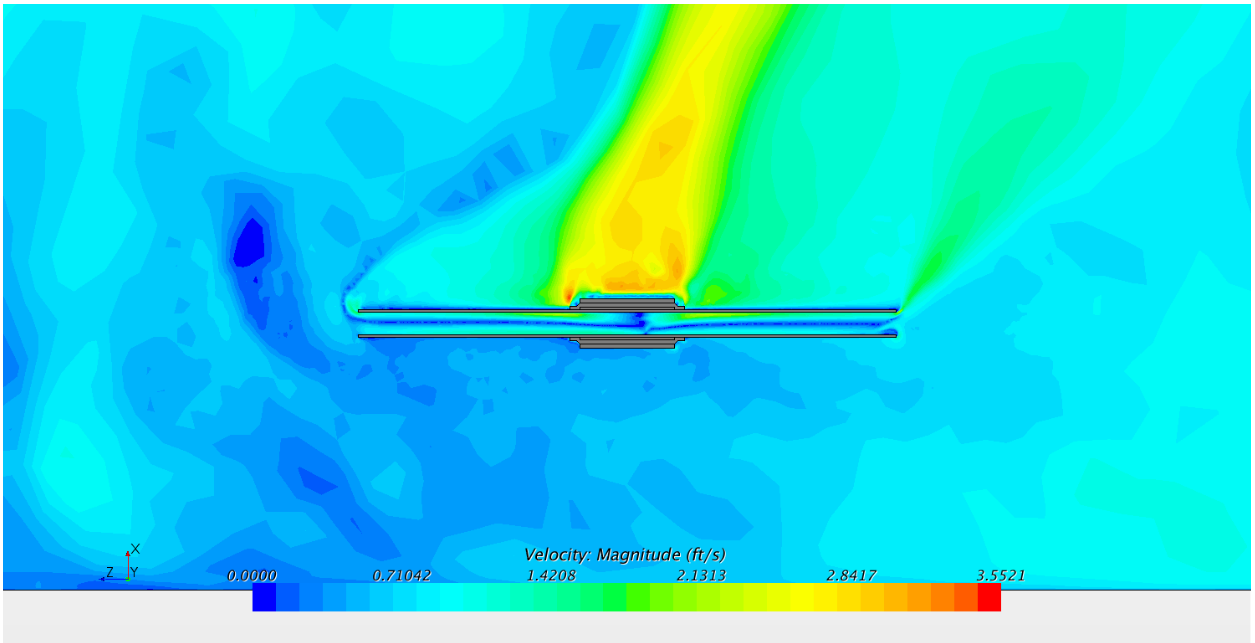

Figure B-16: Velocity contours, cross section of all regions, isometric view (ft/s). 6 inch schedule 120

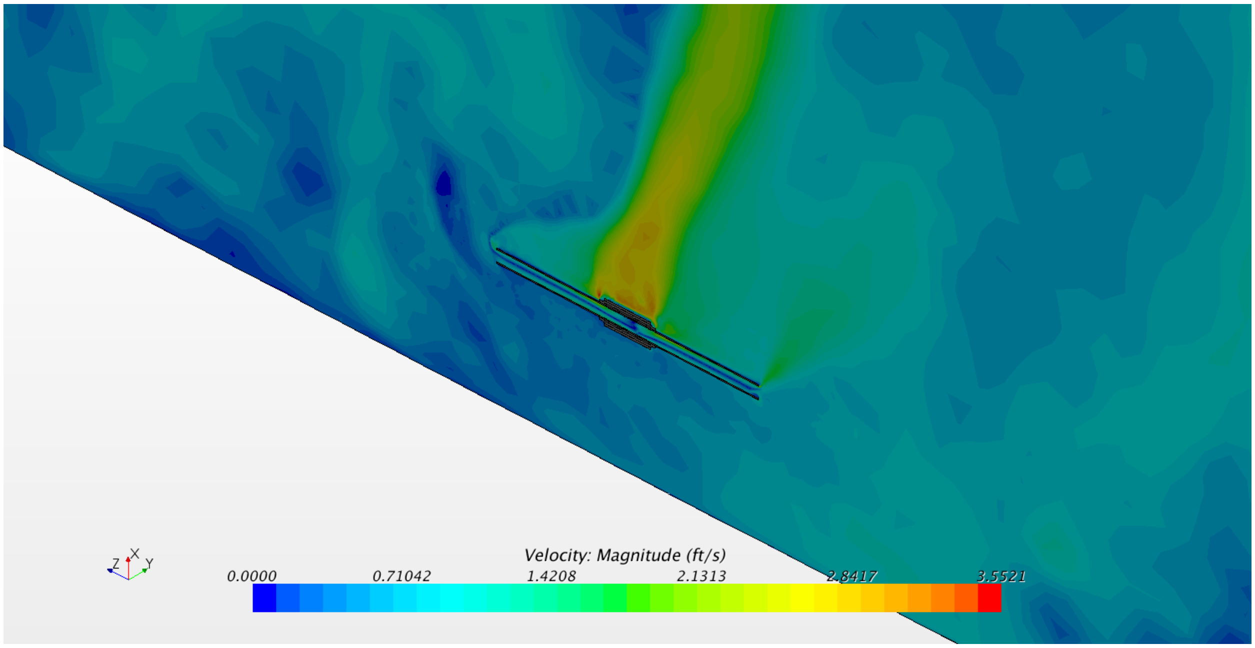

Figure B-17: Temperature contours, cross section of all regions (°F). 6 inch schedule 160

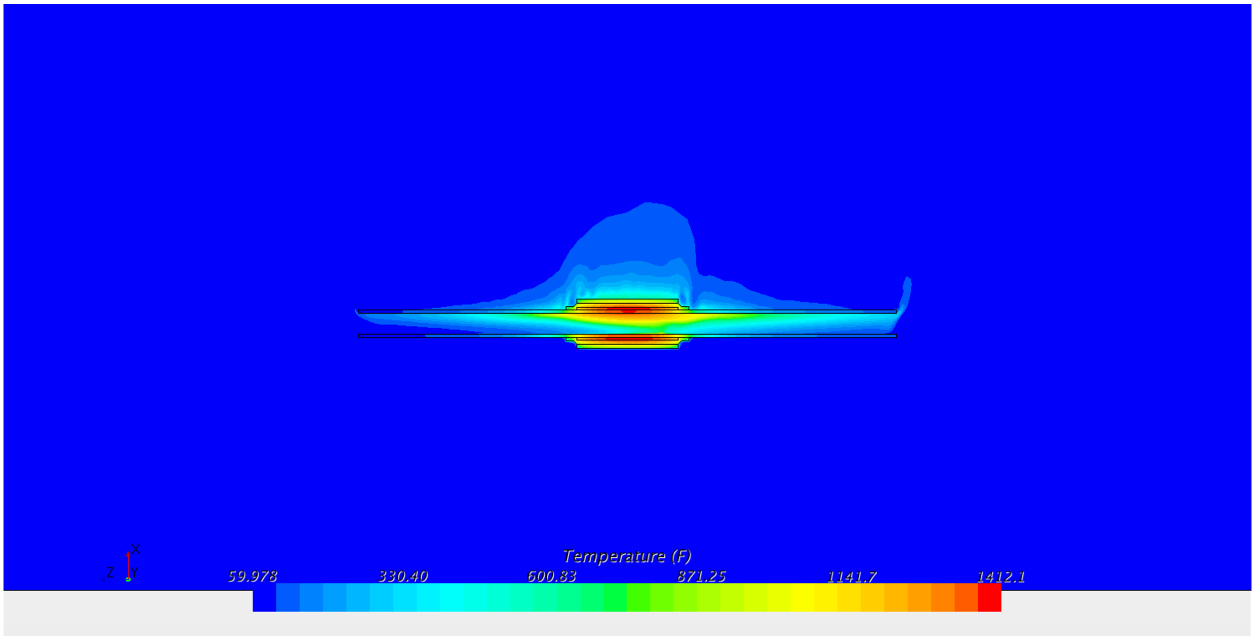

Figure B-18: Temperature contours, cross section of all regions, close-up (°F). 6 inch schedule 160

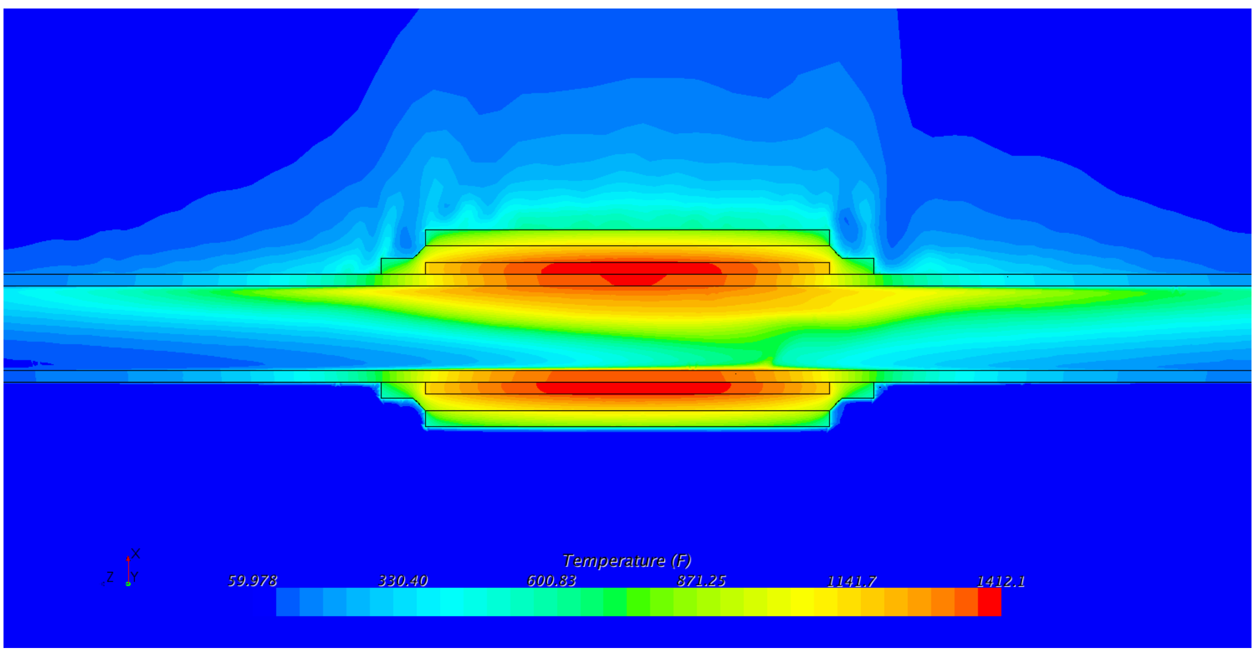

Figure B-19: Temperature contours in pipe wall (°F). 6 inch schedule 160

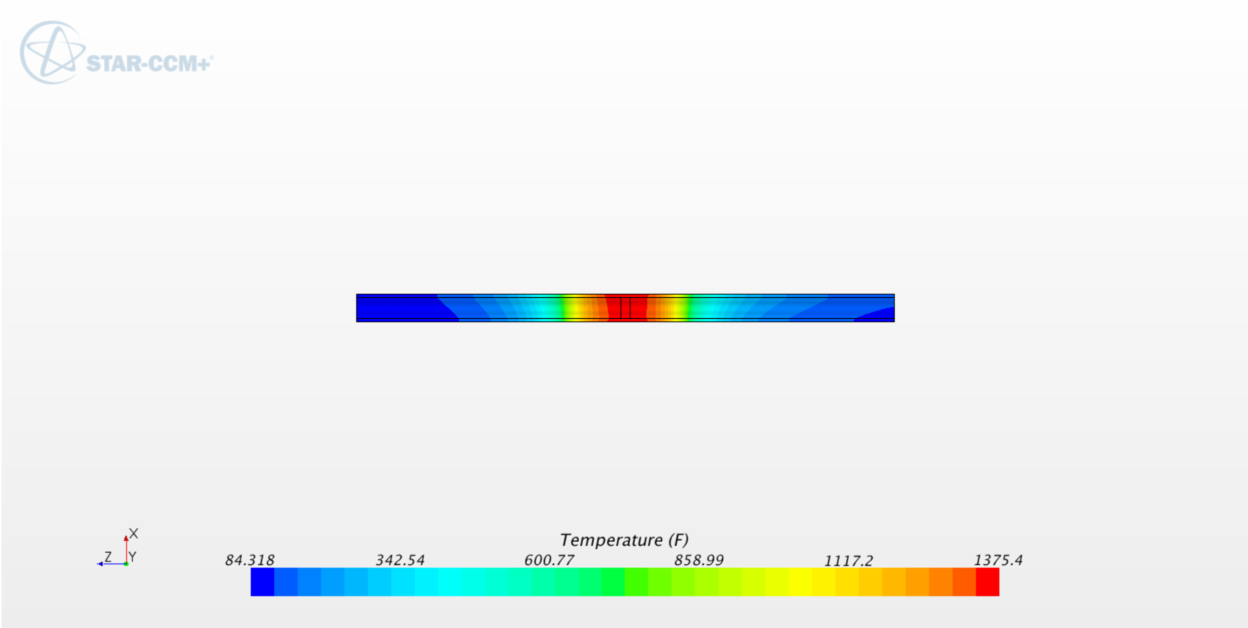

Figure B-20: Temperature contours in pipe wall, close-up (°F). 6 inch schedule 160

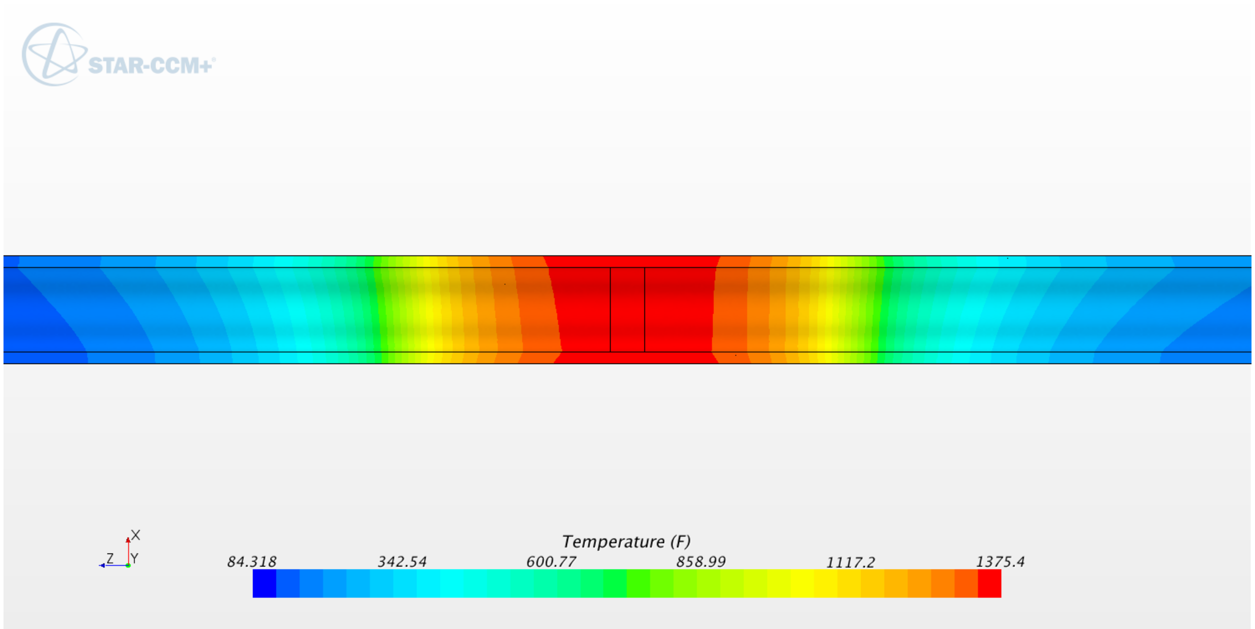

Figure B-21: Temperature contours in SB (°F). 6 inch schedule 160

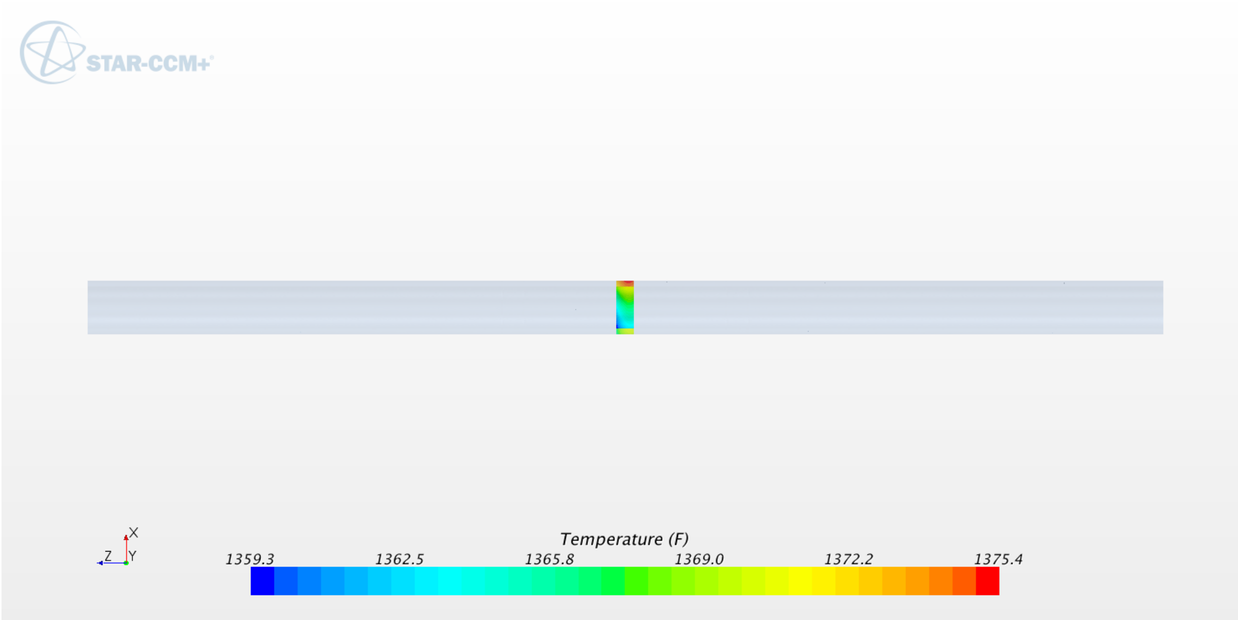

Figure B-22: Temperature contours in SB, isometric view (°F). 6 inch schedule 160

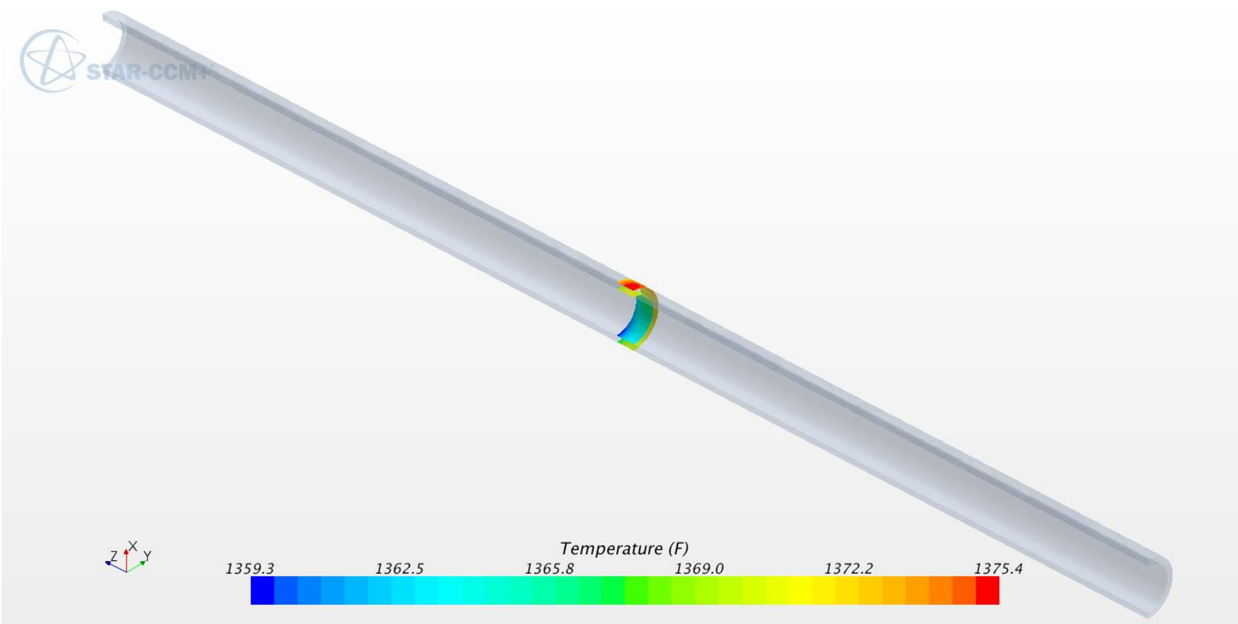

Figure B-23: Velocity contours, cross section of all regions (ft/s). 6 inch schedule 160

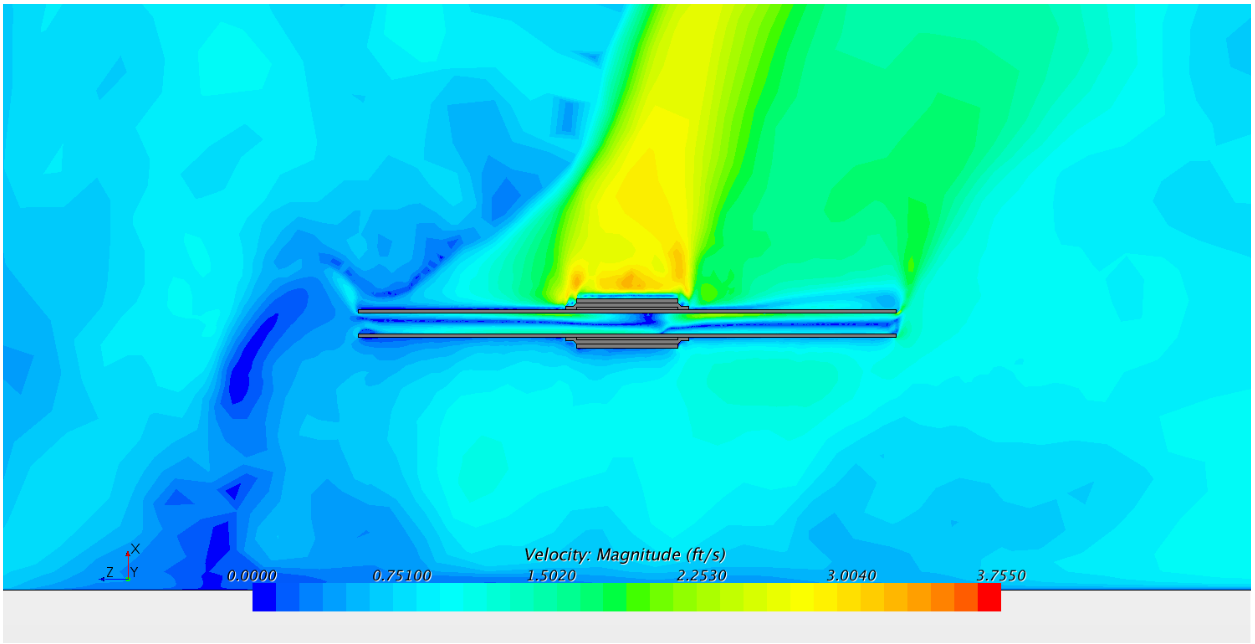

Figure B-24: Velocity contours, cross section of all regions, isometric view (ft/s). 6 inch schedule 160

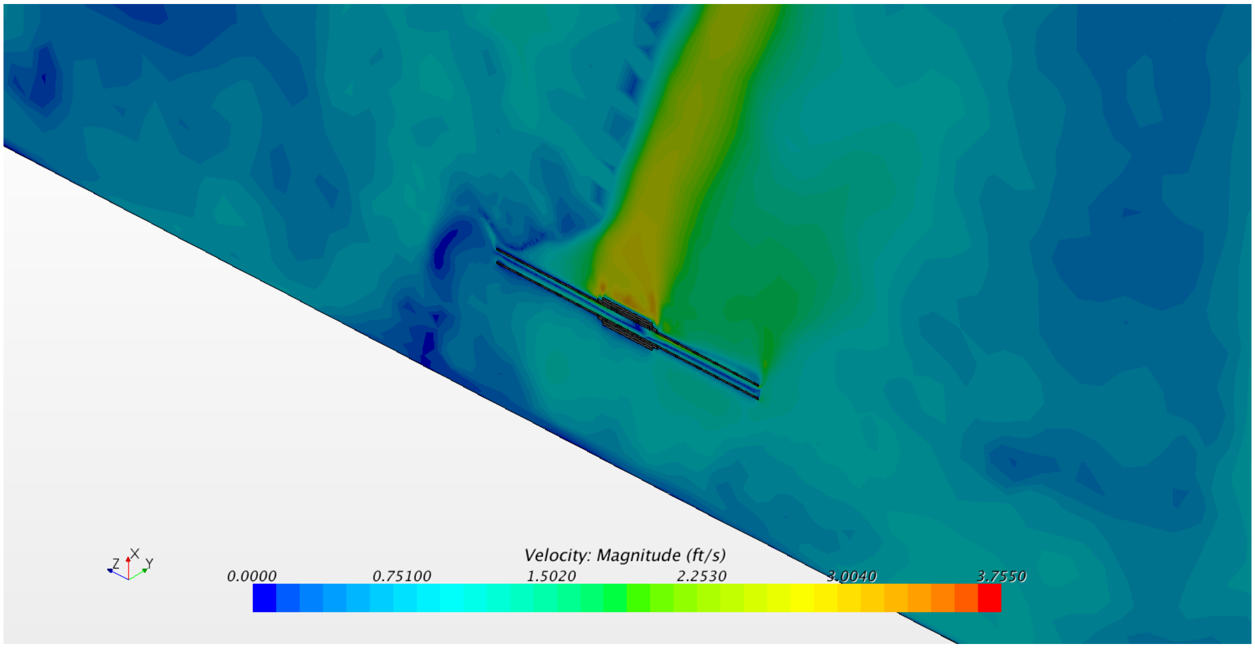

Figure B-25: Temperature contours, cross section of all regions (°F). 10 inch schedule 80

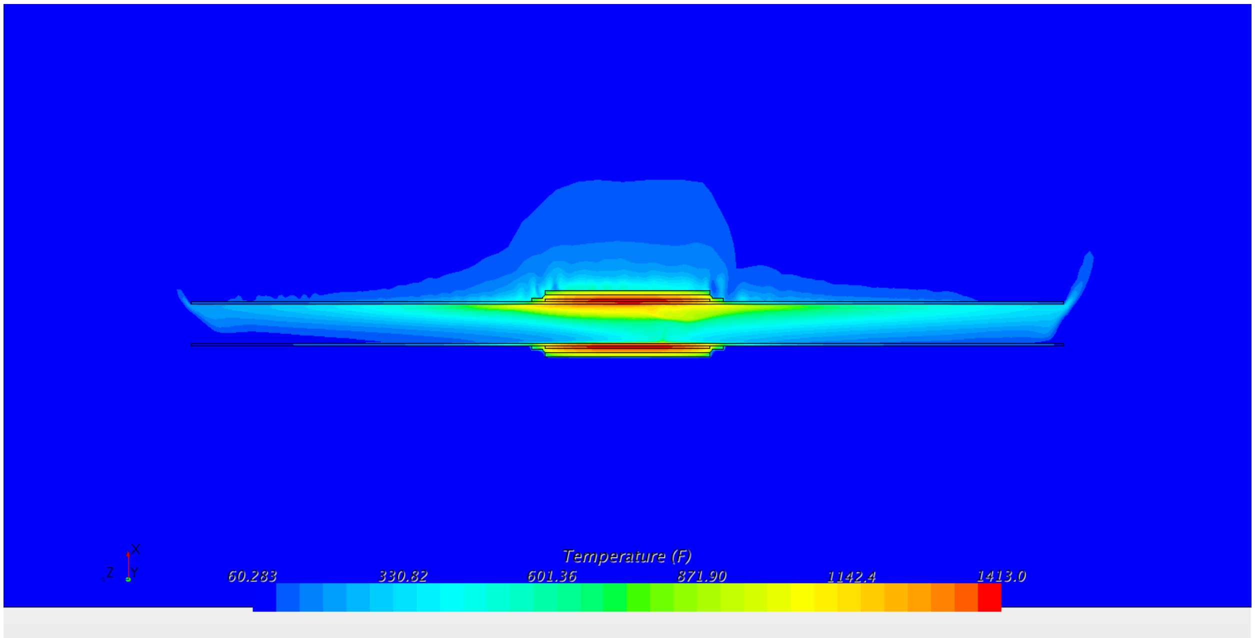

Figure B-26: Temperature contours, cross section of all regions, close-up (°F). 10 inch schedule 80

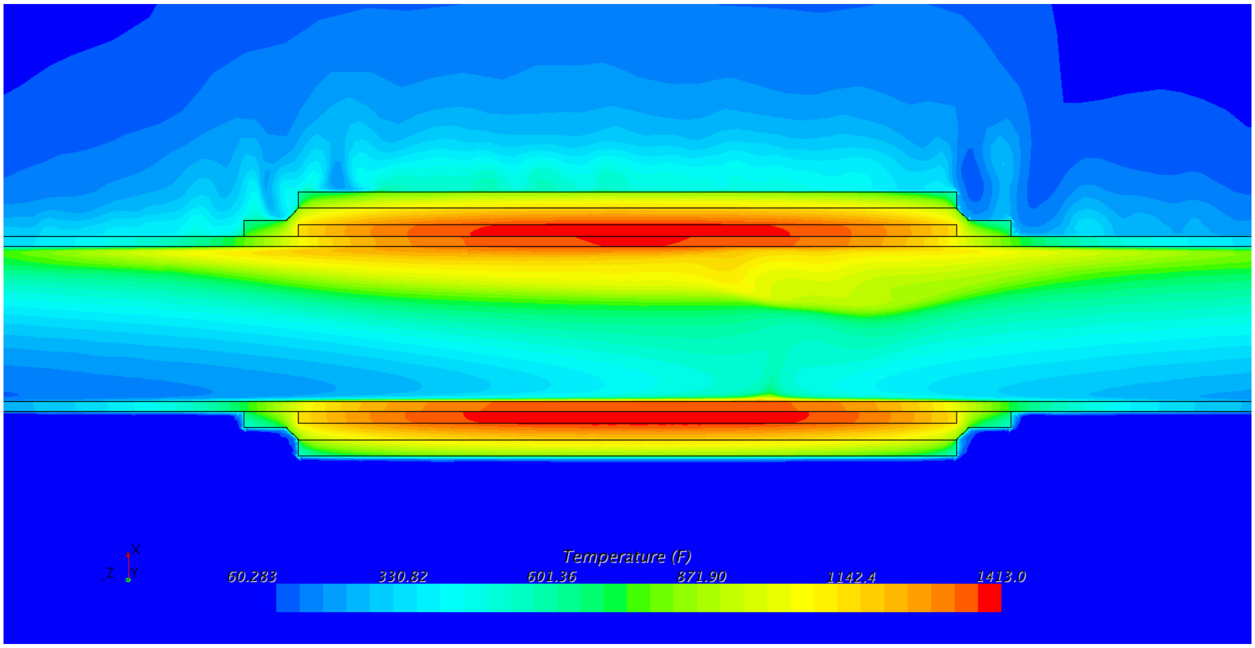

Figure B-27: Temperature contours in pipe wall (°F). 10 inch schedule 80

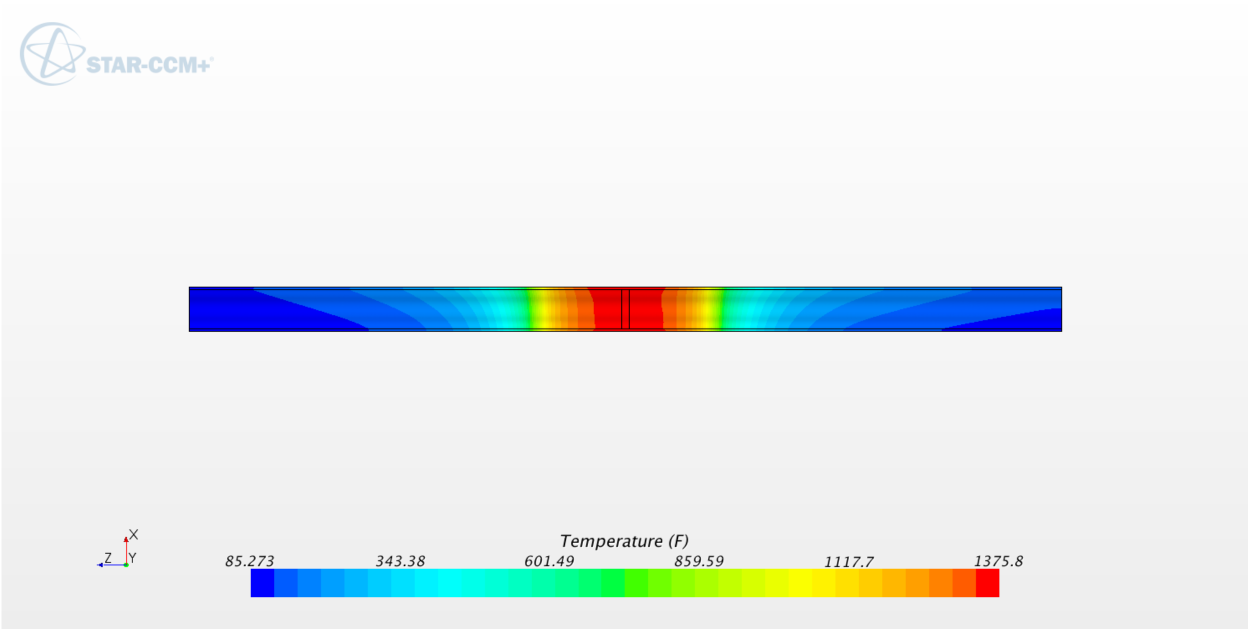

Figure B-28: Temperature contours in pipe wall, close-up (°F). 10 inch schedule 80

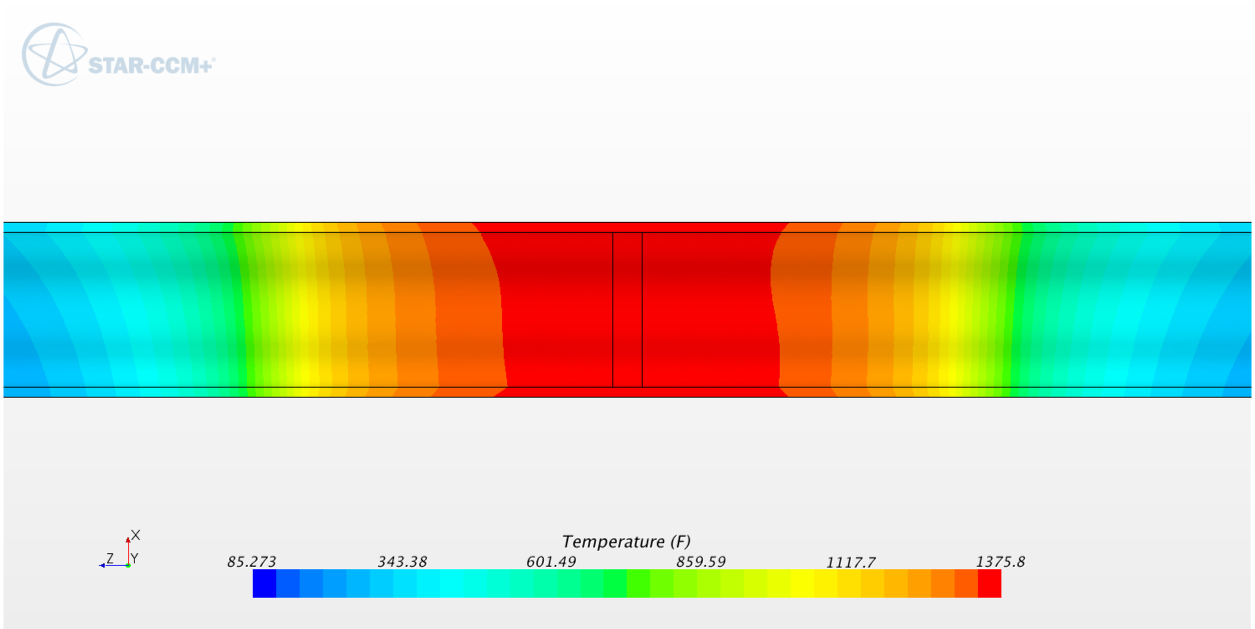

Figure B-29: Temperature contours in SB (°F). 10 inch schedule 80

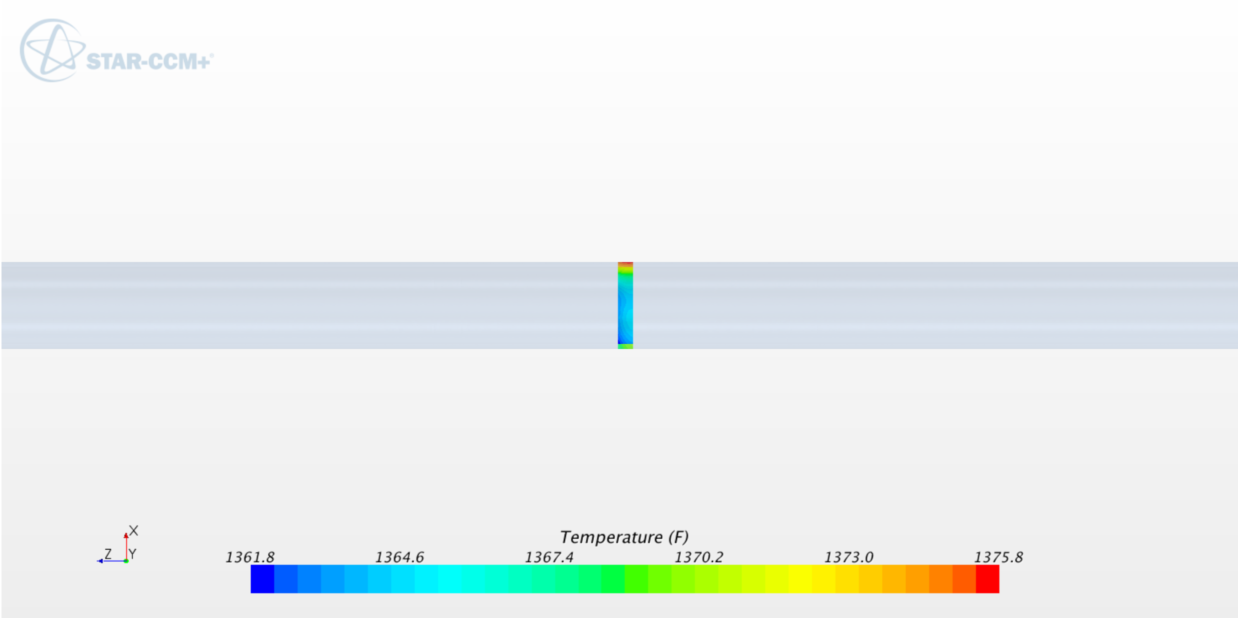

Figure B-30: Temperature contours in SB, isometric view (°F). 10 inch schedule 80

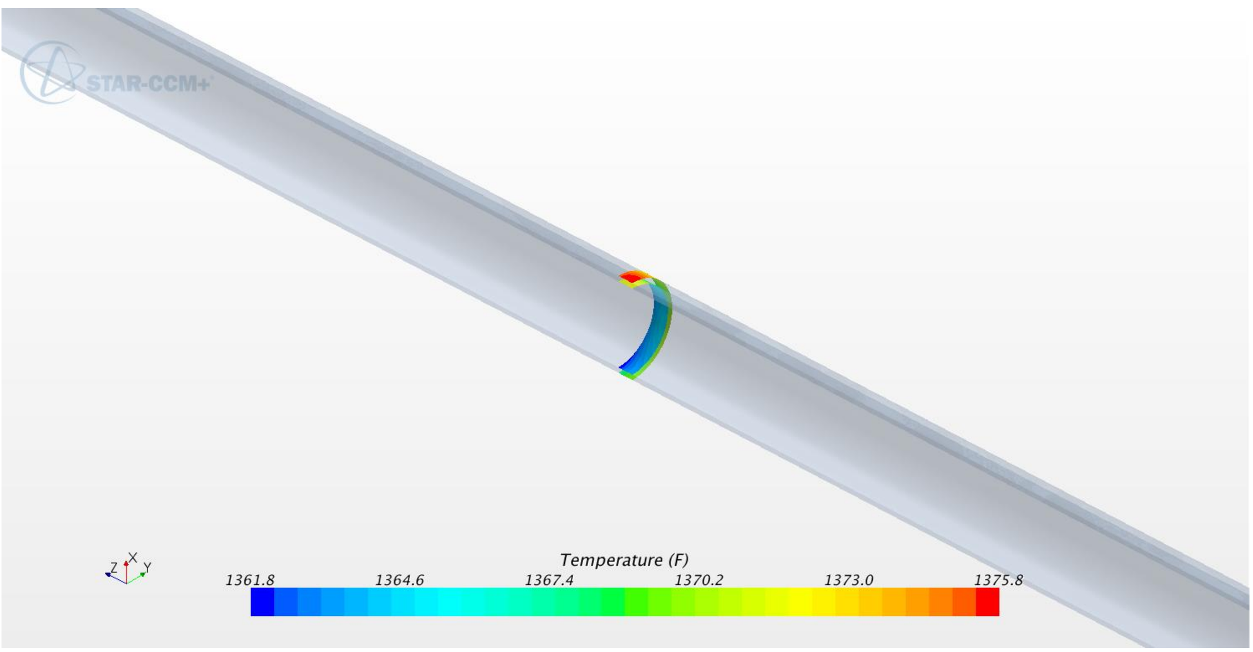

Figure B-31: Velocity contours, cross section of all regions (ft/s). 10 inch schedule 80

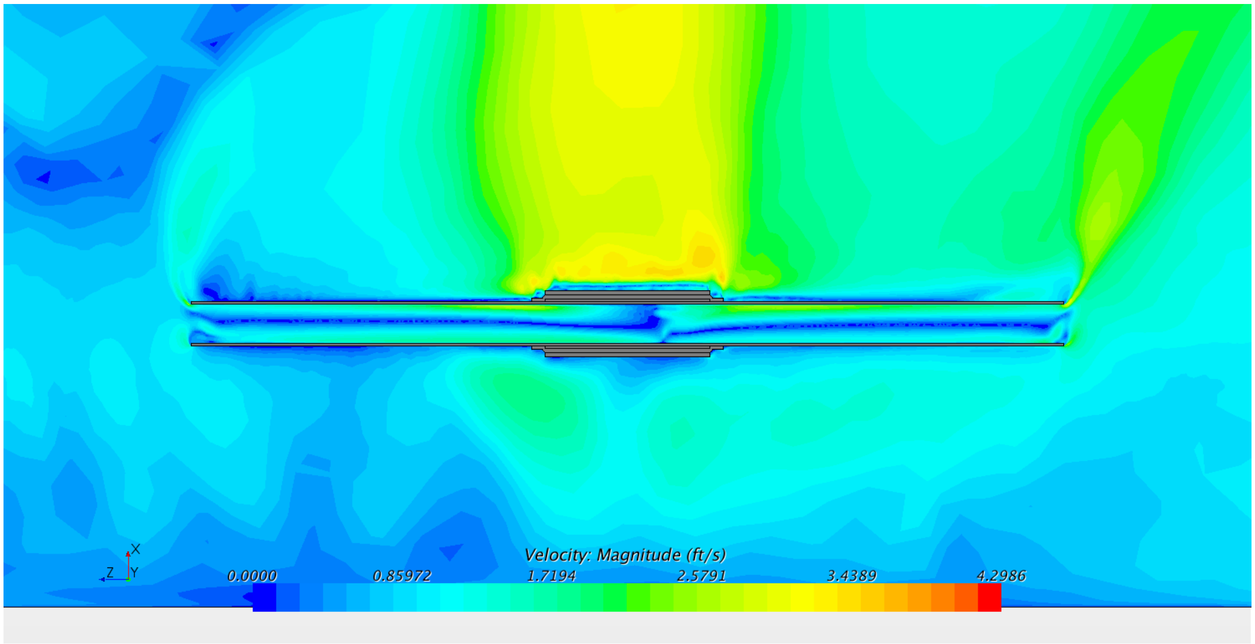

Figure B-32: Velocity contours, cross section of all regions, isometric view (ft/s). 10 inch schedule 80

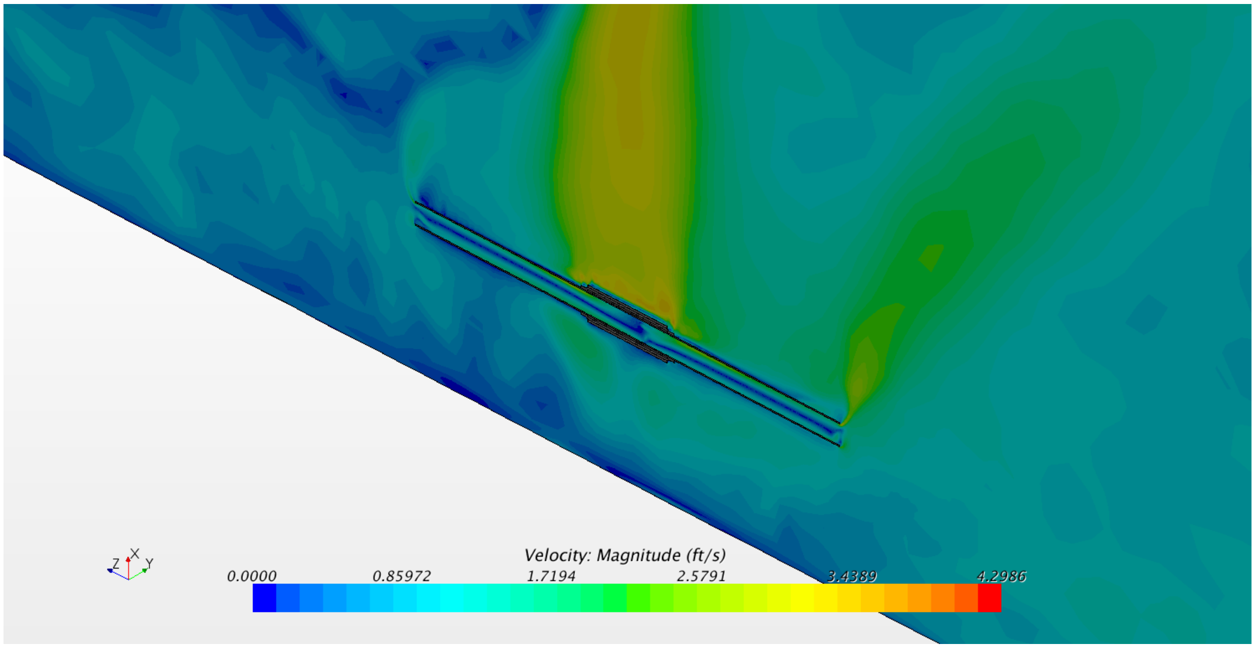

Figure B-33: Temperature contours, cross section of all regions (°F). 10 inch schedule 120

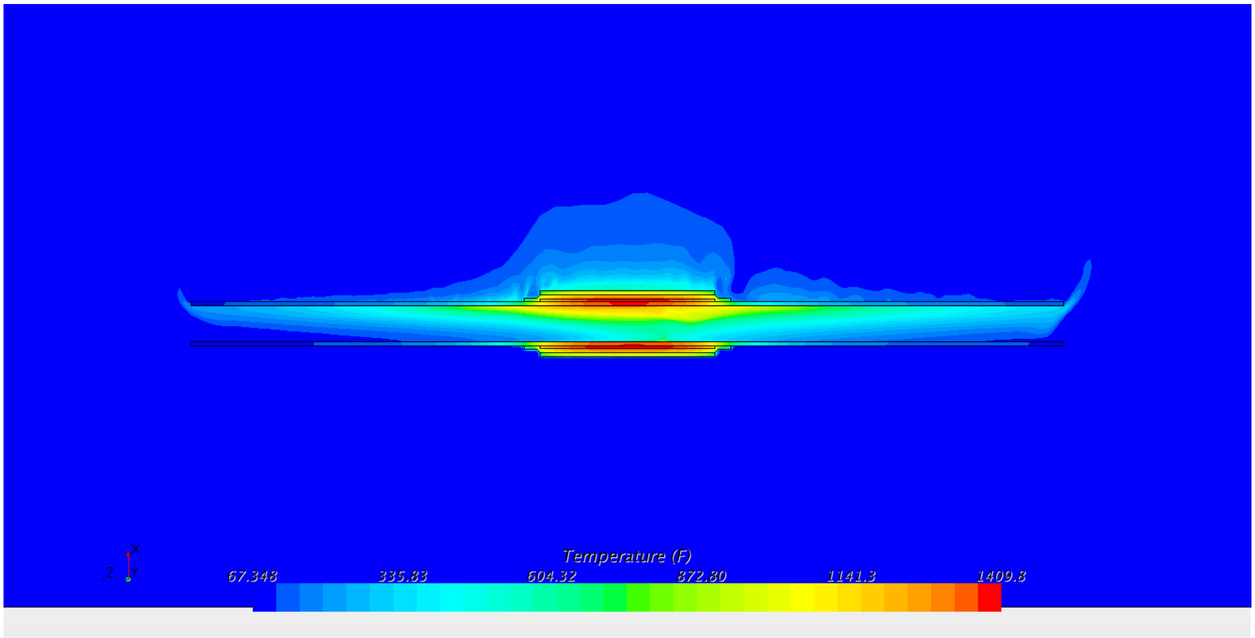

Figure B-34: Temperature contours, cross section of all regions, close-up (°F). 10 inch schedule 120

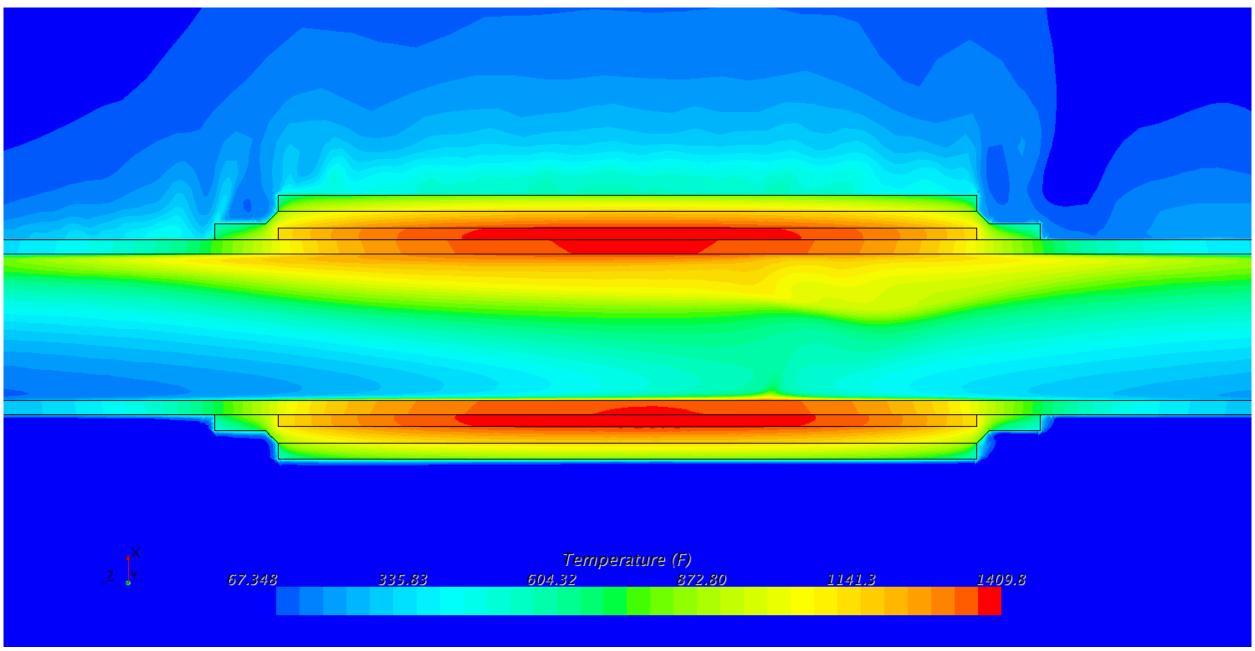

Figure B-35: Temperature contours in pipe wall (°F). 10 inch schedule 120

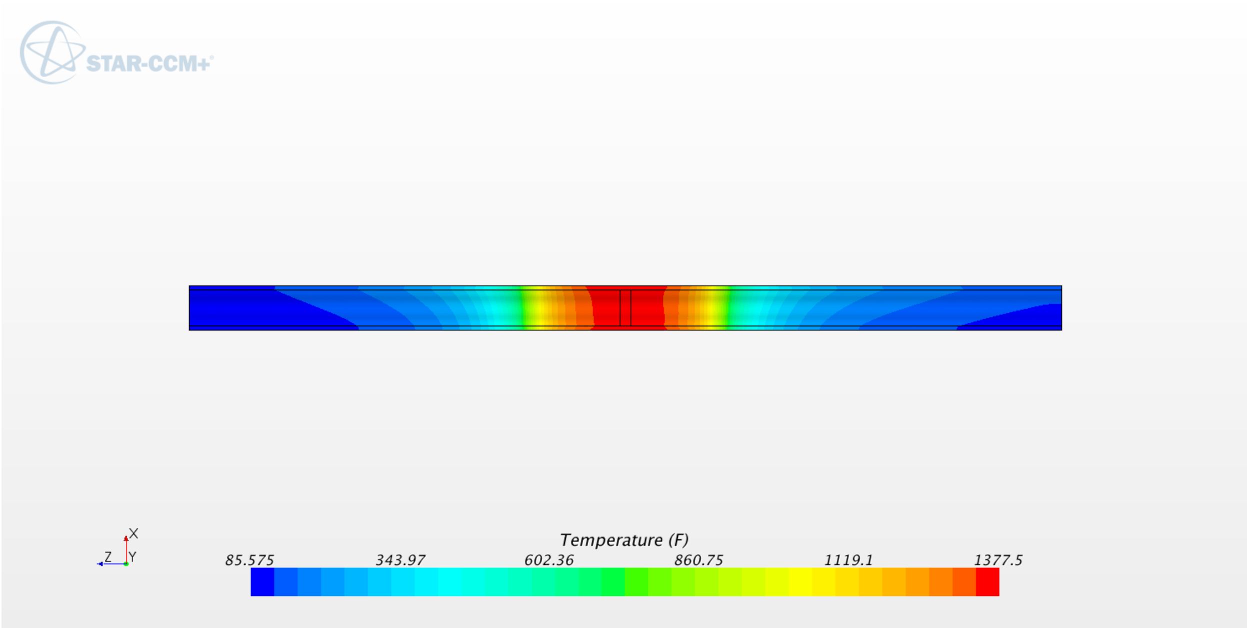

Figure B-36: Temperature contours in pipe wall, close-up (°F). 10 inch schedule 120

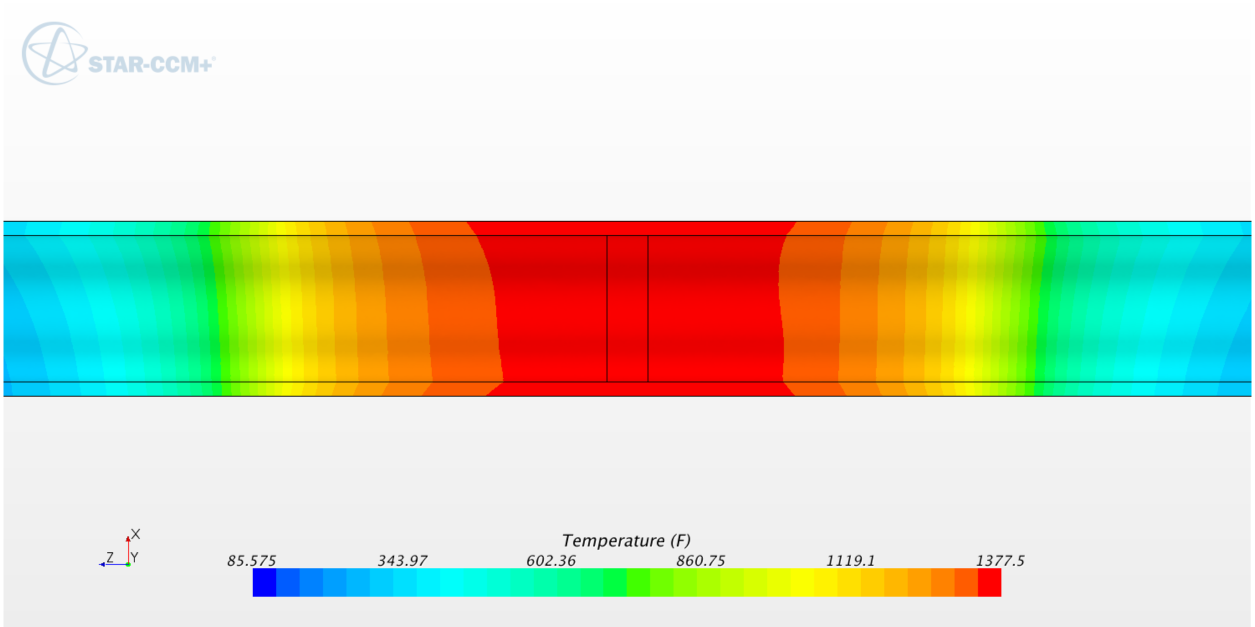

Figure B-37: Temperature contours in SB (°F). 10 inch schedule 120

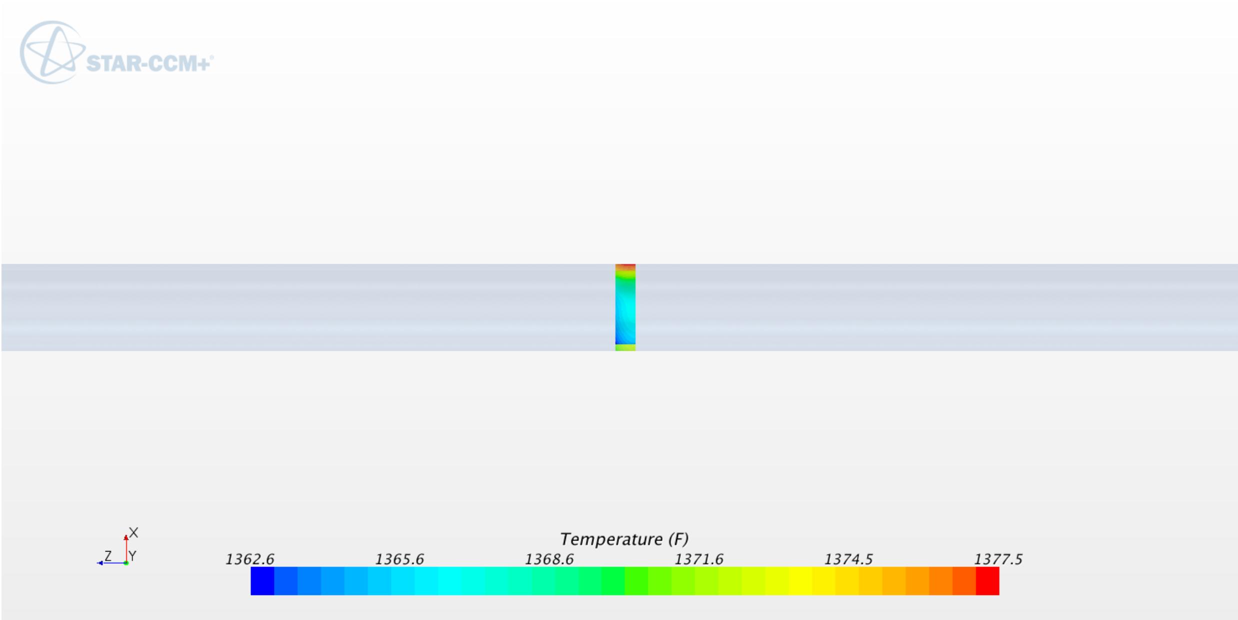

Figure B-38: Temperature contours in SB, isometric view (°F). 10 inch schedule 120

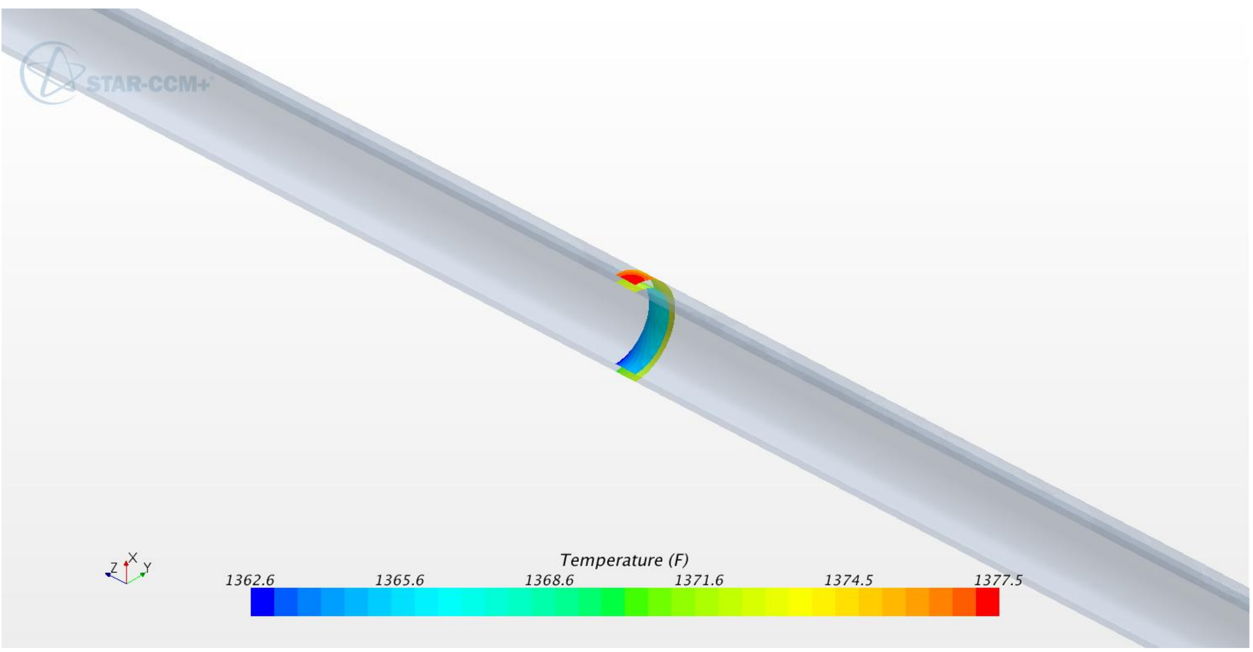

Figure B-39: Velocity contours, cross section of all regions (ft/s). 10 inch schedule 120

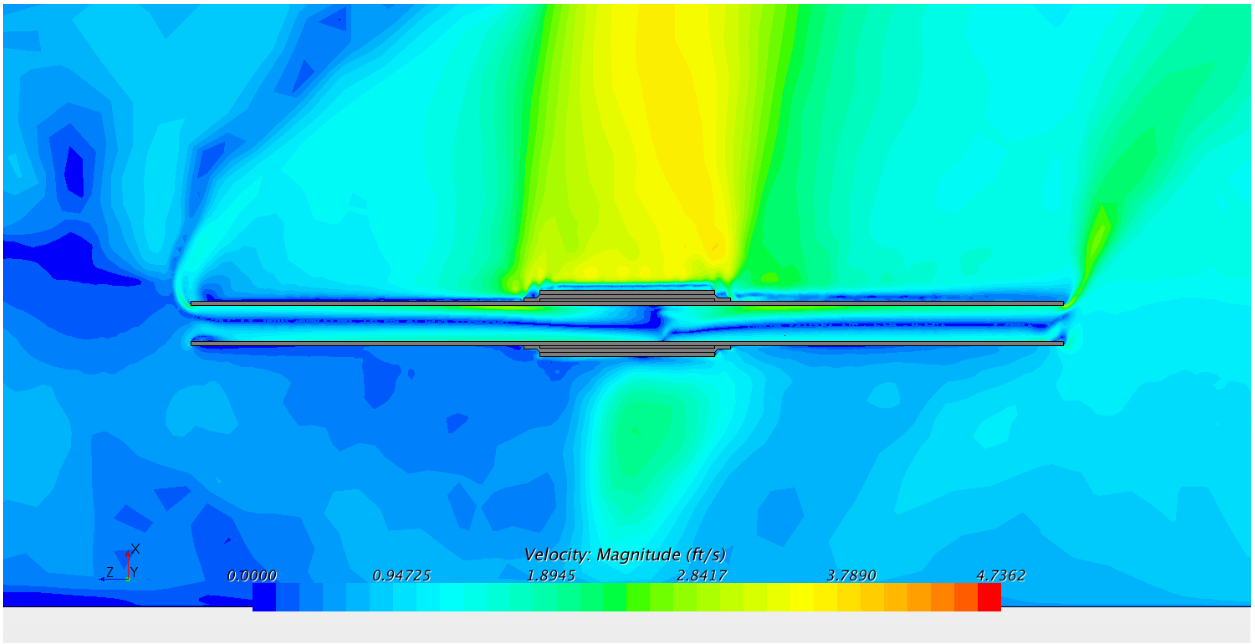

Figure B-40: Velocity contours, cross section of all regions, isometric view (ft/s). 10 inch schedule 120

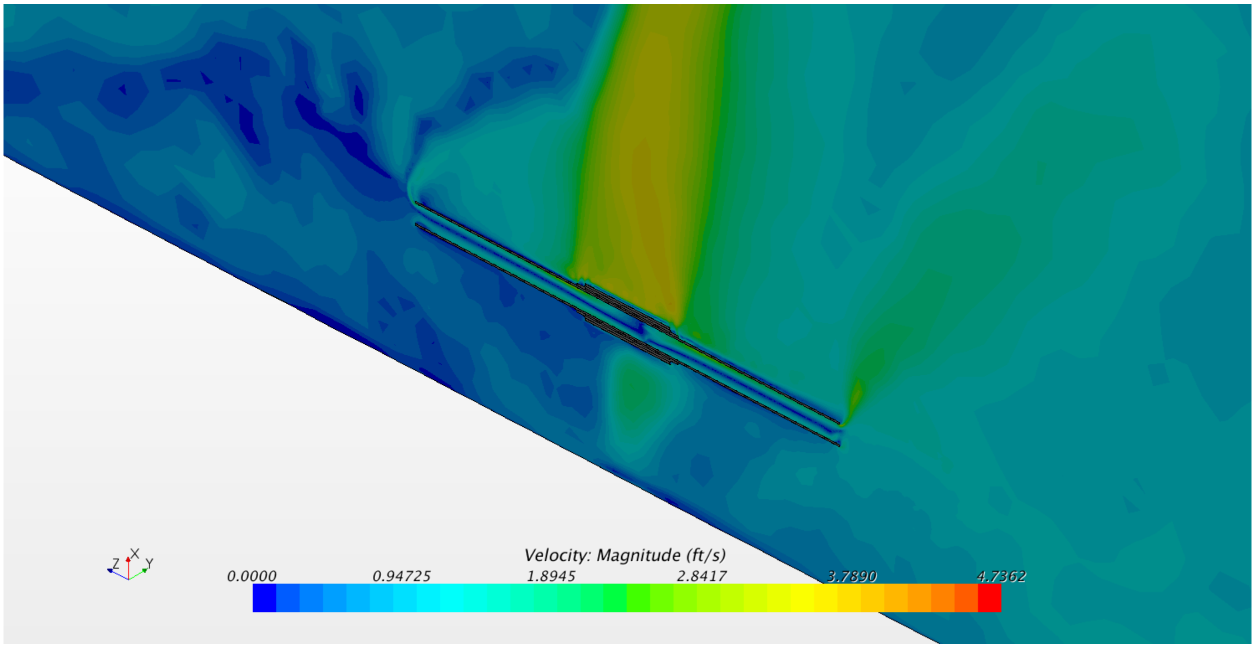

Figure B-41: Temperature contours, cross section of all regions (°F). 10 inch schedule 160

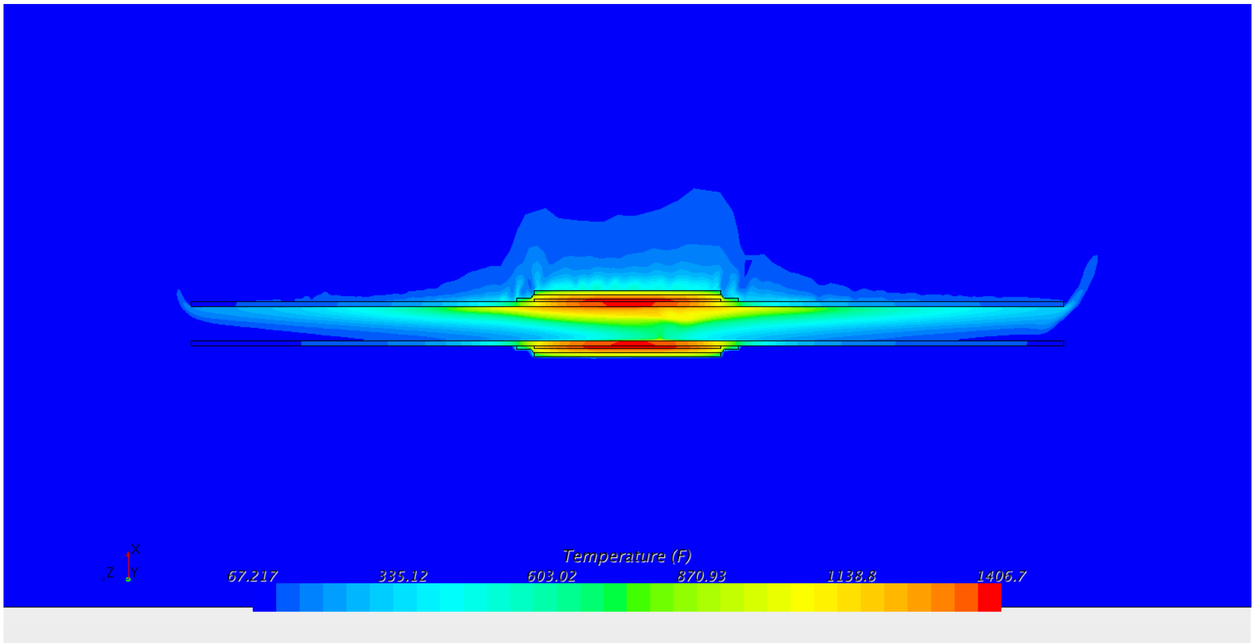

Figure B-42: Temperature contours, cross section of all regions, close-up (°F). 10 inch schedule 160

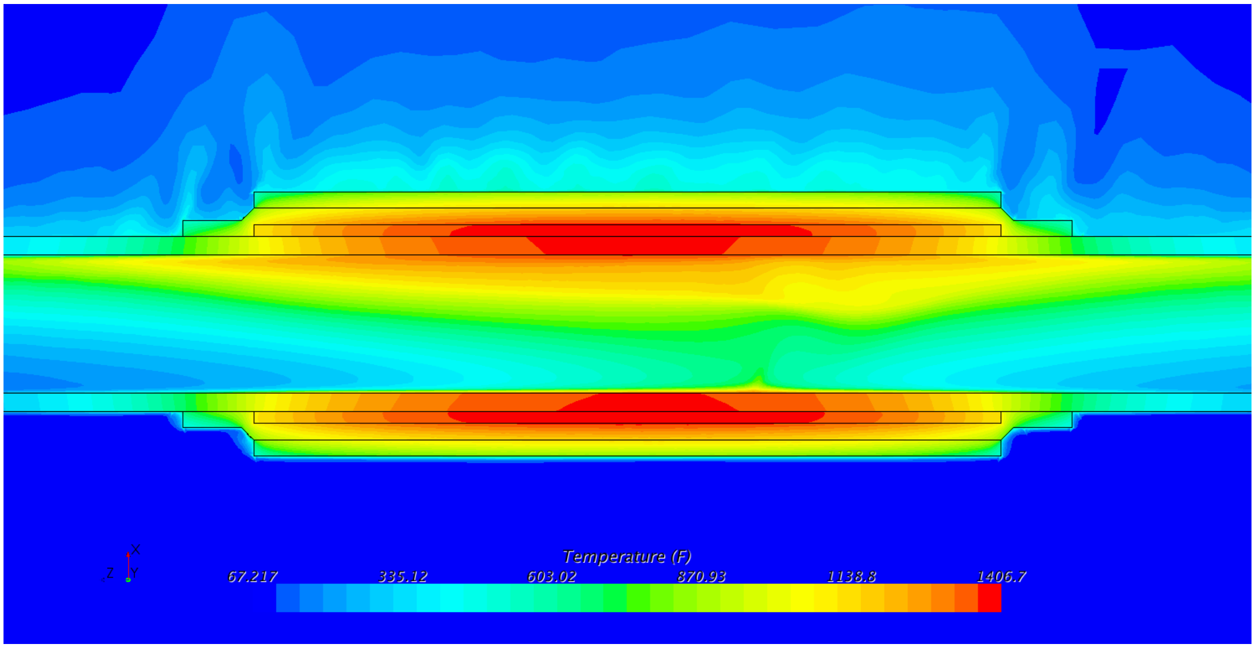

Figure B-43: Temperature contours in pipe wall (°F). 10 inch schedule 160

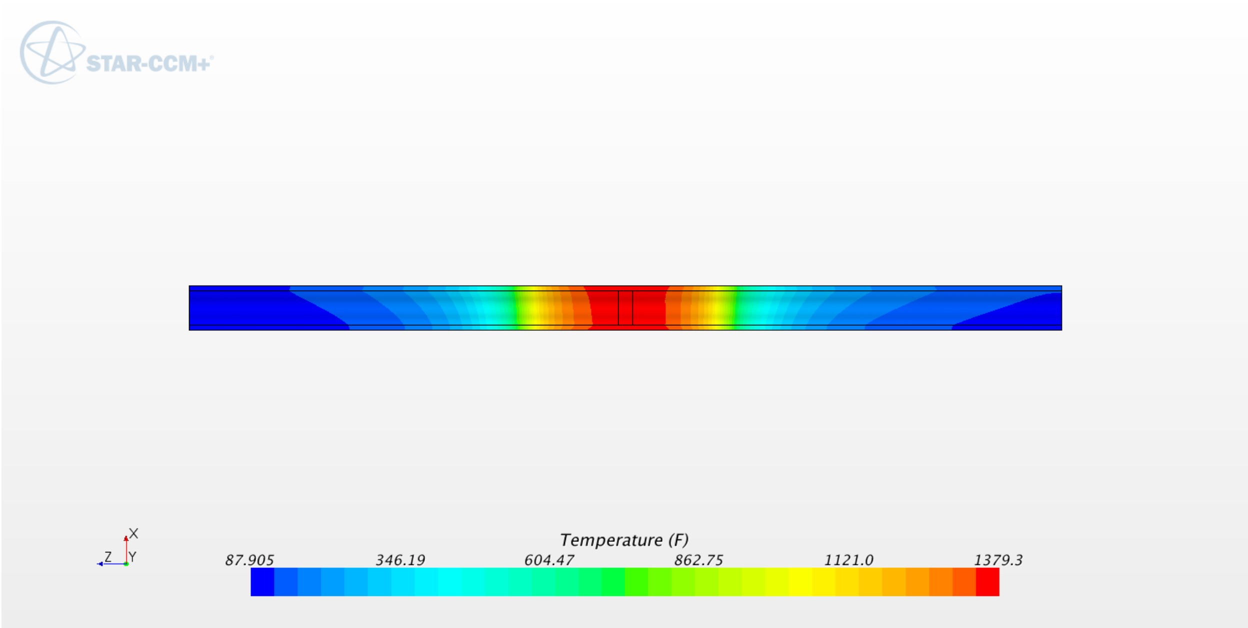

Figure B-44: Temperature contours in pipe wall, close-up (°F). 10 inch schedule 160

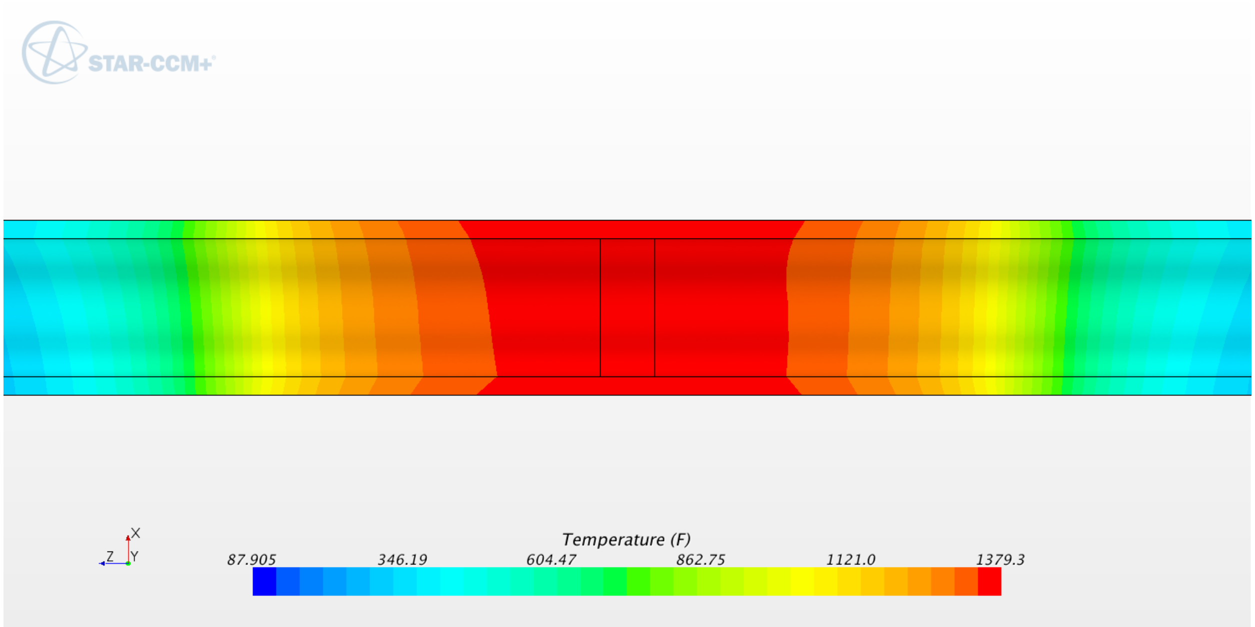

Figure B-45: Temperature contours in SB (°F). 10 inch schedule 160

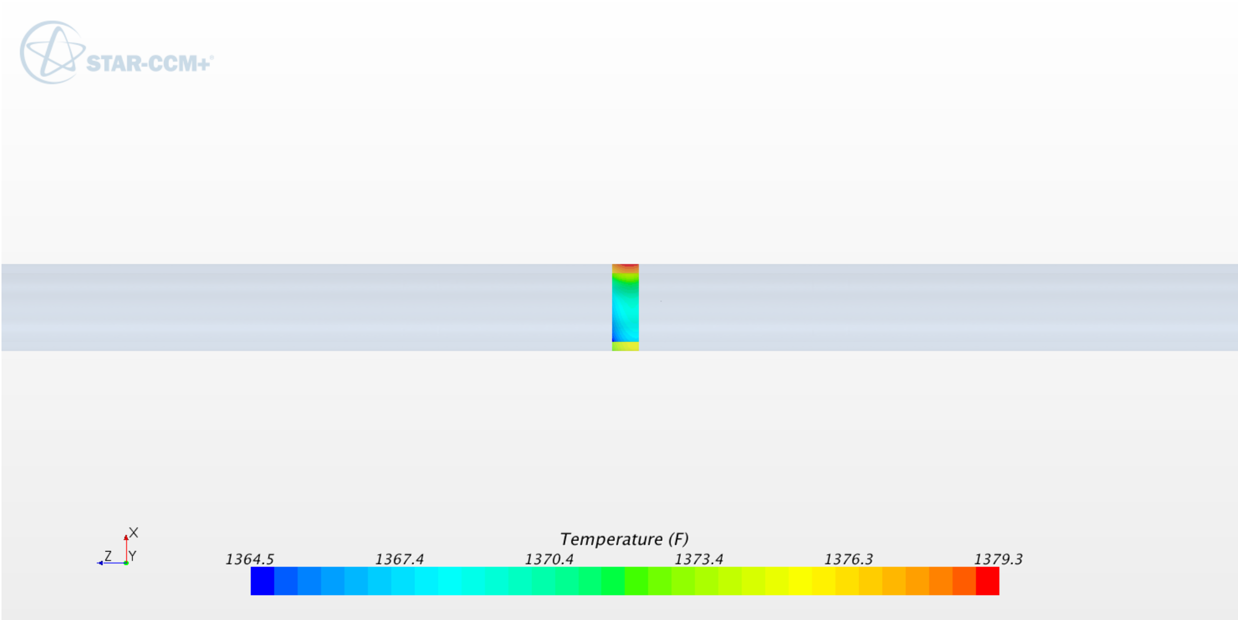

Figure B-46: Temperature contours in SB, isometric view (°F). 10 inch schedule 160

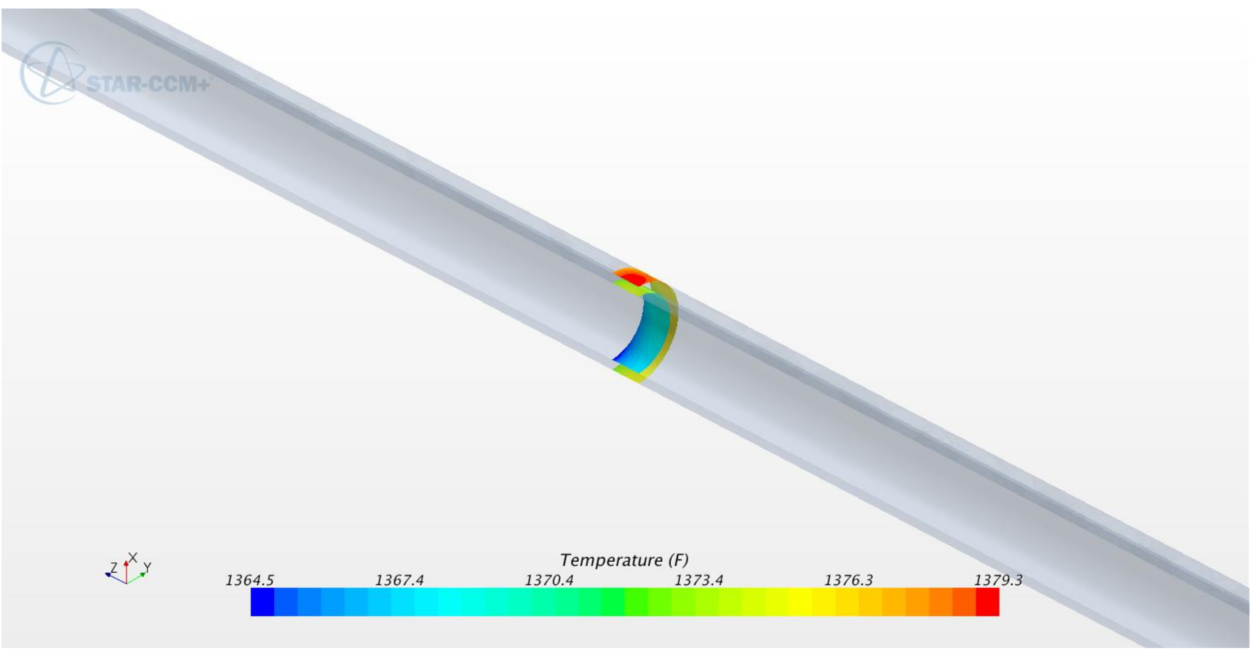

Figure B-47: Velocity contours, cross section of all regions (ft/s). 10 inch schedule 160

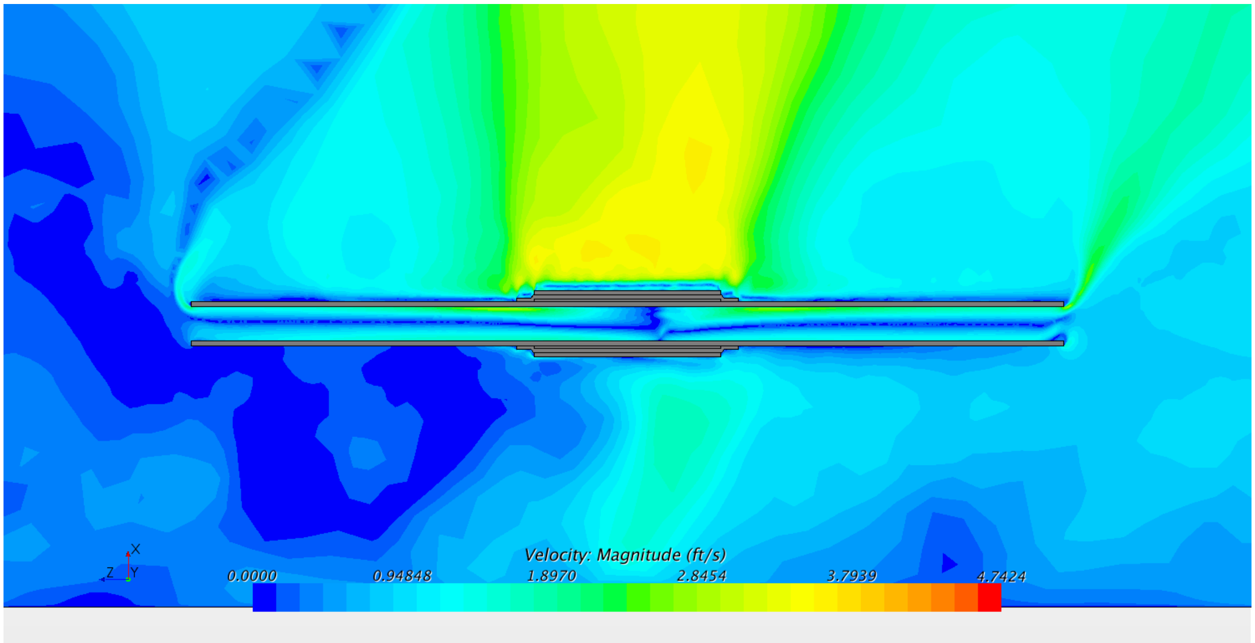

Figure B-48: Velocity contours, cross section of all regions, isometric view (ft/s). 10 inch schedule 160

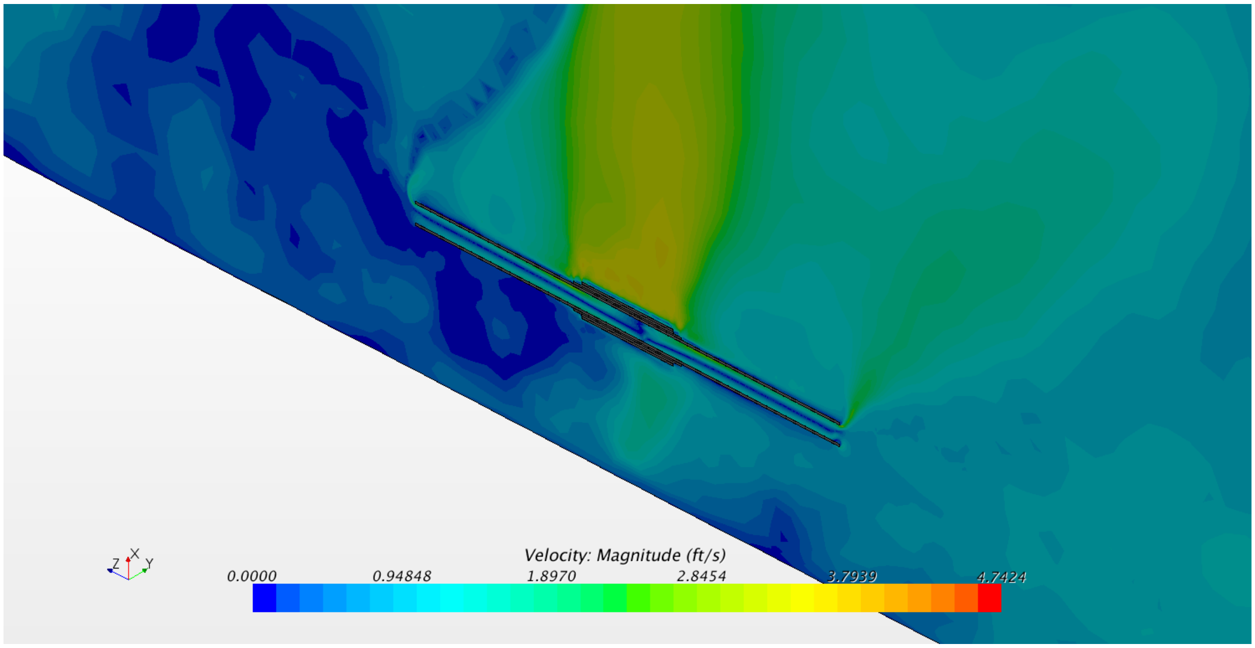

Figure B-49: Temperature contours, cross section of all regions (°F). 14 inch schedule 80

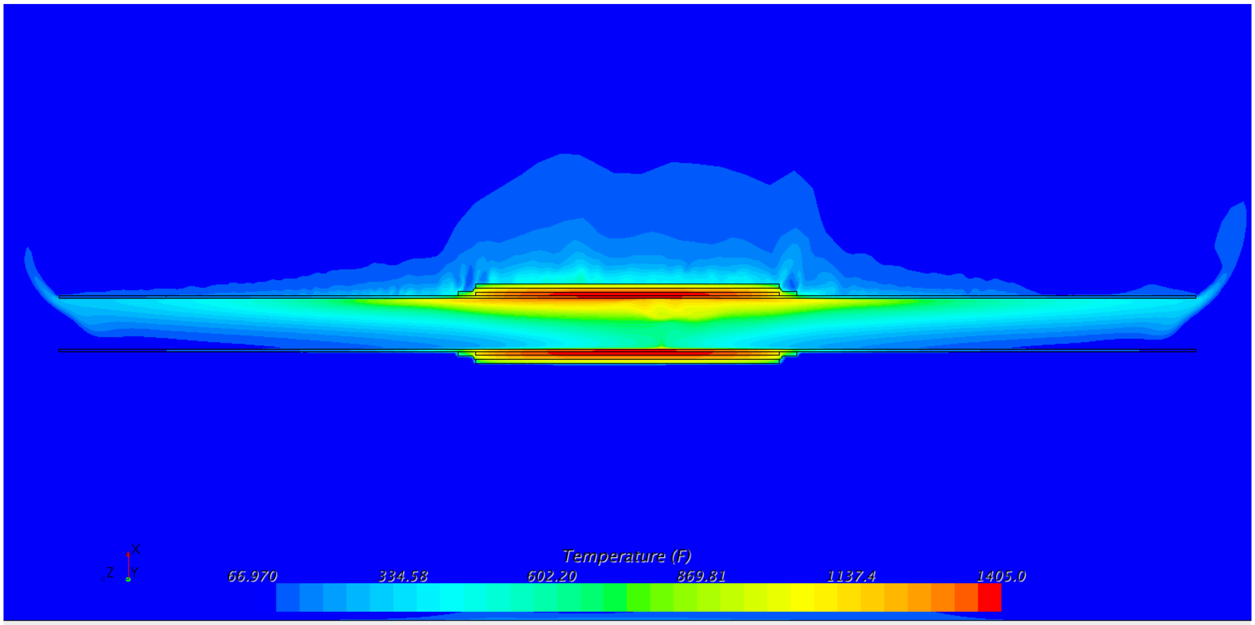

Figure B-50: Temperature contours, cross section of all regions, close-up (°F). 14 inch schedule 80

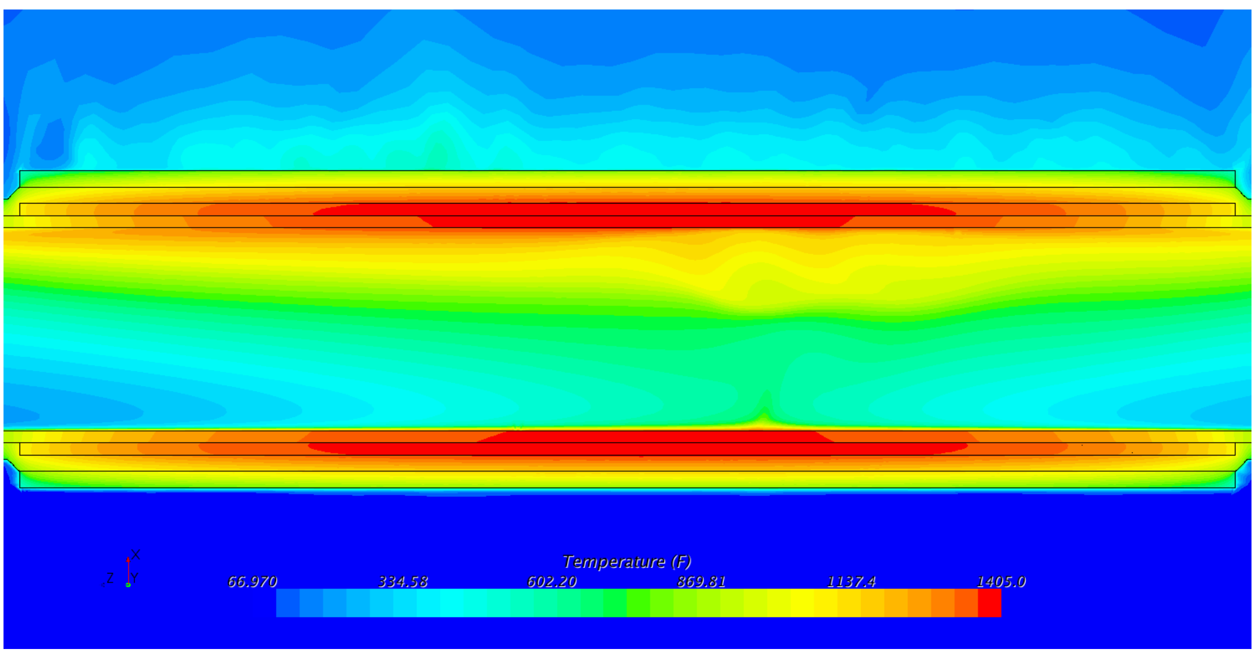

Figure B-51: Temperature contours in pipe wall (°F). 14 inch schedule 80

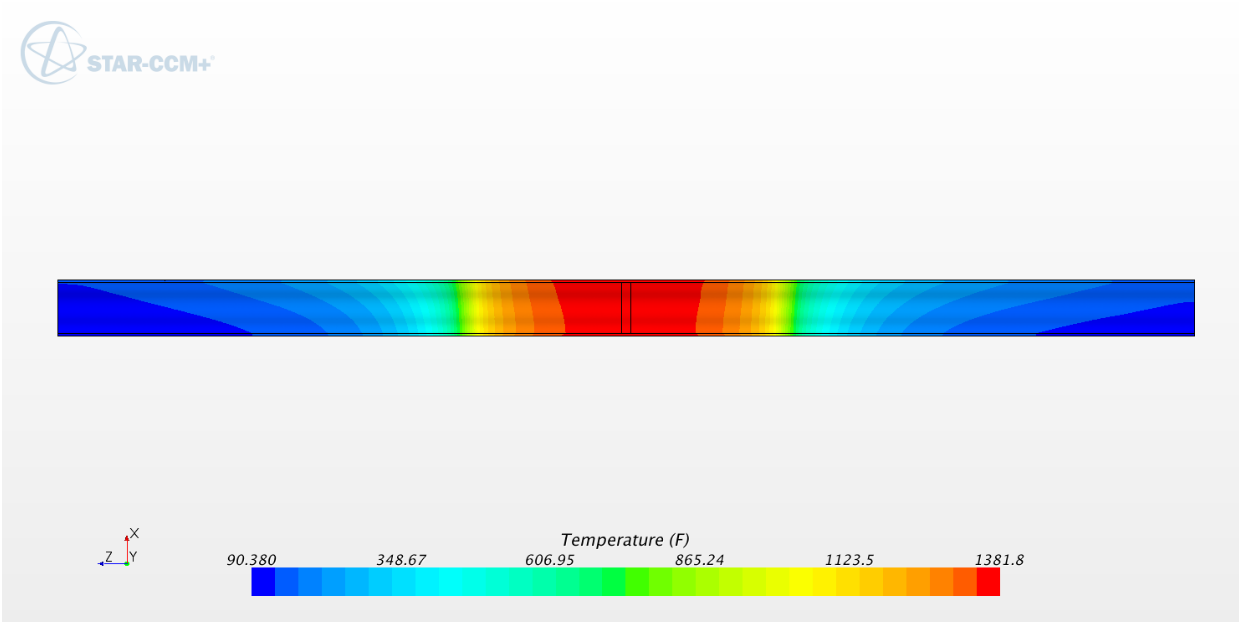

Figure B-52: Temperature contours in pipe wall, close-up (°F). 14 inch schedule 80

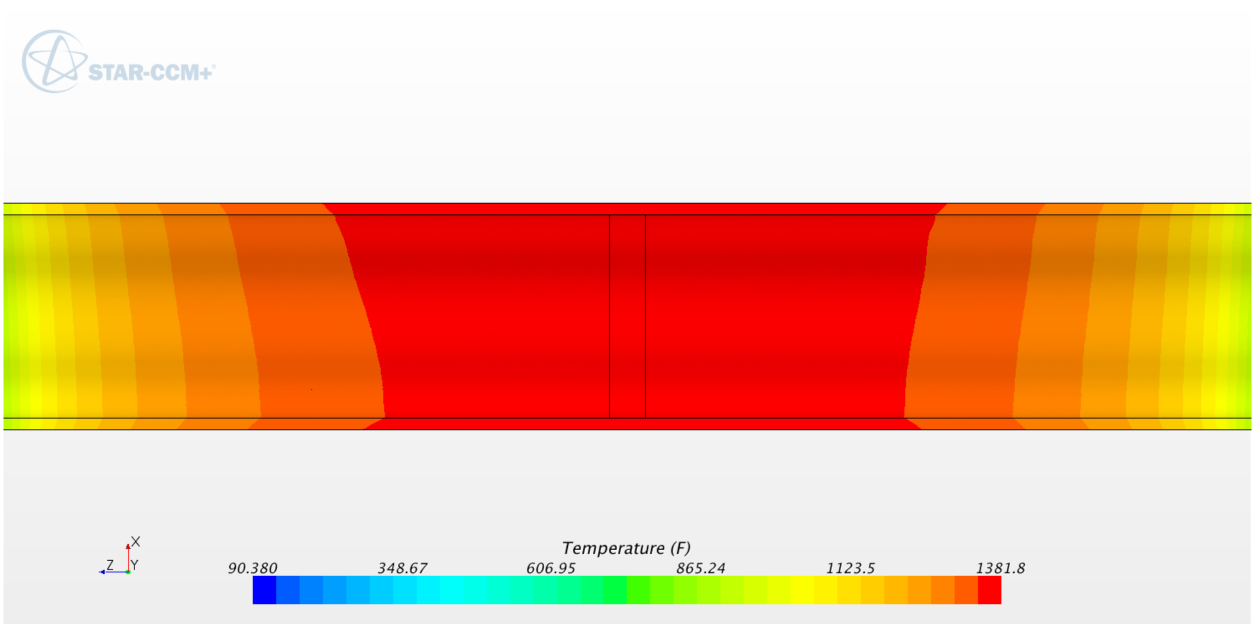

Figure B-53: Temperature contours in SB (°F). 14 inch schedule 80

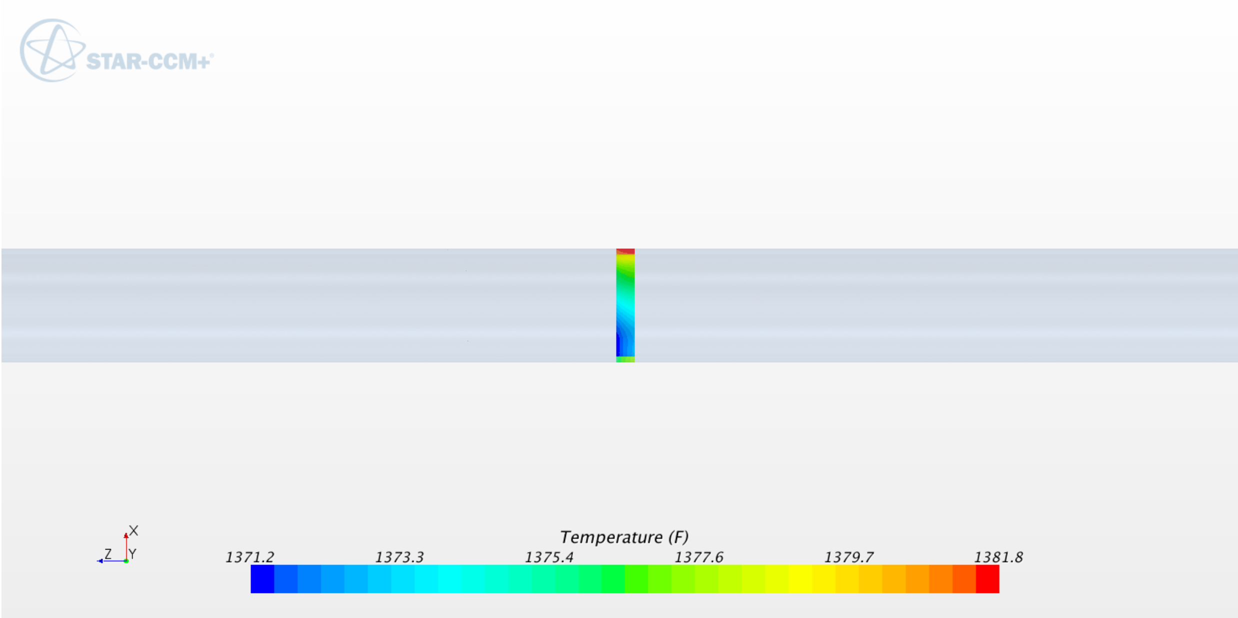

Figure B-54: Temperature contours in SB, isometric view (°F). 14 inch schedule 80

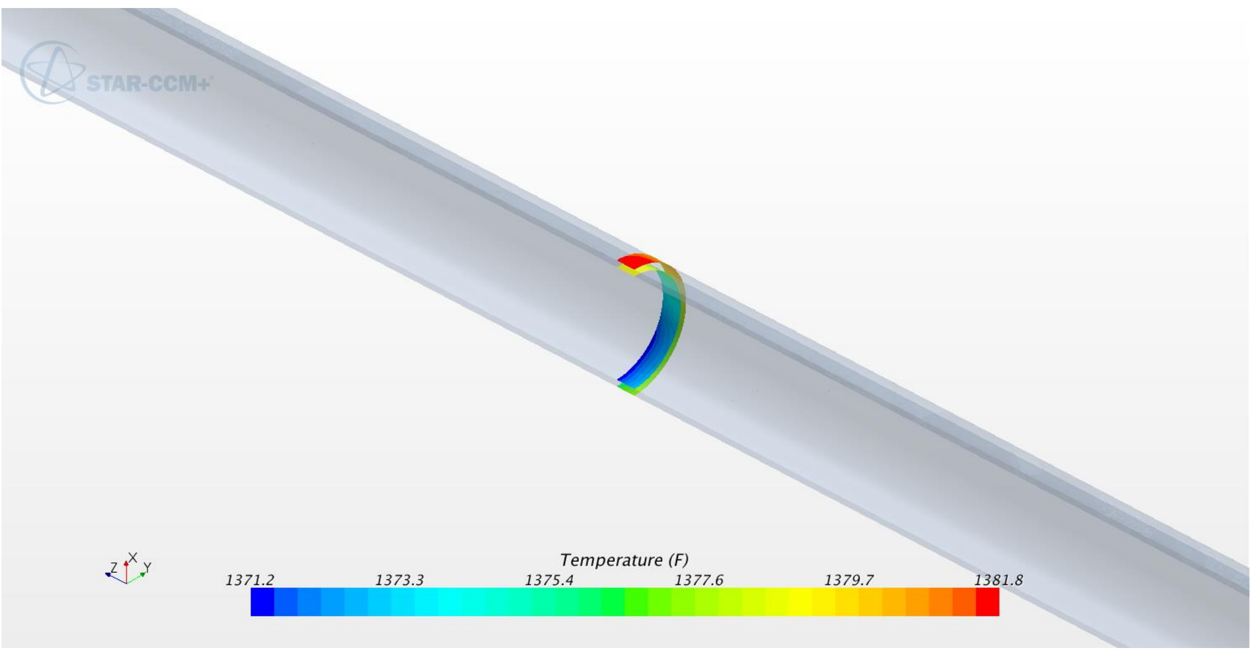

Figure B-55: Velocity contours, cross section of all regions (ft/s). 14 inch schedule 80

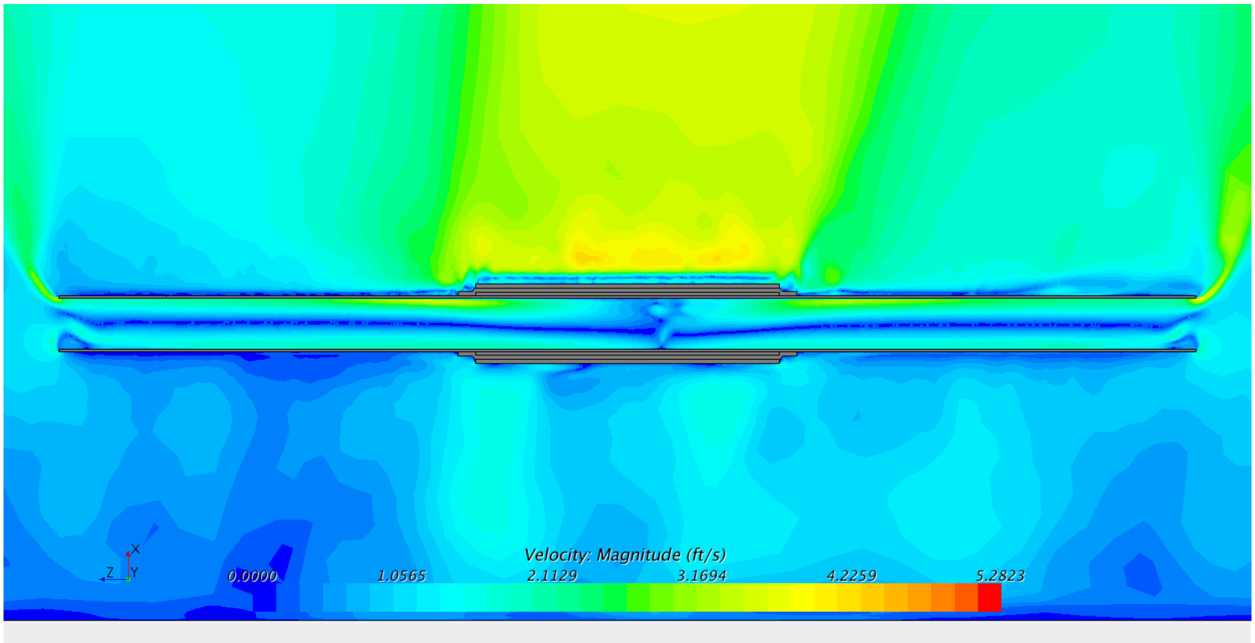

Figure B-56: Velocity contours, cross section of all regions, isometric view (ft/s). 14 inch schedule 80

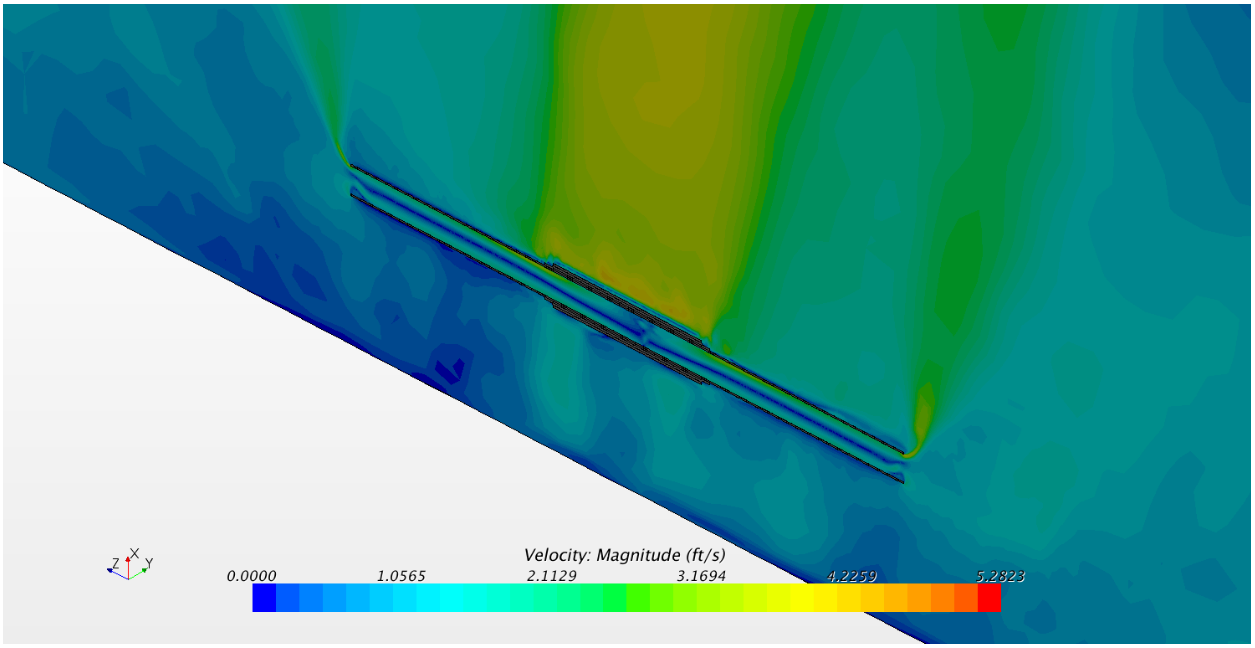

Figure B-57: Temperature contours, cross section of all regions (°F). 14 inch schedule 120

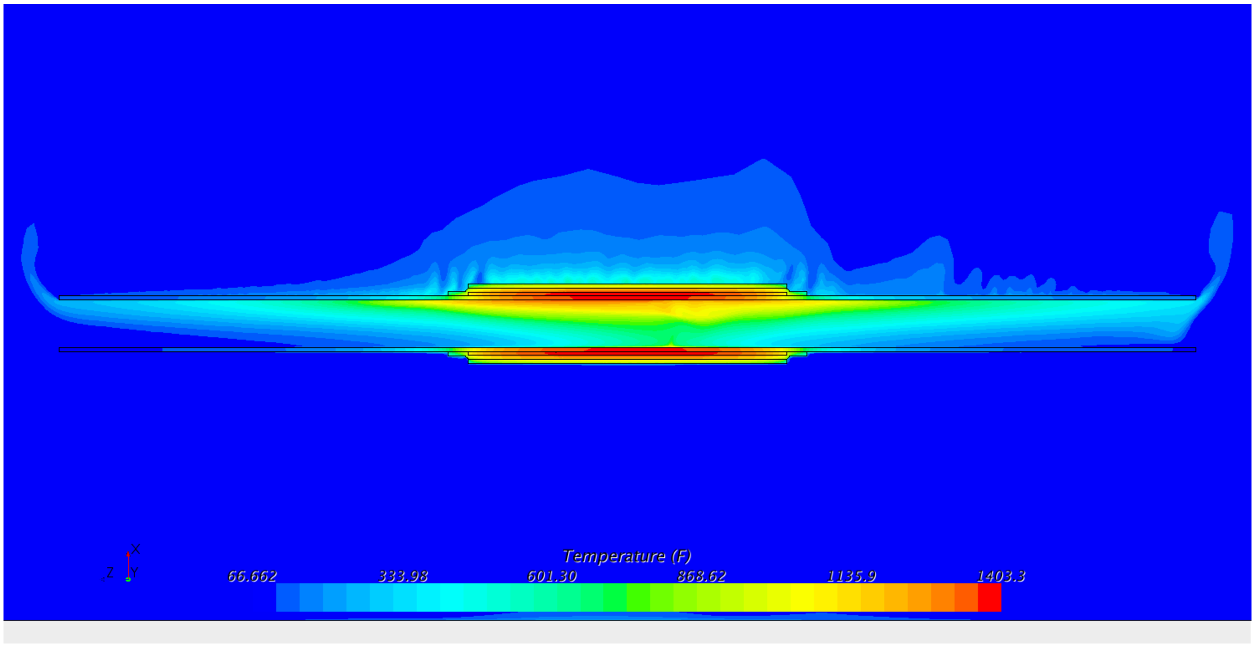

Figure B-58: Temperature contours, cross section of all regions, close-up (°F). 14 inch schedule 120

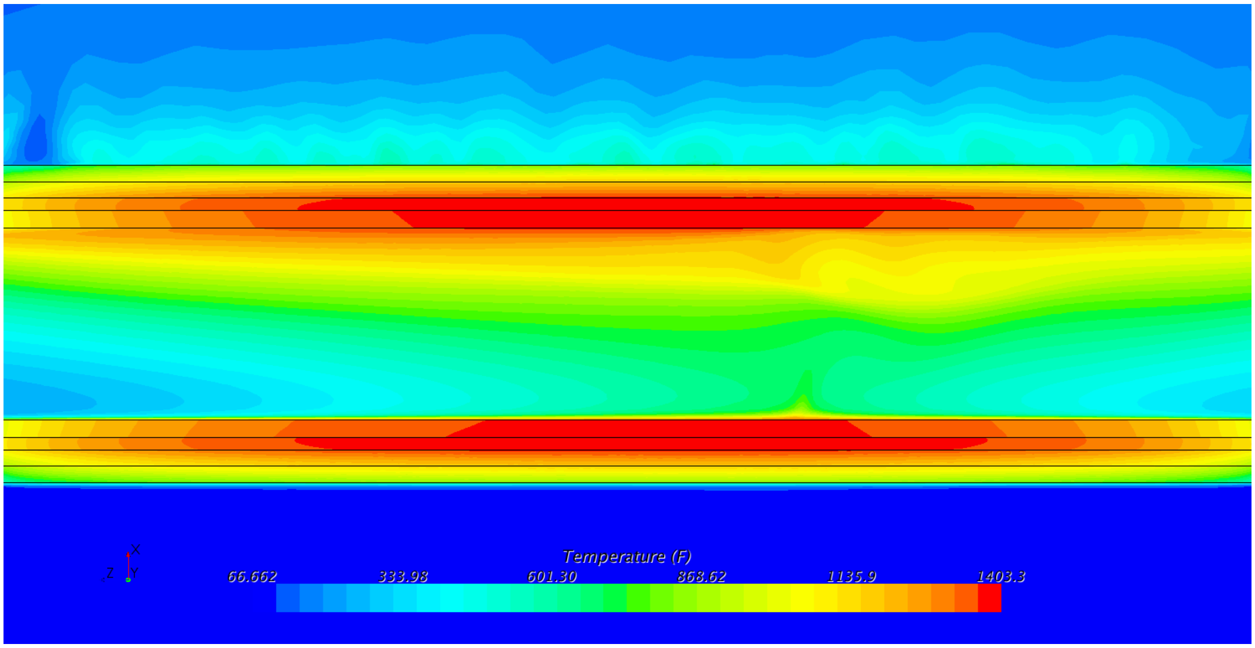

Figure B-59: Temperature contours in pipe wall (°F). 14 inch schedule 120

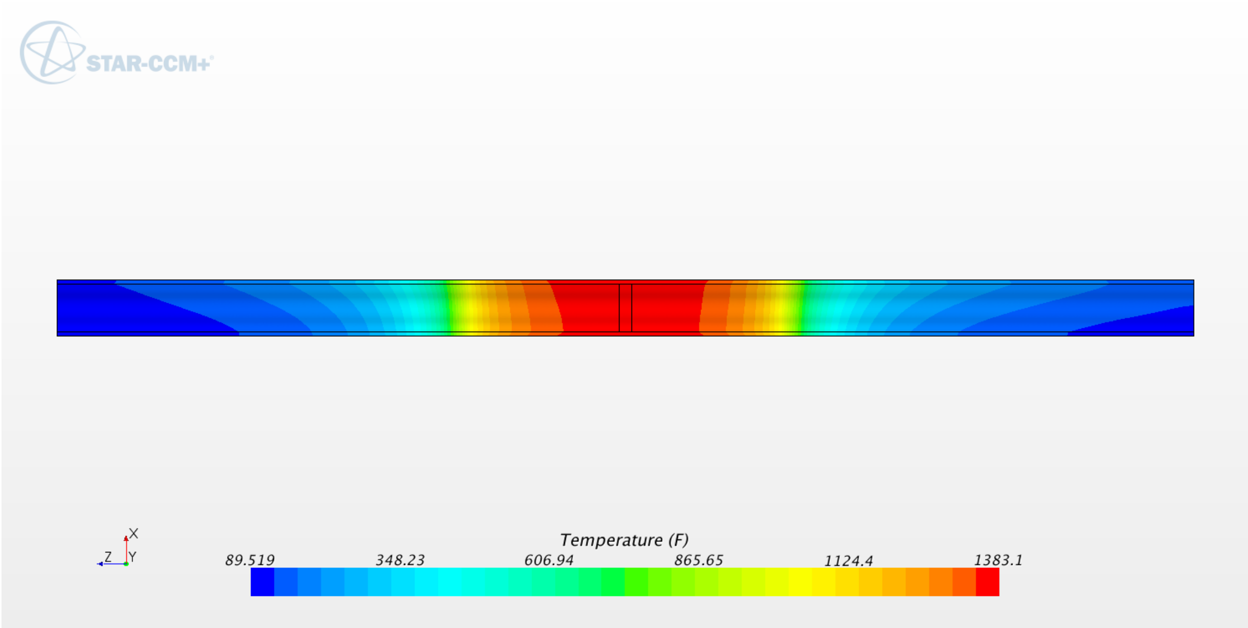

Figure B-60: Temperature contours in pipe wall, close-up (°F). 14 inch schedule 120

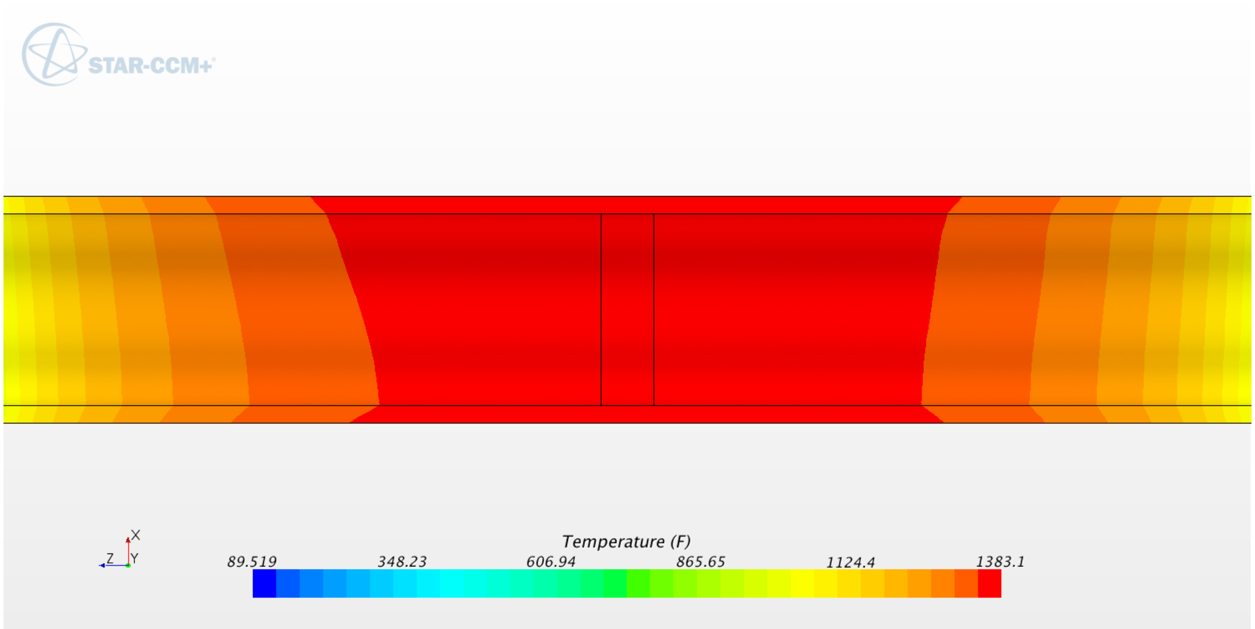

Figure B-61: Temperature contours in SB (°F). 14 inch schedule 120

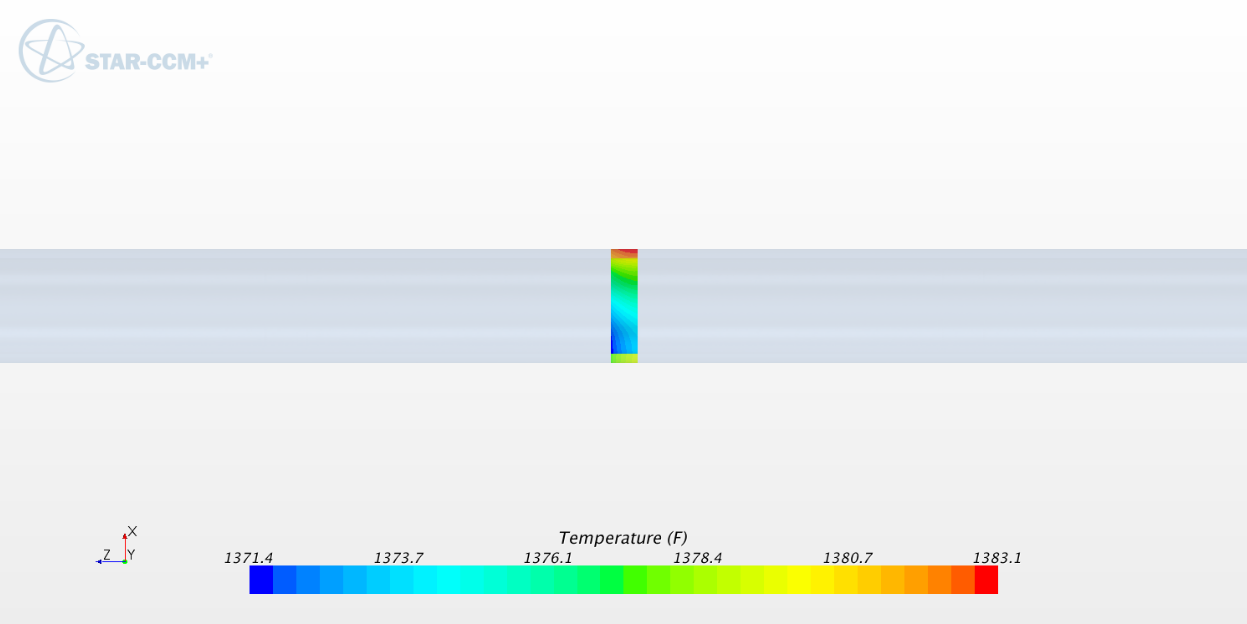

Figure B-62: Temperature contours in SB, isometric view (°F). 14 inch schedule 120.

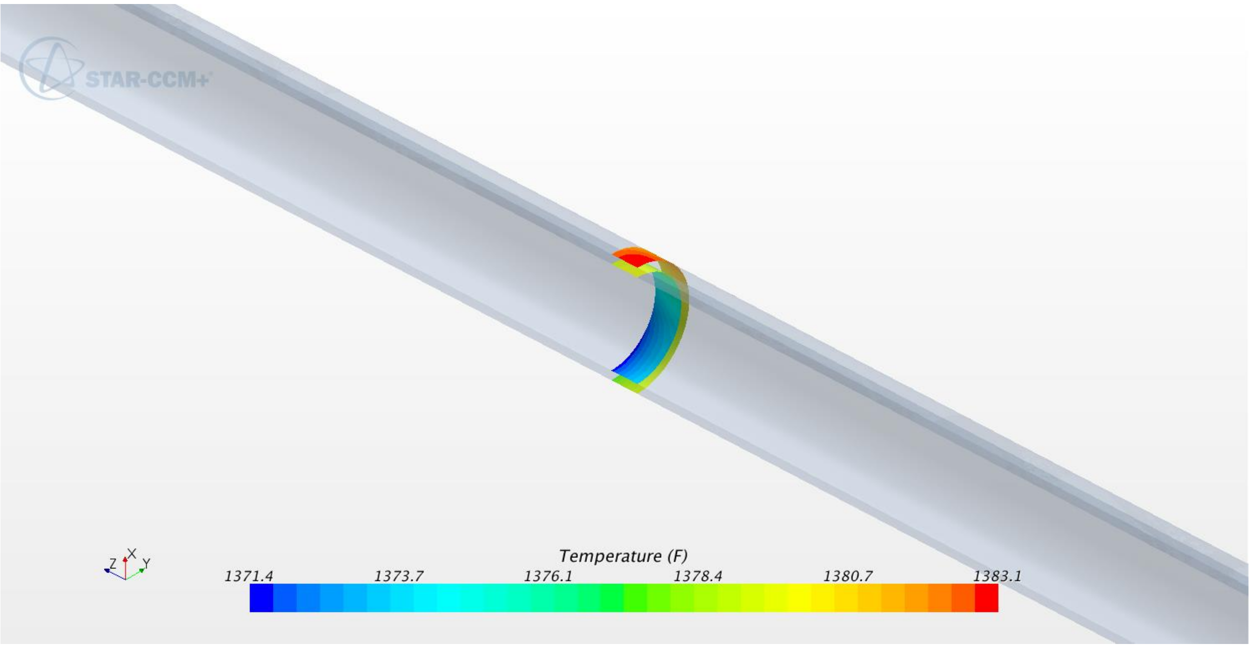

Figure B-63: Velocity contours, cross section of all regions (ft/s). 14 inch schedule 120

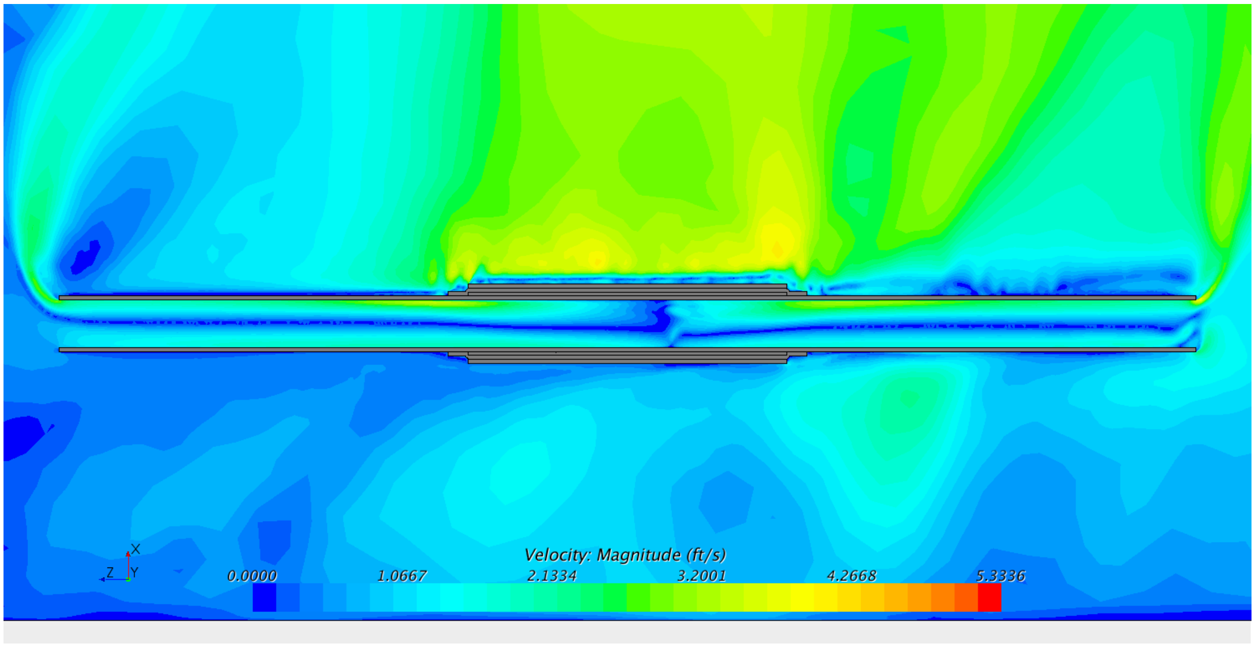

Figure B-64: Velocity contours, cross section of all regions, isometric view (ft/s). 14 inch schedule 120

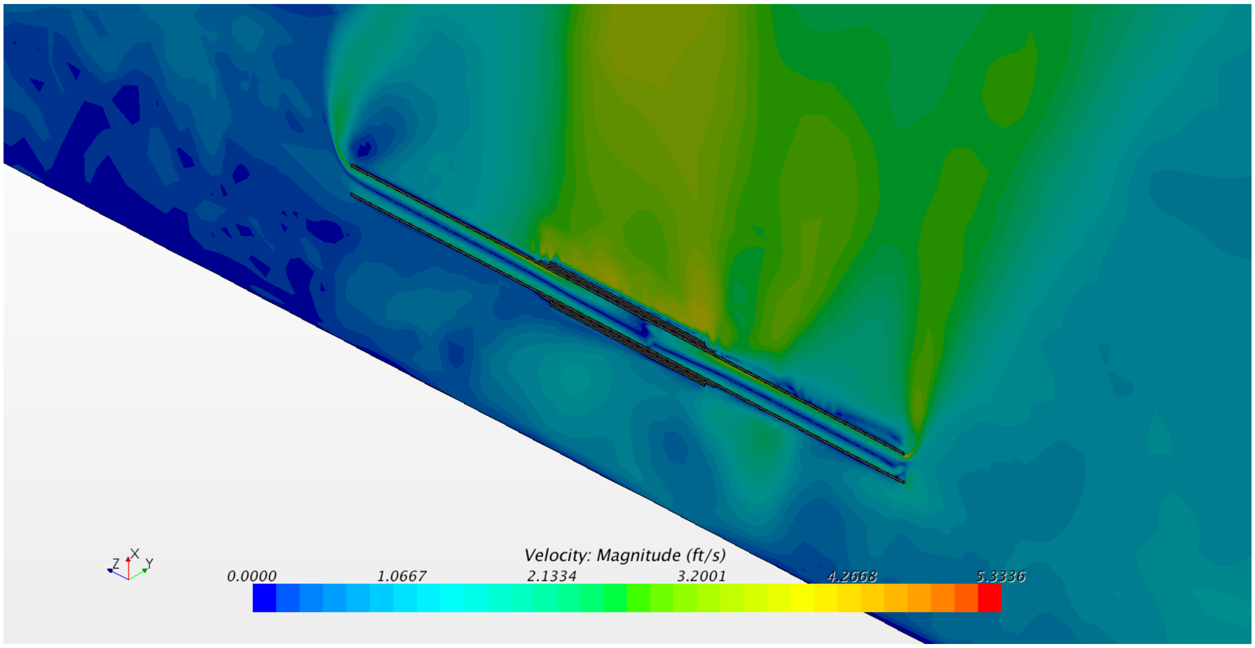

Figure B-65: Temperature contours, cross section of all regions (°F). 14 inch schedule 160

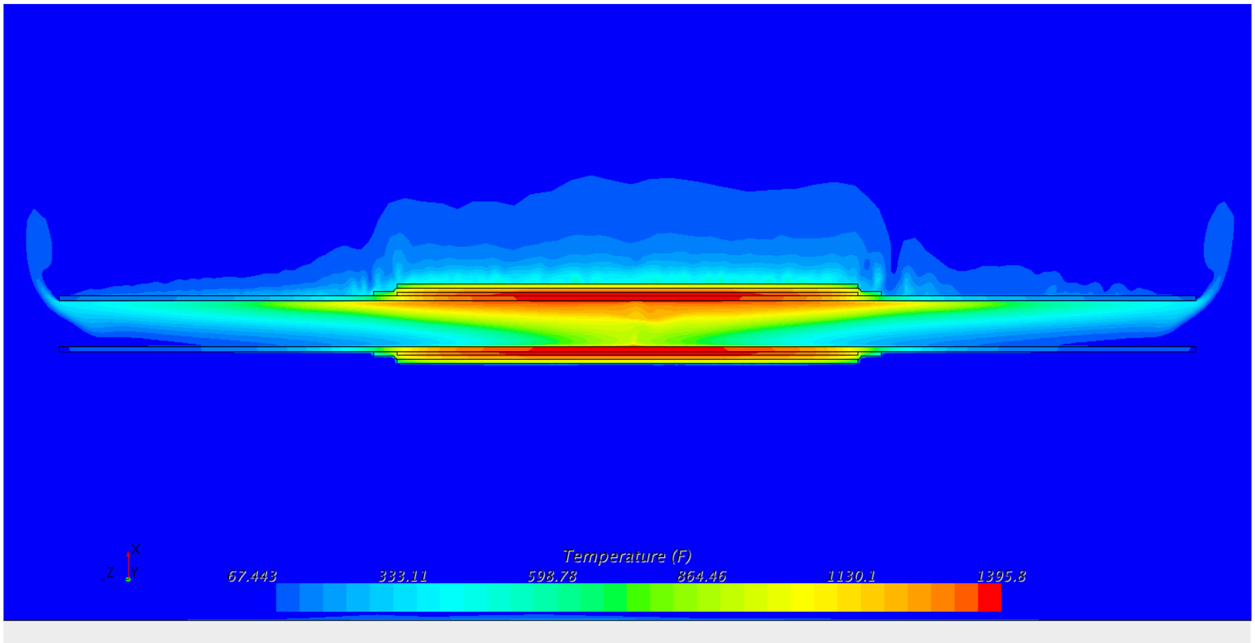

Figure B-66: Temperature contours, cross section of all regions, close-up (°F). 14 inch schedule 160

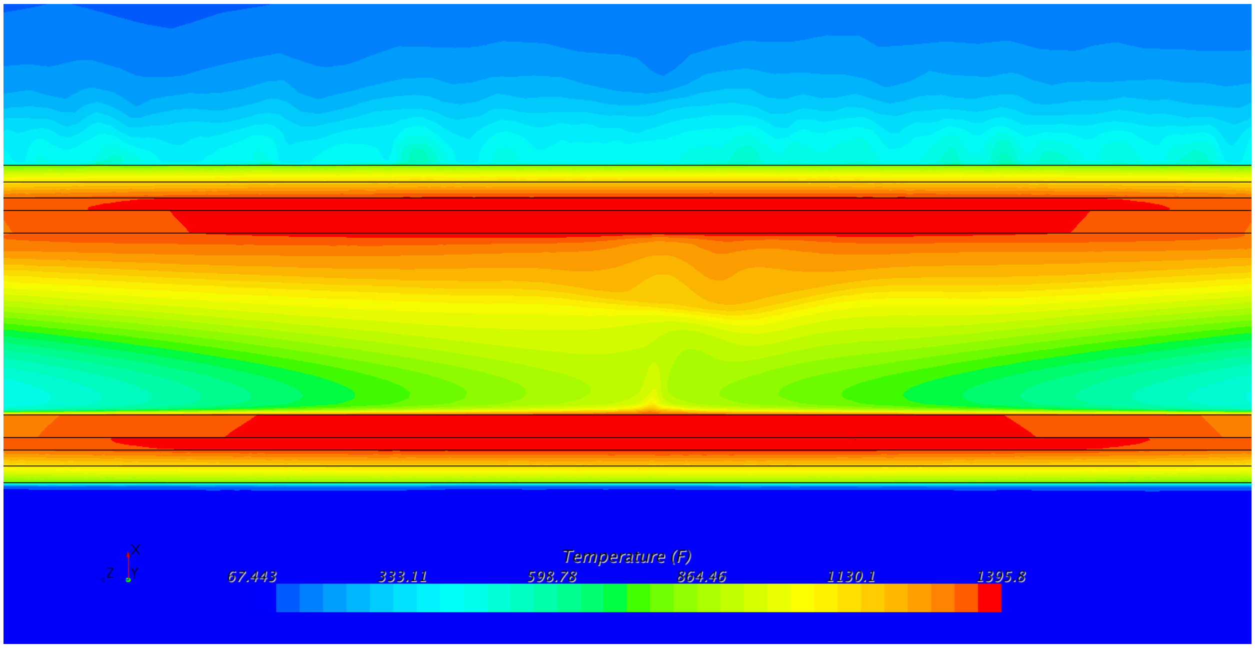

Figure B-67: Temperature contours in pipe wall (°F). 14 inch schedule 160

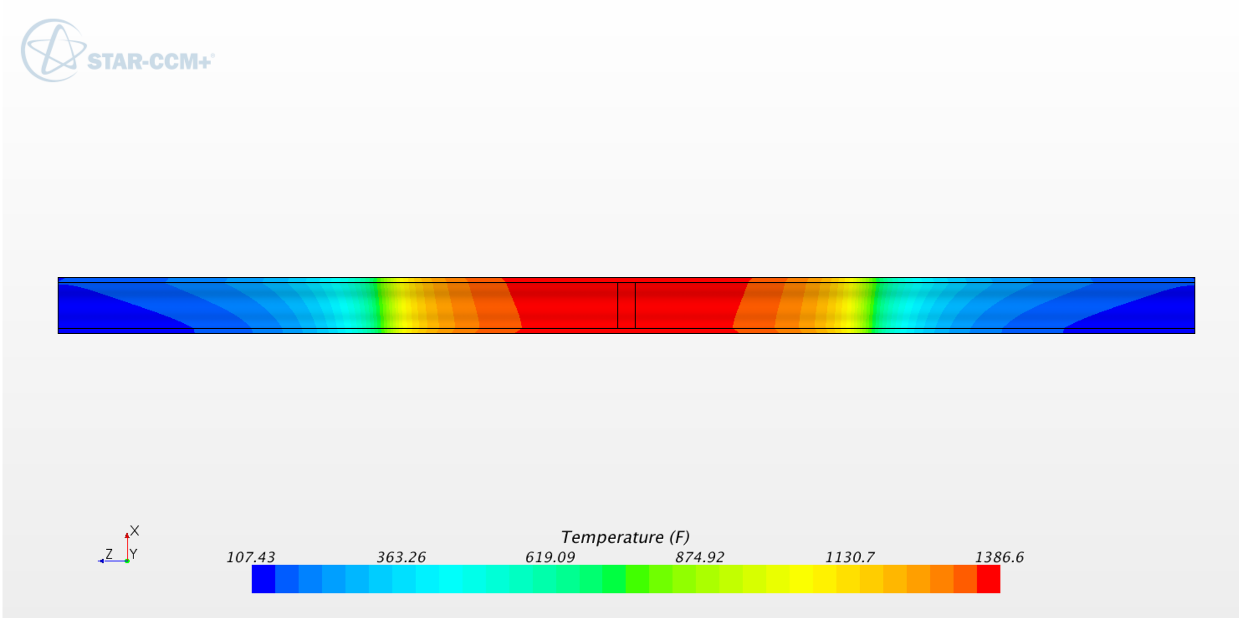

Figure B-68: Temperature contours in pipe wall, close-up (°F). 14 inch schedule 160

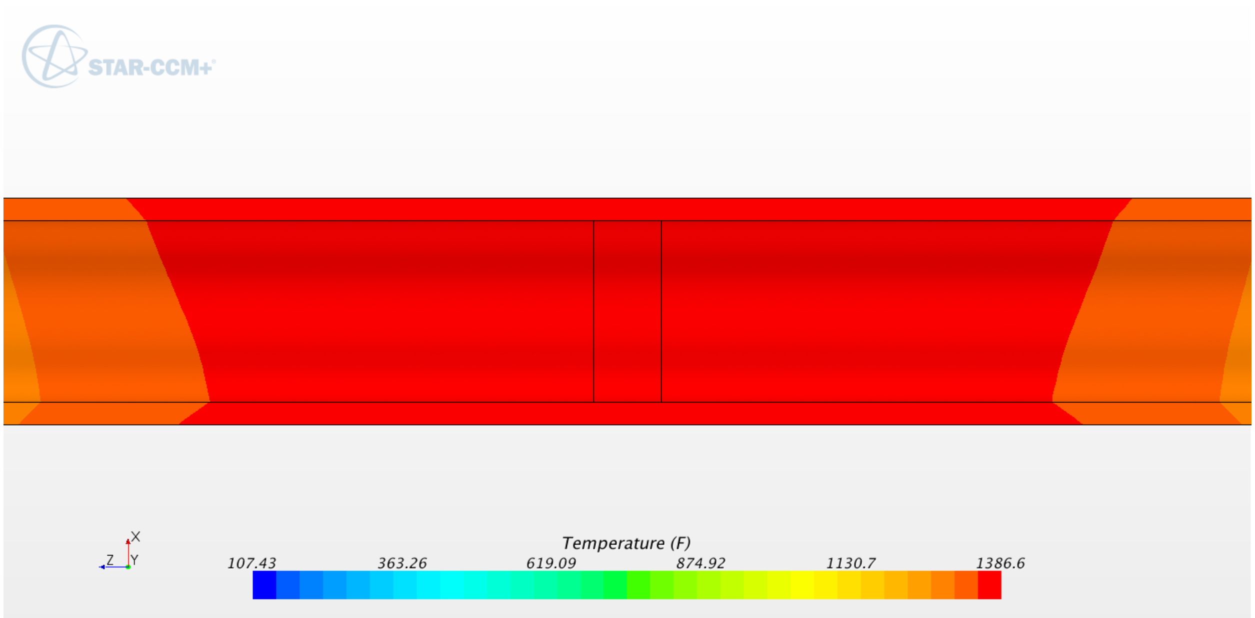

Figure B-69: Temperature contours in SB (°F). 14 inch schedule 160

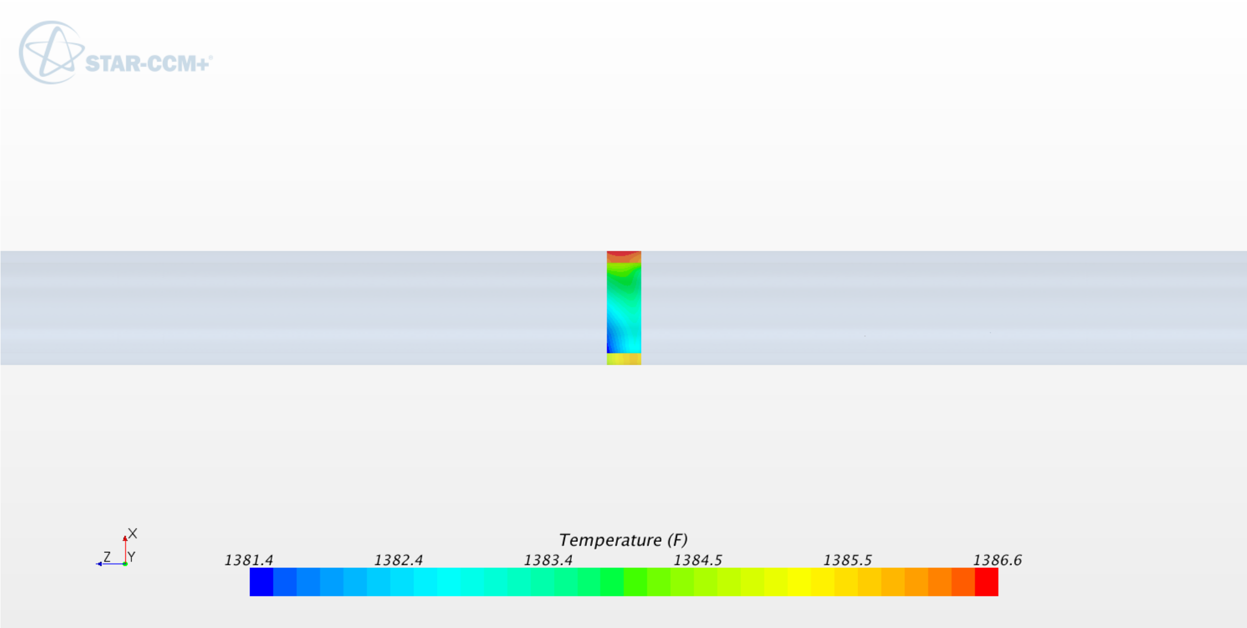

Figure B-70: Temperature contours in SB, isometric view (°F). 14 inch schedule 160

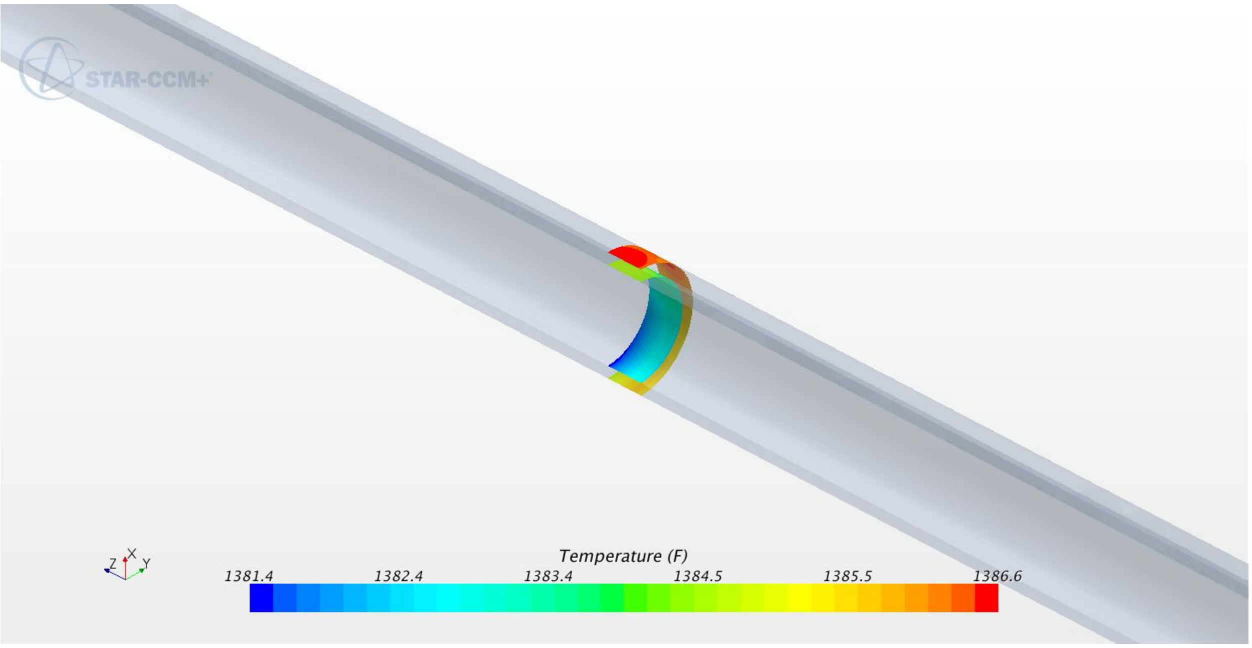

Figure B-71: Velocity contours, cross section of all regions (ft/s). 14 inch schedule 160

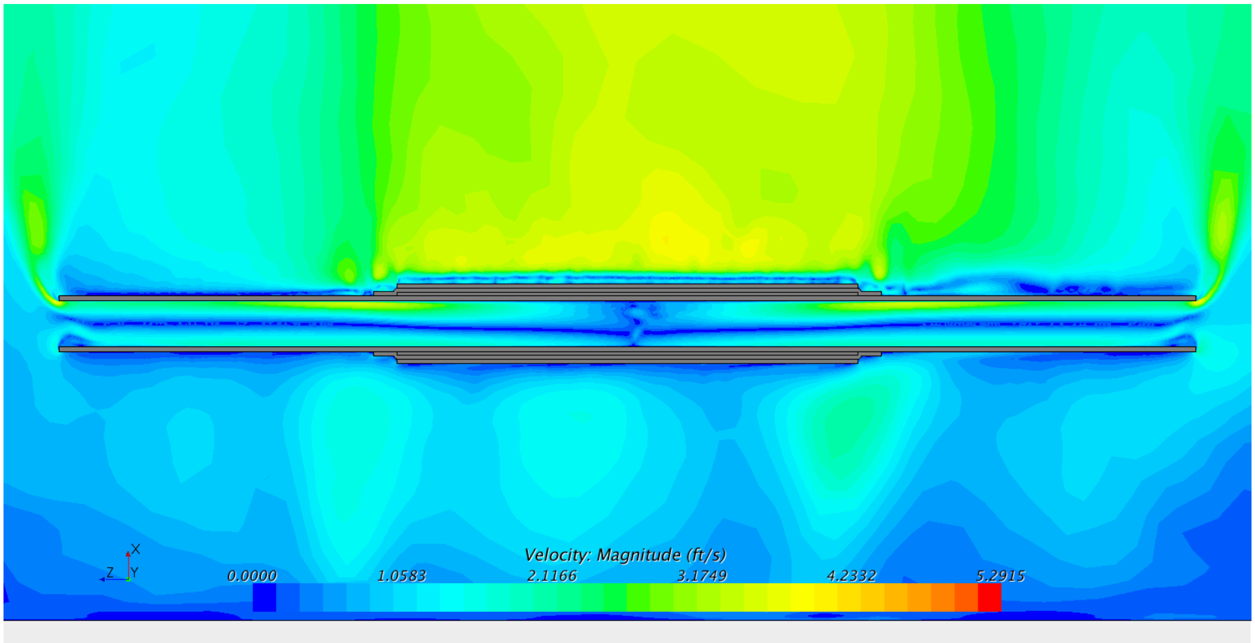

Figure B-72: Velocity contours, cross section of all regions, isometric view (ft/s). 14 inch schedule 160

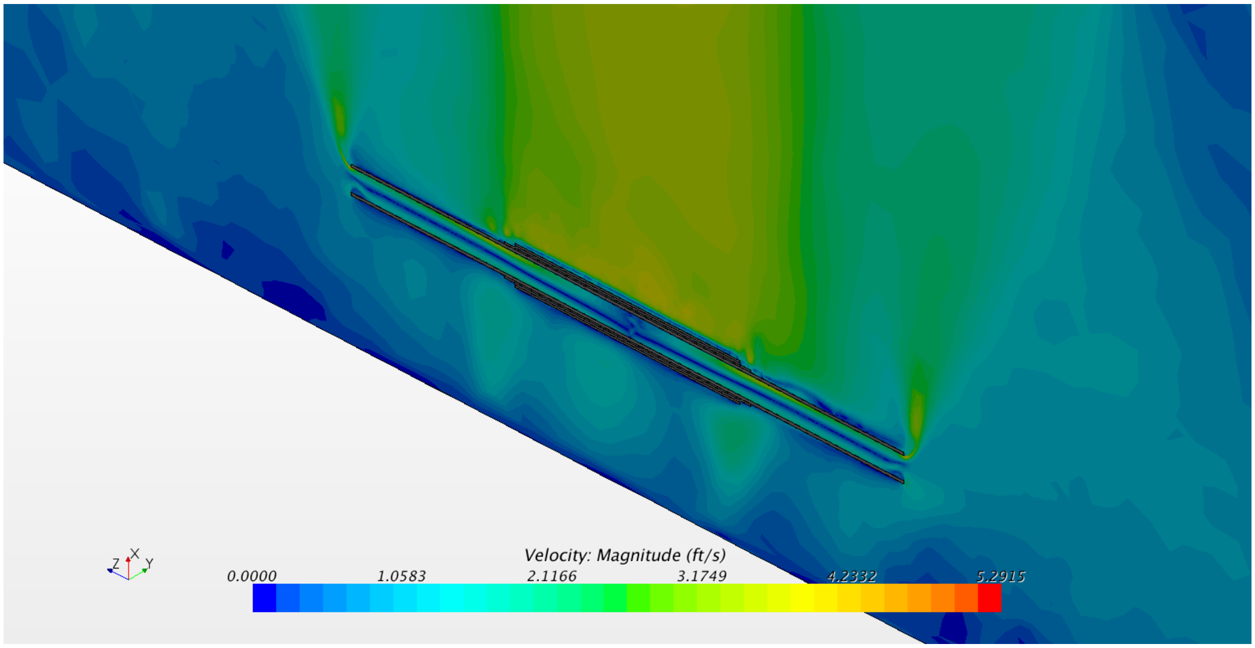

Figure B-73: Temperature contours, cross section of all regions (°F). 24 inch schedule 80

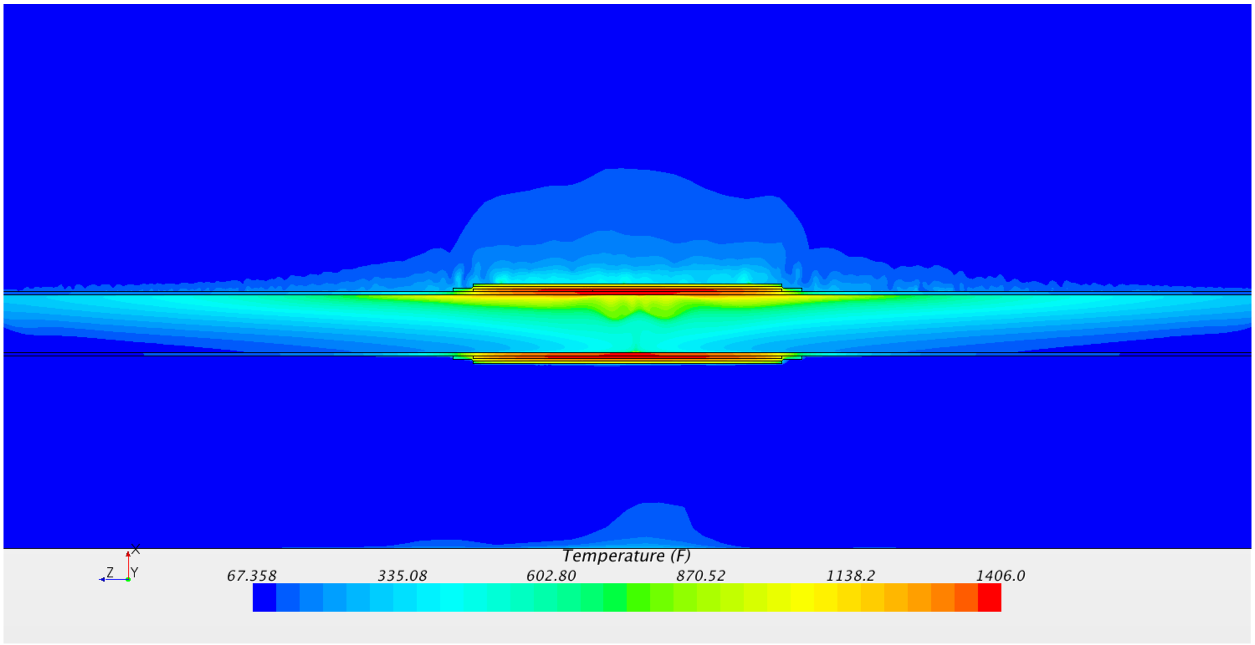

Figure B-74: Temperature contours, cross section of all regions, close-up (°F). 24 inch schedule 80

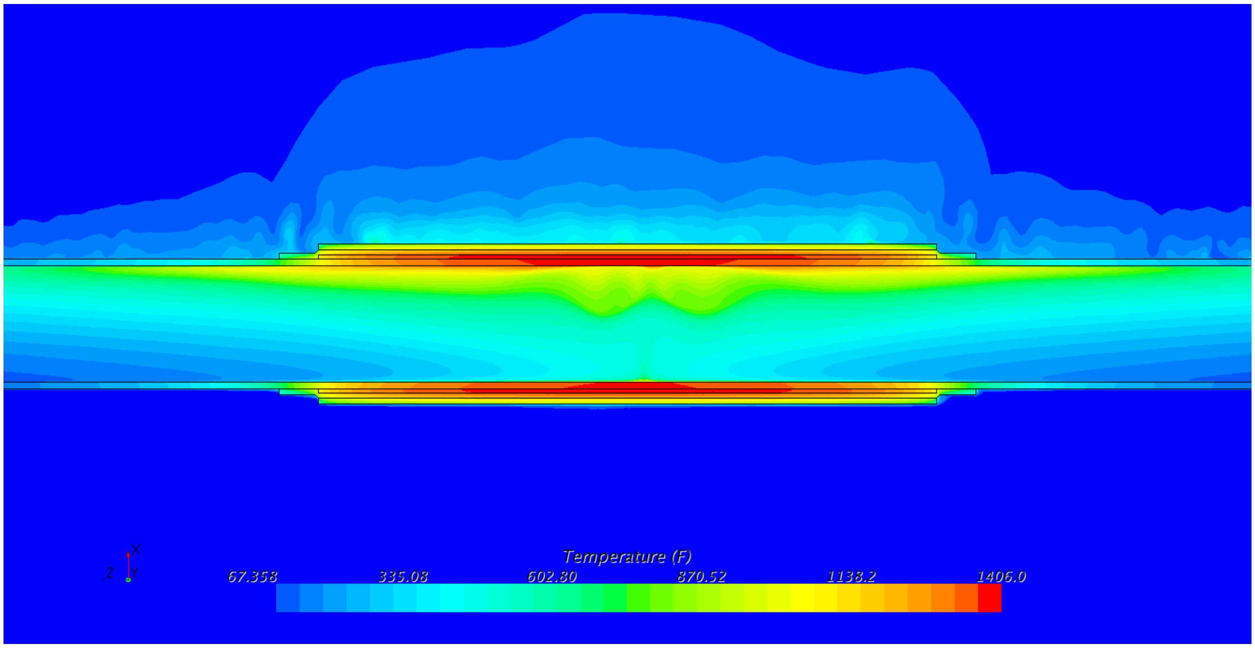

Figure B-75: Temperature contours in pipe wall (°F). 24 inch schedule 80

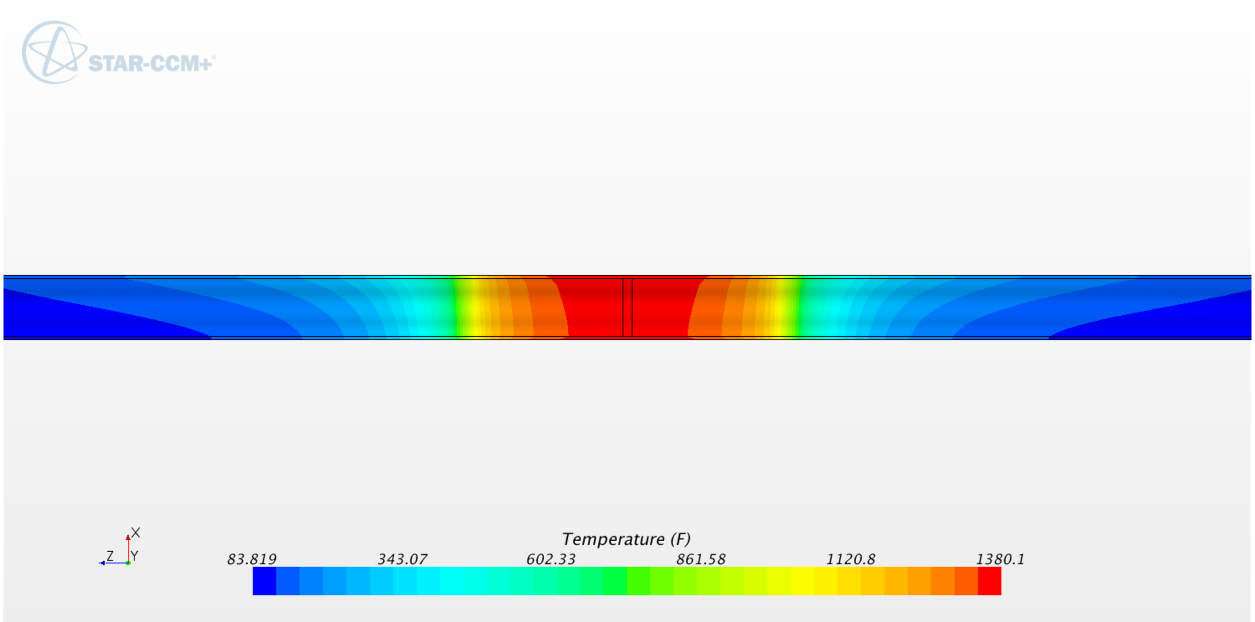

Figure B-76: Temperature contours in pipe wall, close-up (°F). 24 inch schedule 80

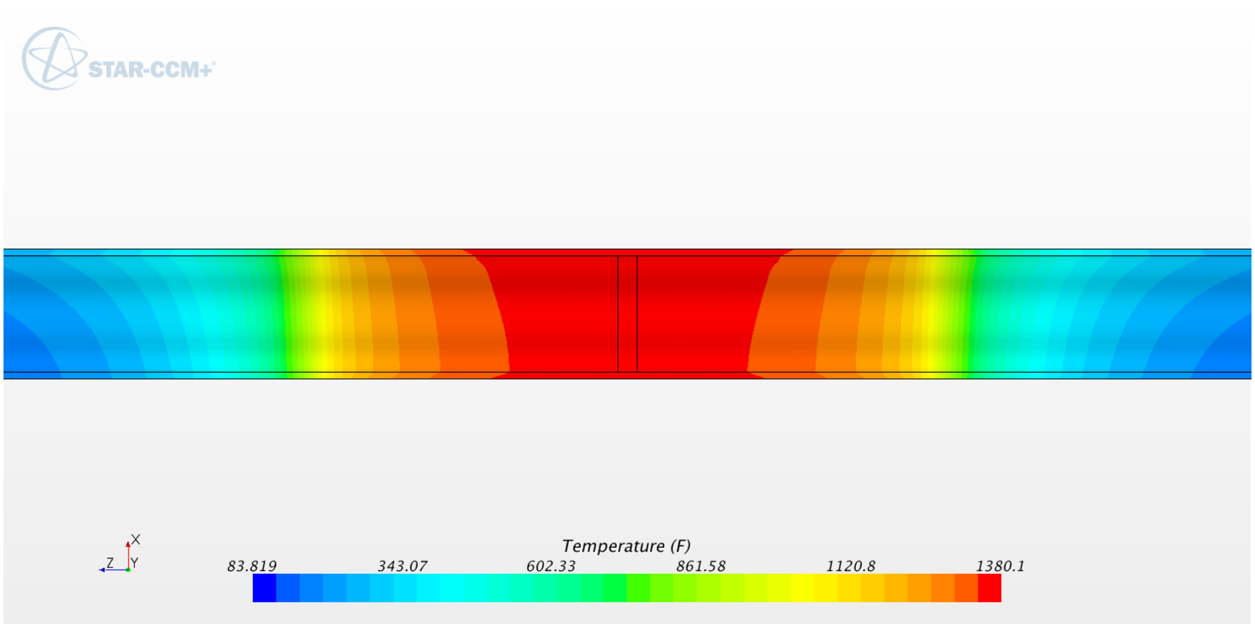

Figure B-77: Temperature contours in SB (°F). 24 inch schedule 80

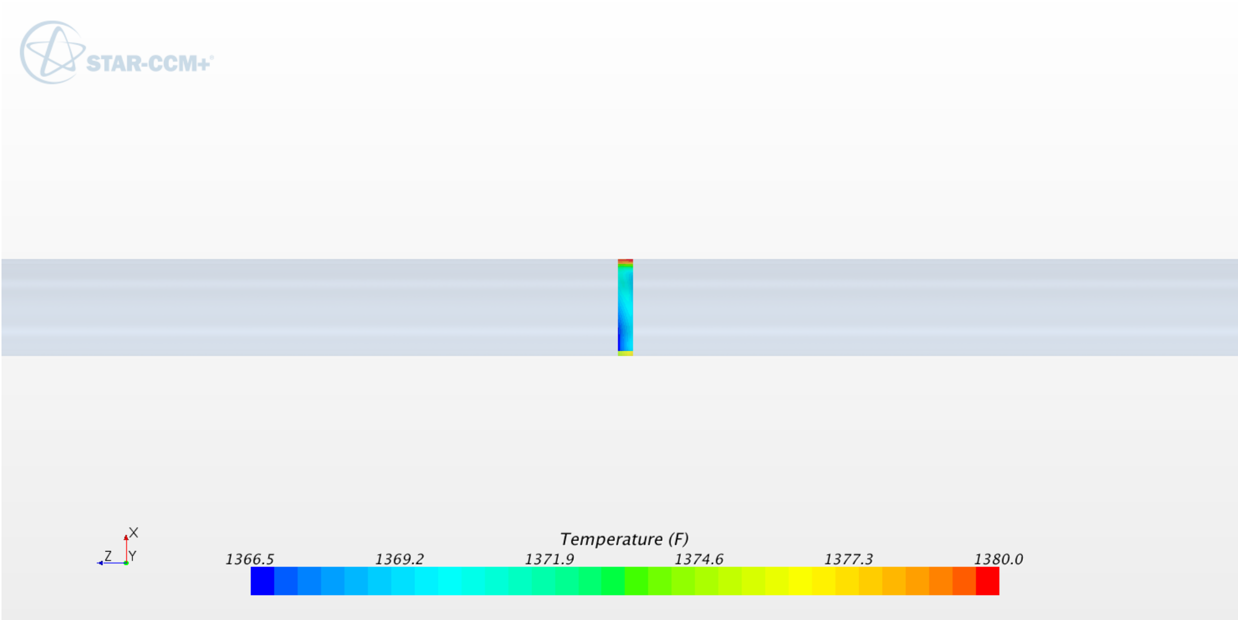

Figure B-78: Temperature contours in SB, isometric view (°F). 24 inch schedule 80

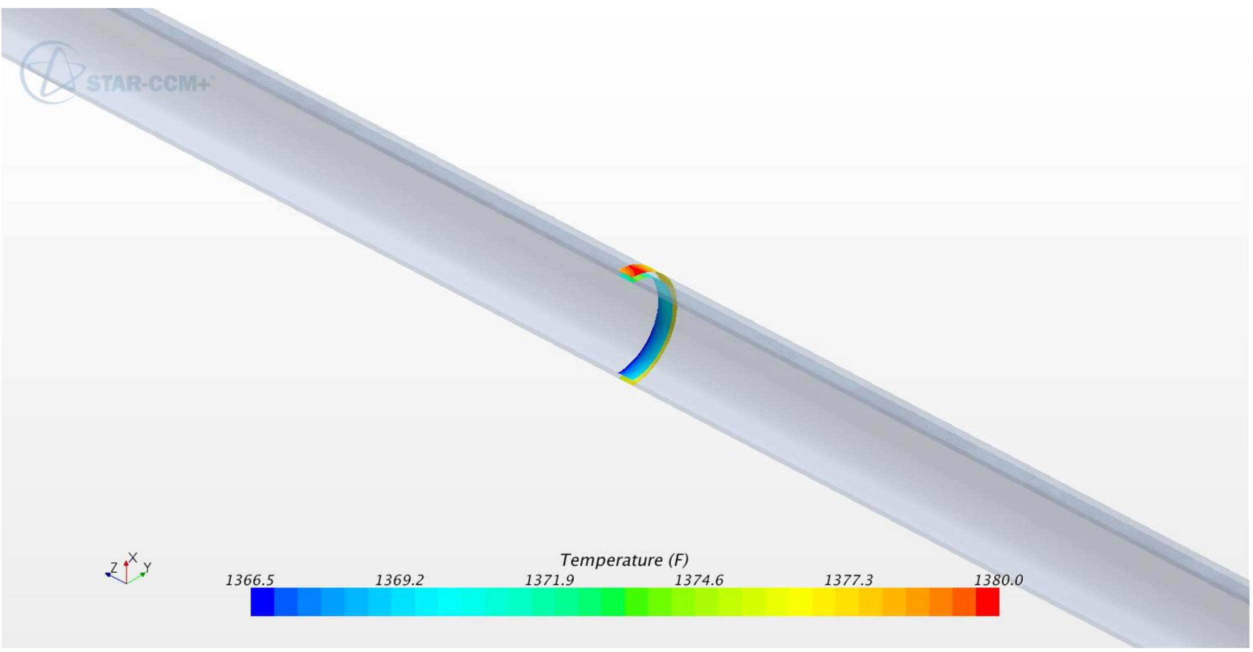

Figure B-79: Velocity contours, cross section of all regions (ft/s). 24 inch schedule 80

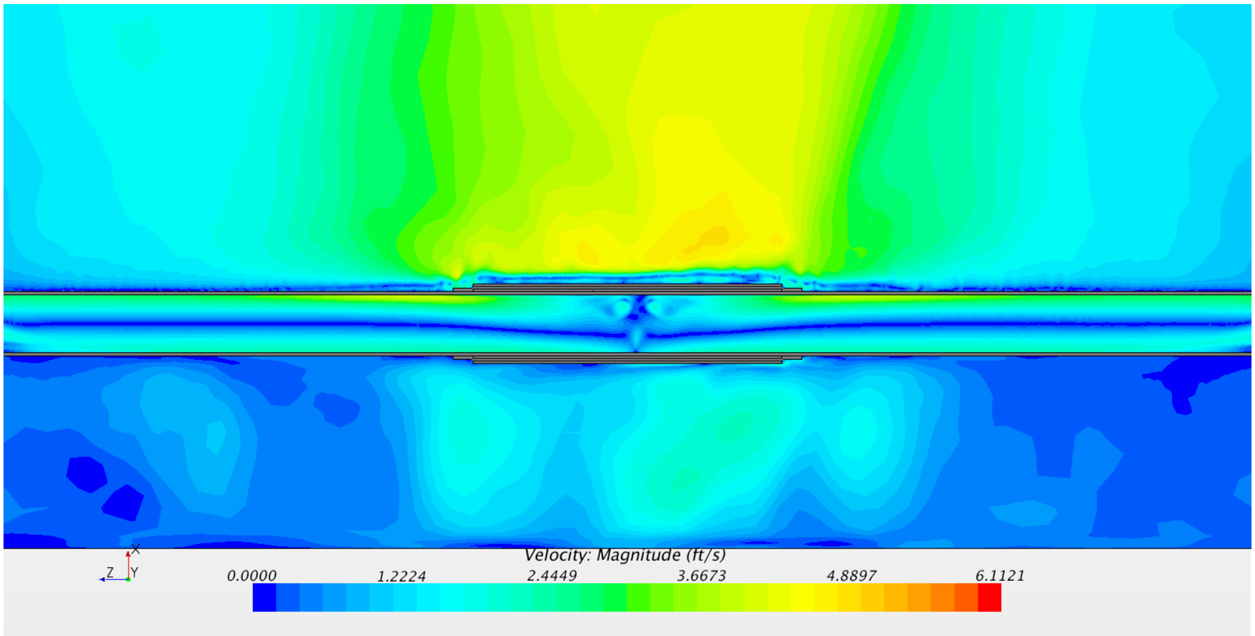

Figure B-80: Velocity contours, cross section of all regions, isometric view (ft/s). 24 inch schedule 80

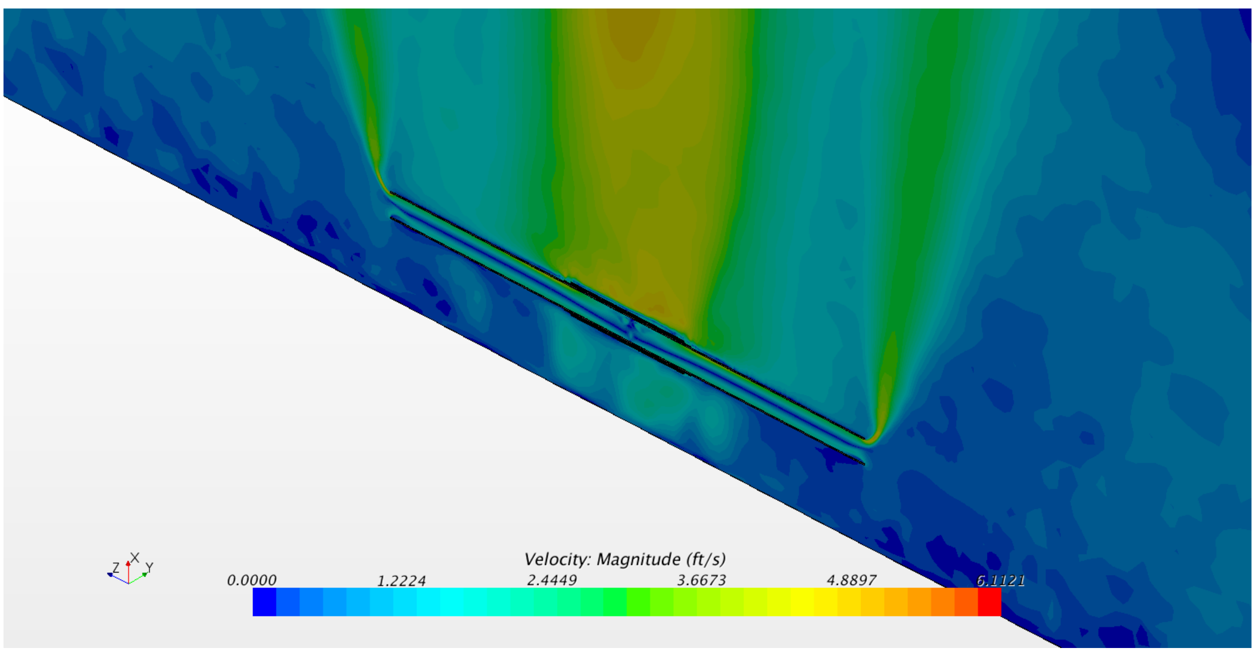

Figure B-81: Temperature contours, cross section of all regions (°F). 24 inch schedule 120

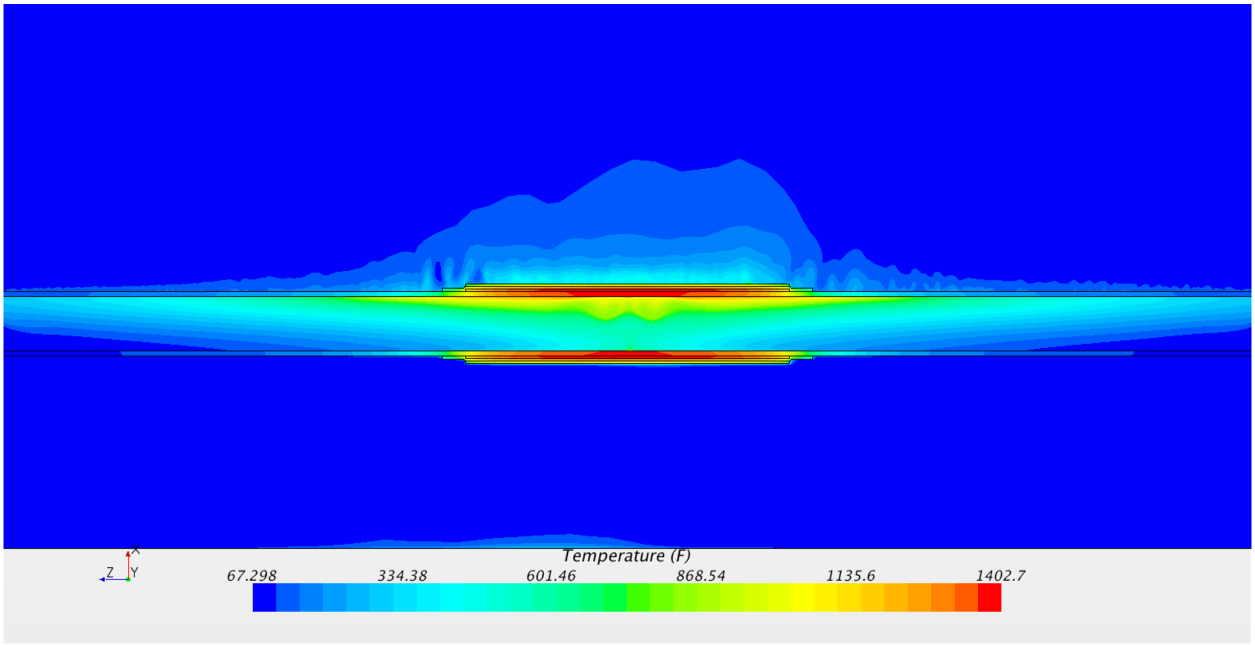

Figure B-82: Temperature contours, cross section of all regions, close-up (°F). 24 inch schedule 120

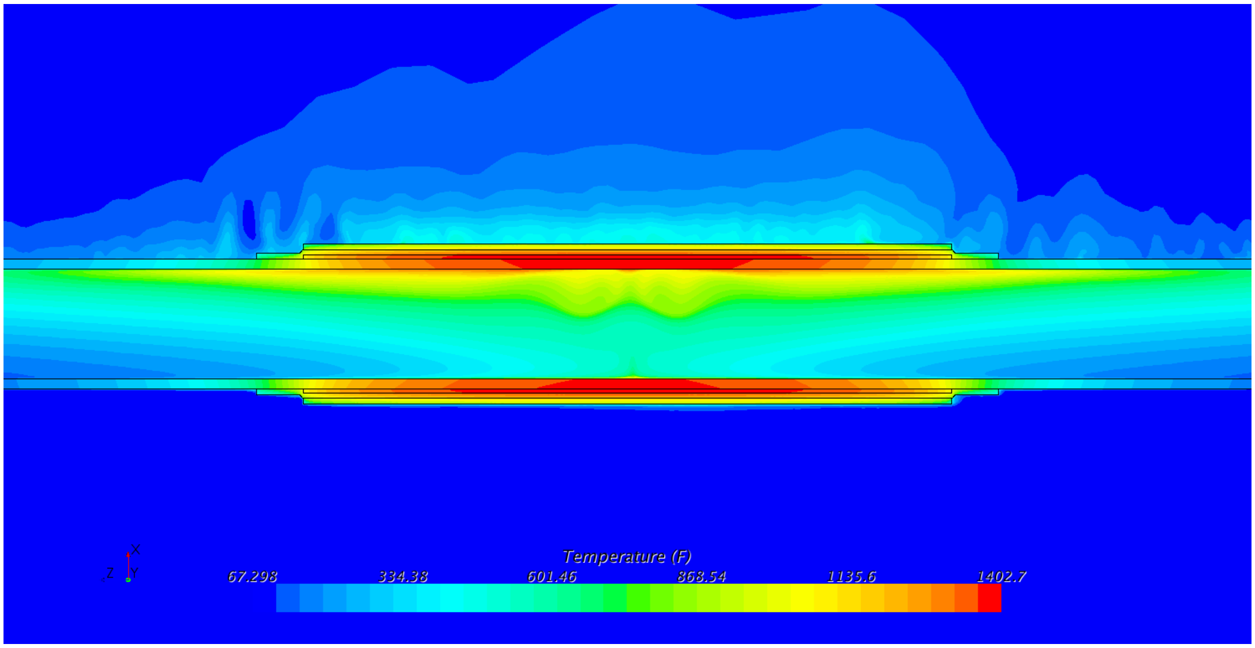

Figure B-83: Temperature contours in pipe wall (°F). 24 inch schedule 120

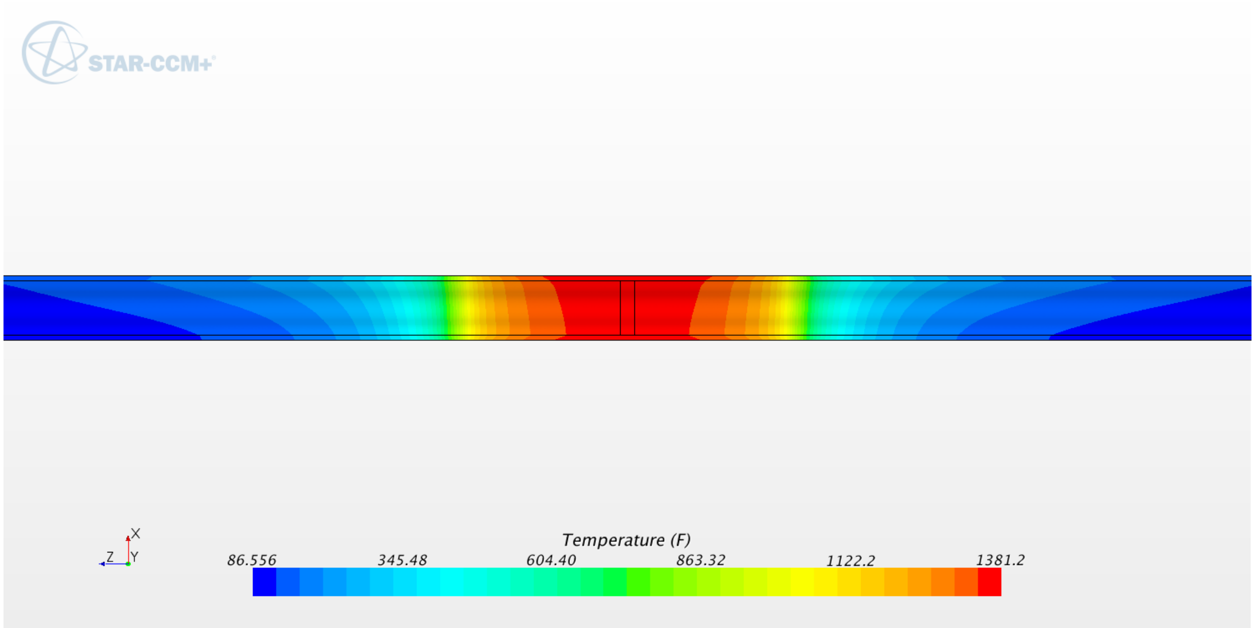

Figure B-84: Temperature contours in pipe wall, close-up (°F). 24 inch schedule 120

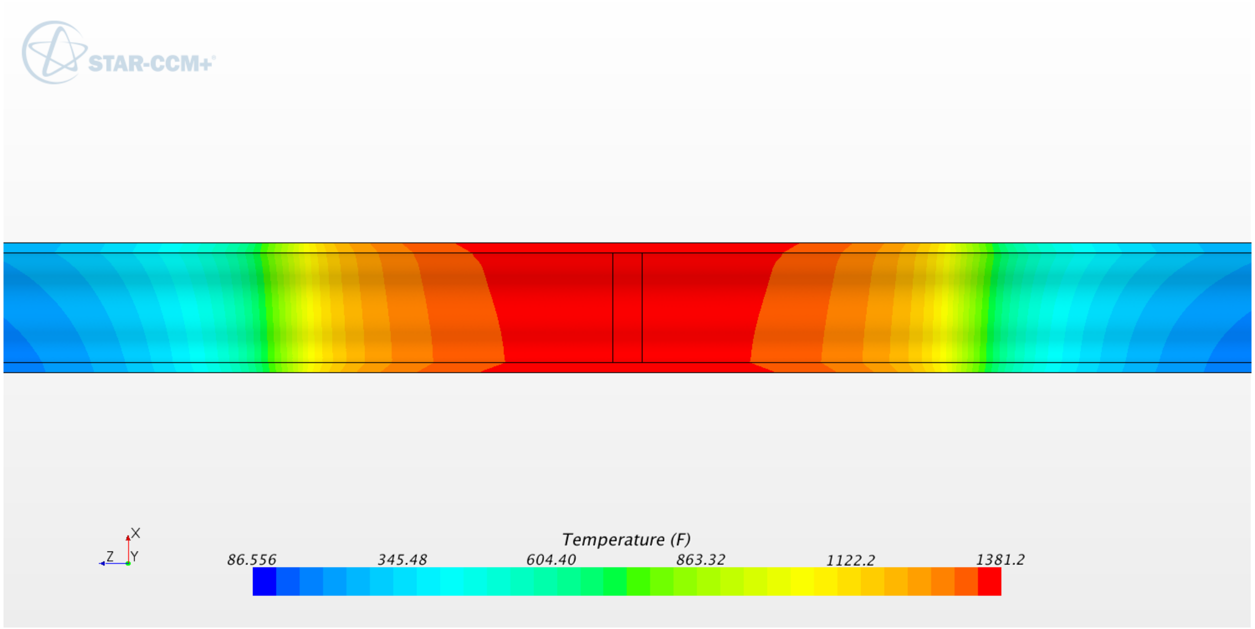

Figure B-85: Temperature contours in SB (°F). 24 inch schedule 120

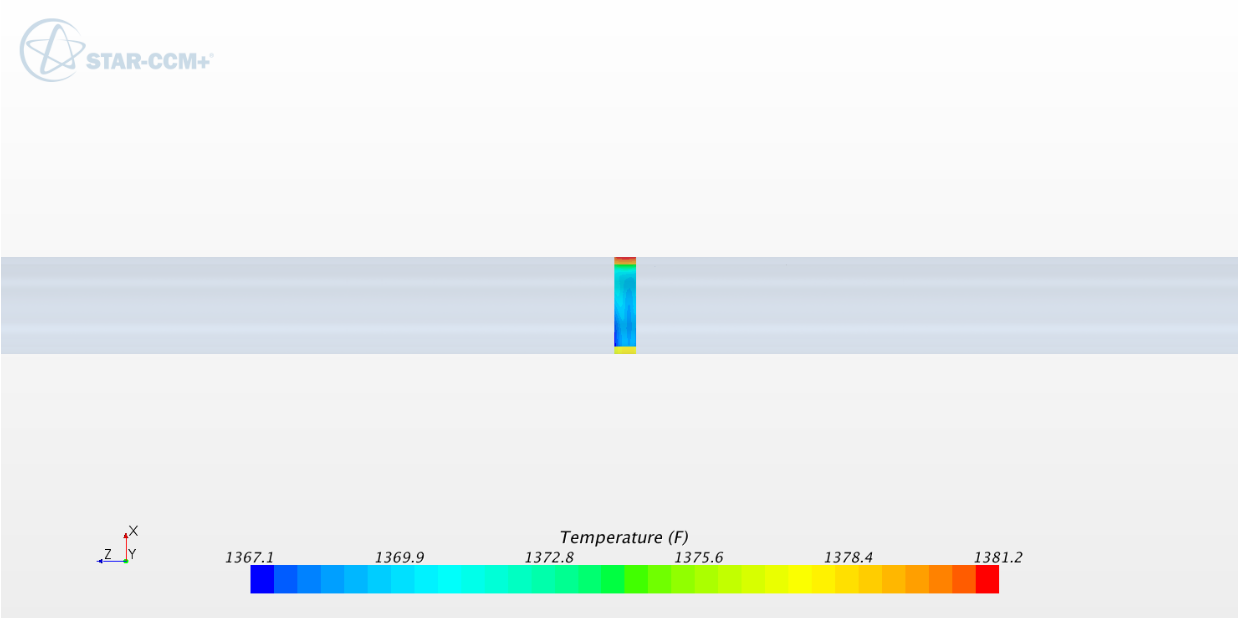

Figure B-86: Temperature contours in SB, isometric view (°F). 24 inch schedule 120

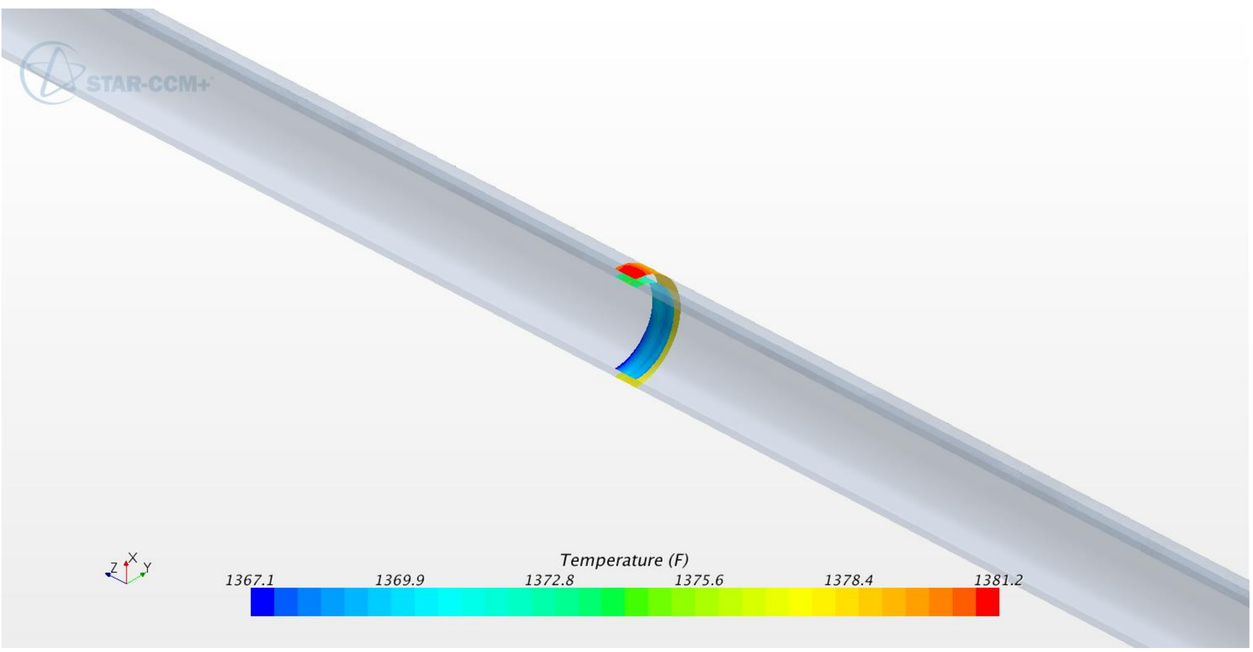

Figure B-87: Velocity contours, cross section of all regions (ft/s). 24 inch schedule 120

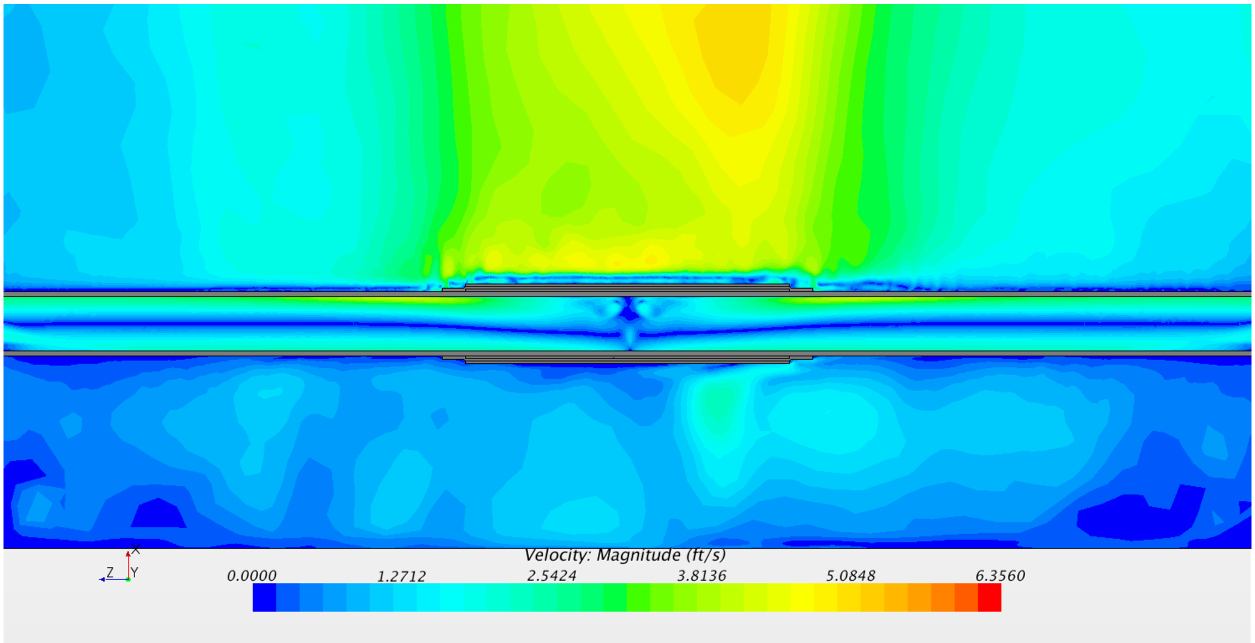

Figure B-88: Velocity contours, cross section of all regions, isometric view (ft/s). 24 inch schedule 120

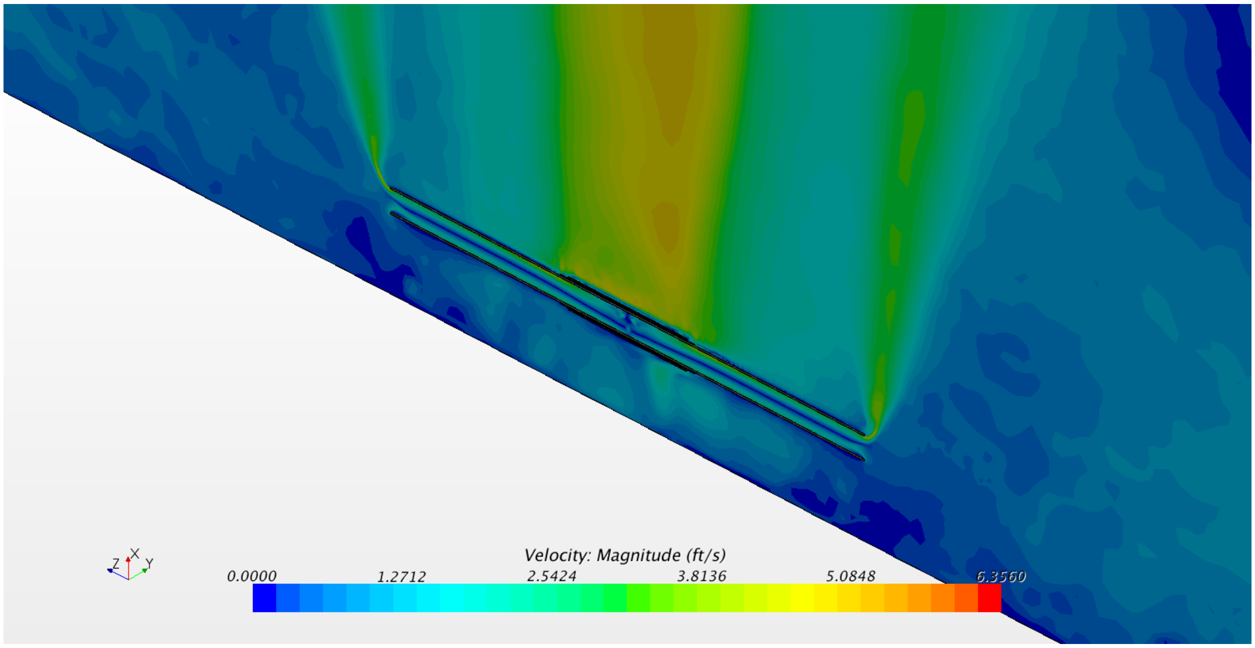

Figure B-89: Temperature contours, cross section of all regions (°F). 24 inch schedule 160

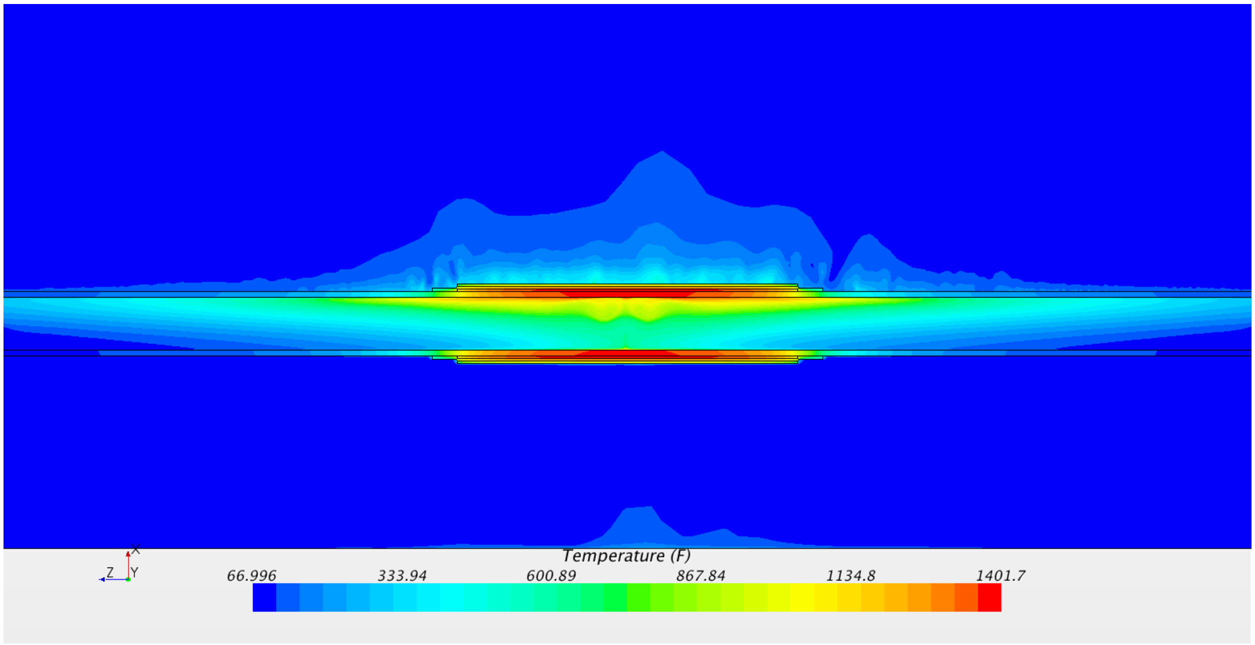

Figure B-90: Temperature contours, cross section of all regions, close-up (°F). 24 inch schedule 160

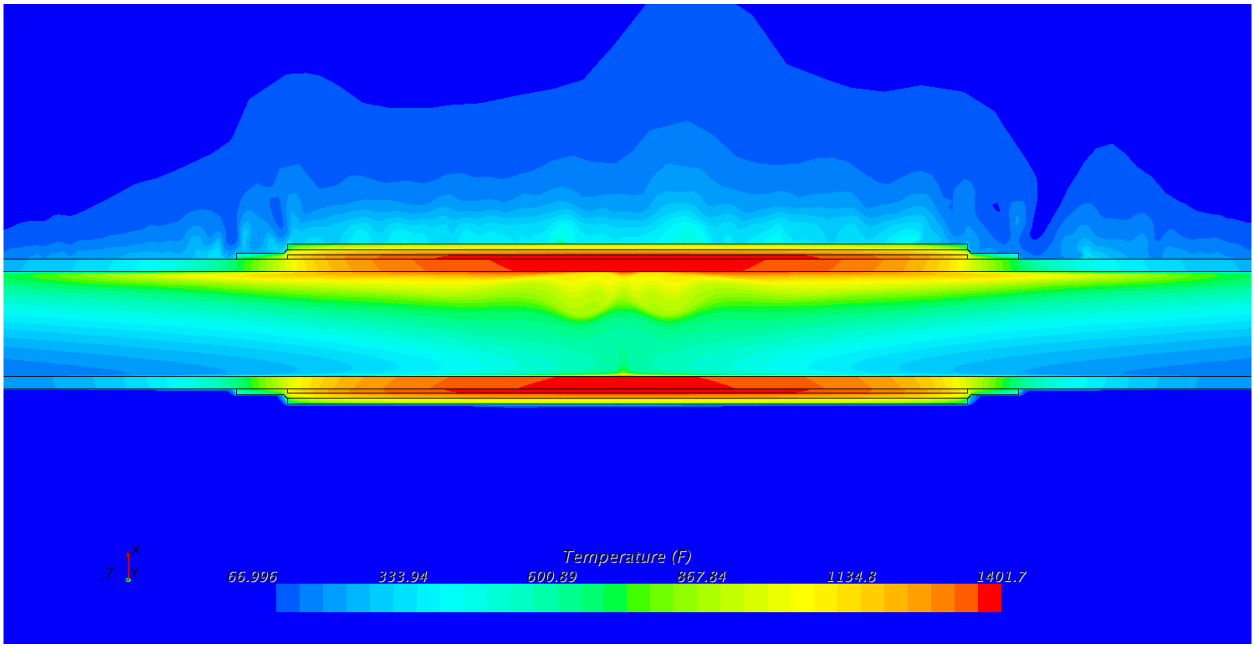

Figure B-91: Temperature contours in pipe wall (°F). 24 inch schedule 160

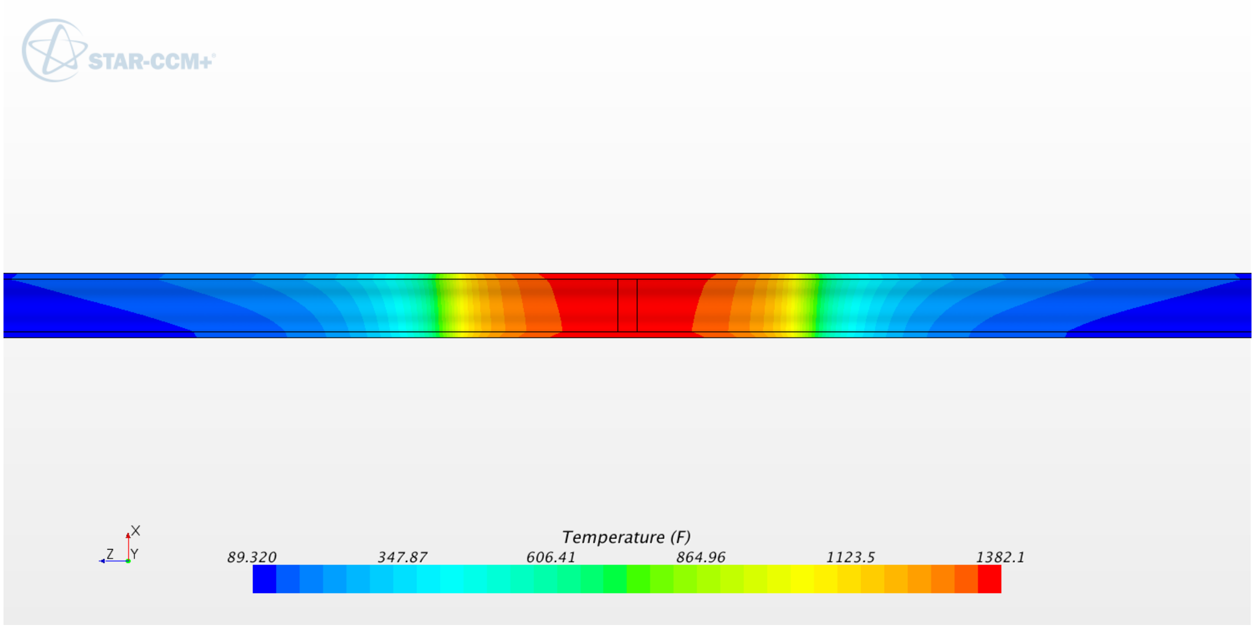

Figure B-92: Temperature contours in pipe wall, close-up (°F). 24 inch schedule 160

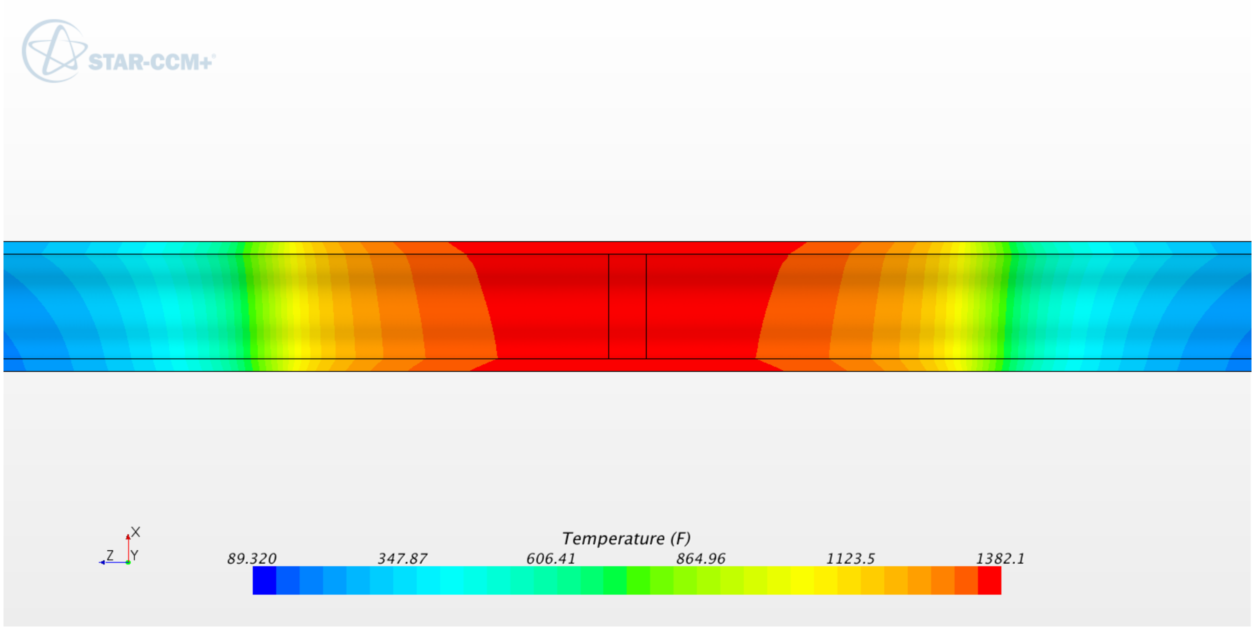

Figure B-93: Temperature contours in SB (°F). 24 inch schedule 160

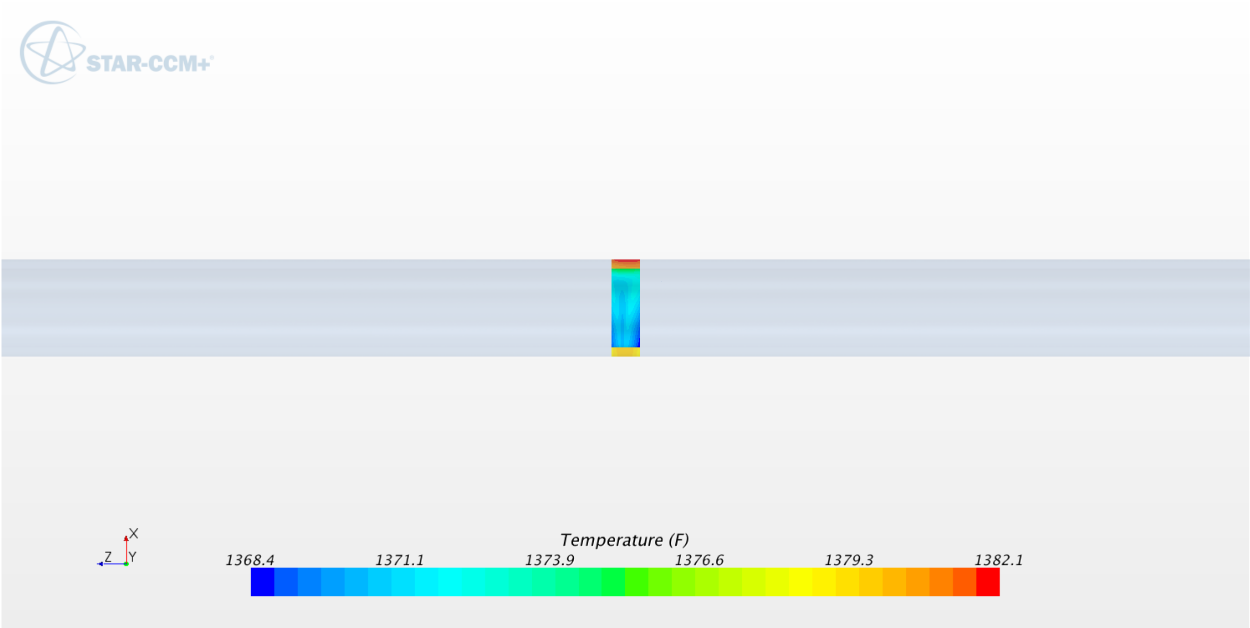

Figure B-94: Temperature contours in SB, isometric view (°F). 24 inch schedule 160

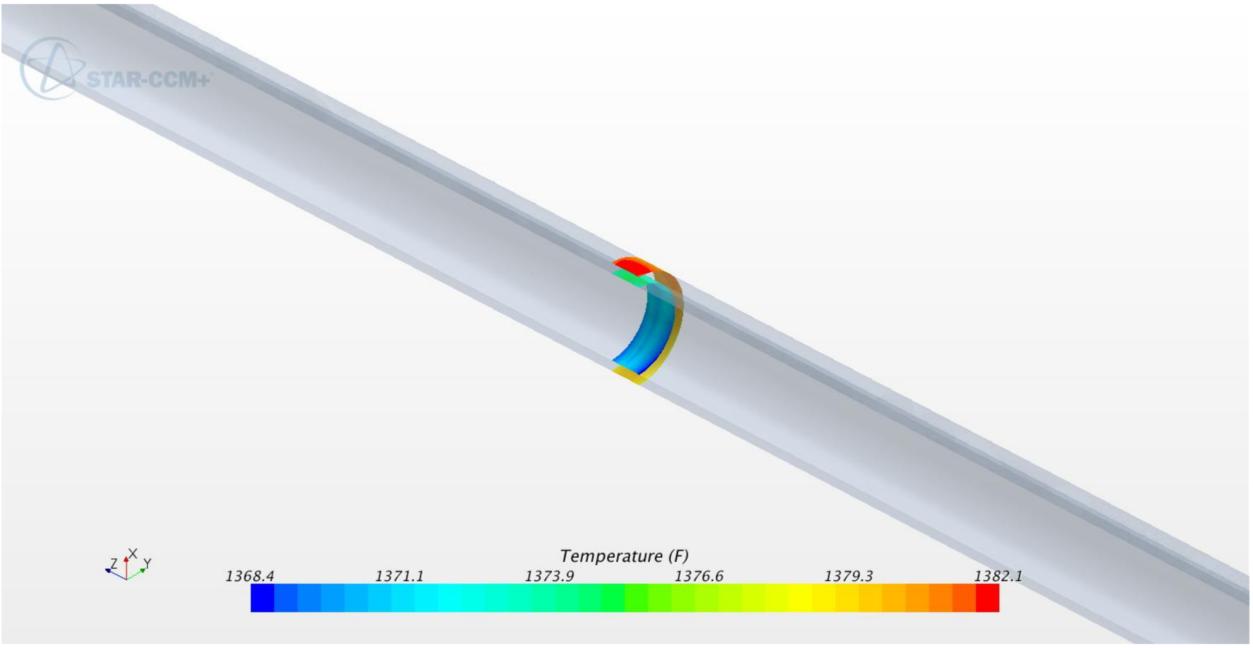

Figure B-95: Velocity contours, cross section of all regions (ft/s). 24 inch schedule 160

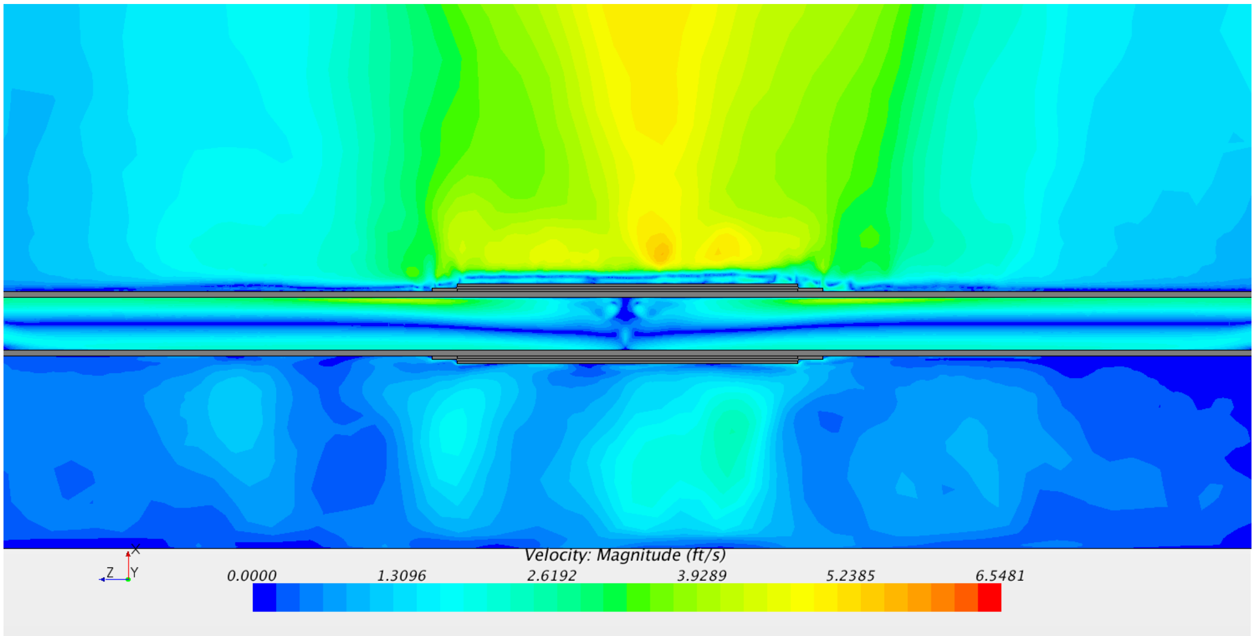

Figure B-96: Velocity contours, cross section of all regions, isometric view (ft/s). 24 inch schedule 160

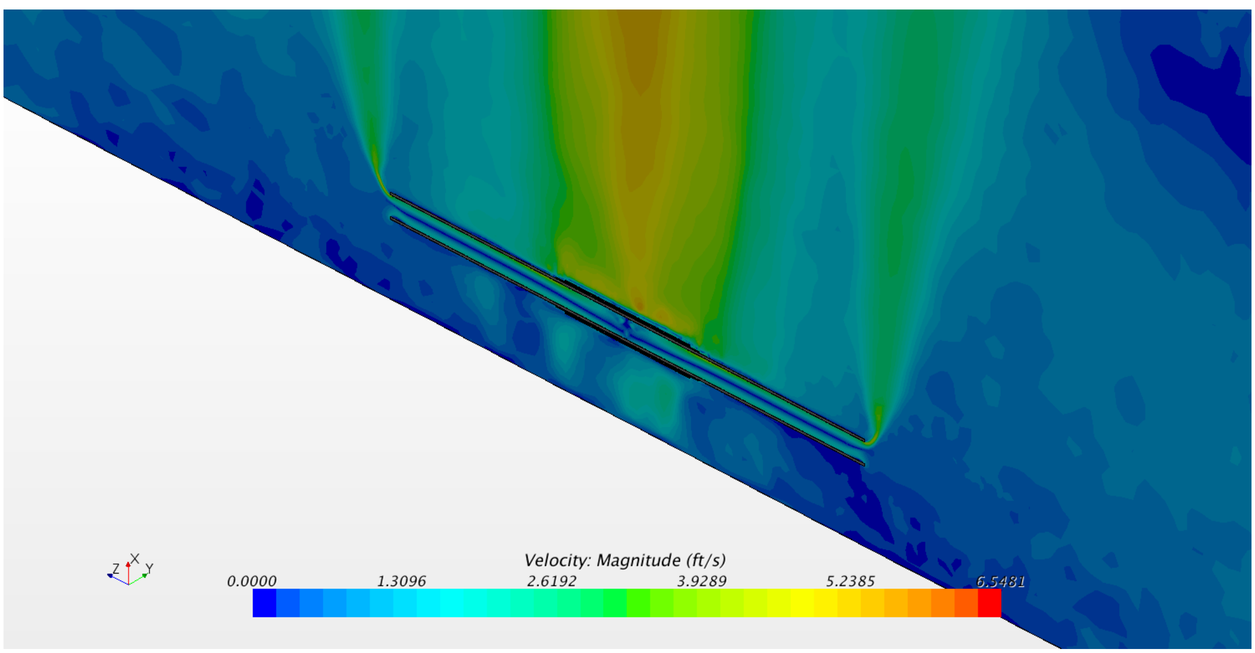

Figure B-97: Temperature contours, cross section of all regions (°F). 30 inch schedule 80

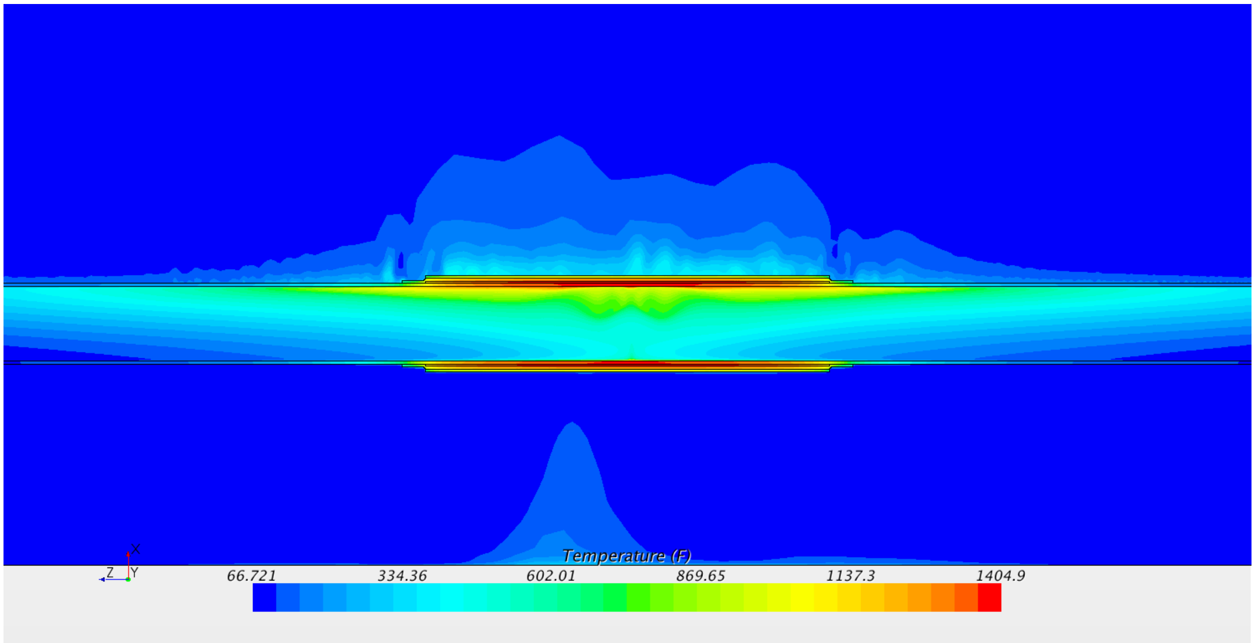

Figure B-98: Temperature contours, cross section of all regions, close-up (°F). 30 inch schedule 80

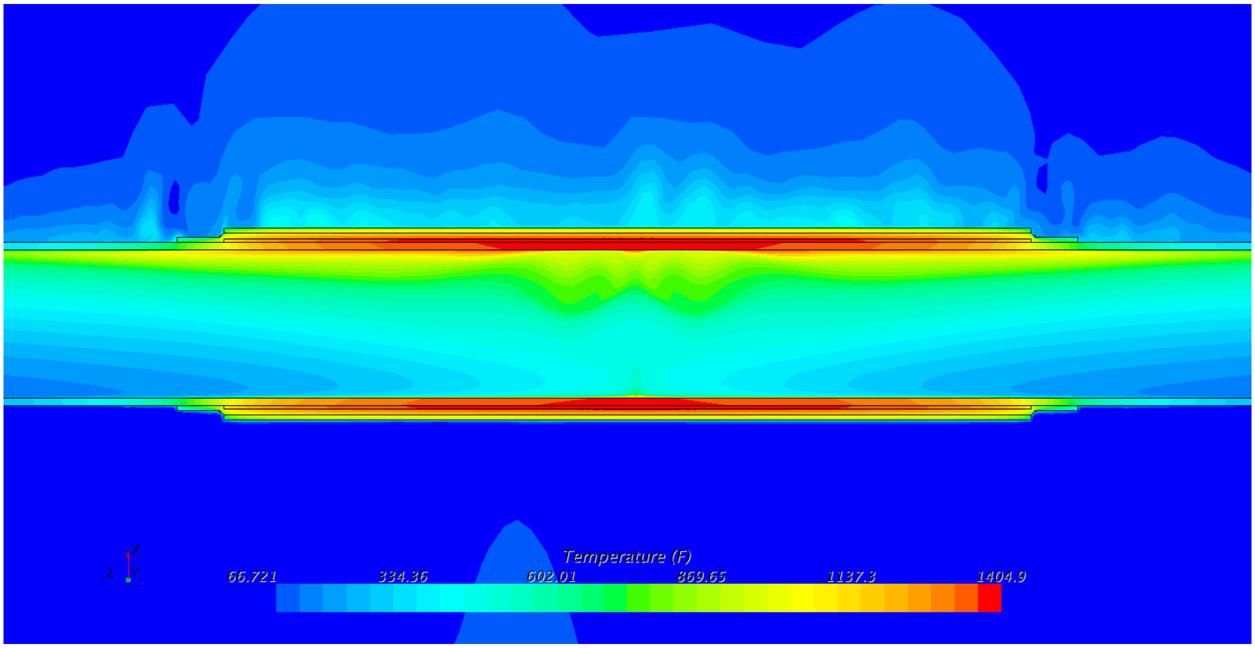

Figure B-99: Temperature contours in pipe wall (°F). 30 inch schedule 80

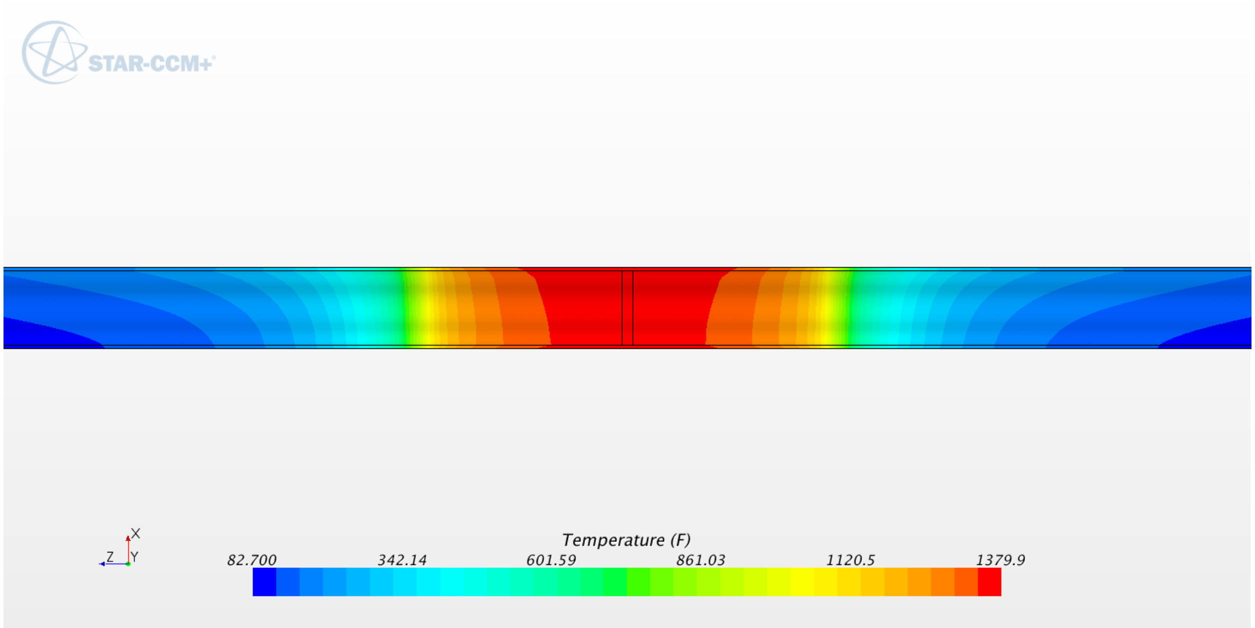

Figure B-100: Temperature contours in pipe wall, close-up (°F). 30 inch schedule 80

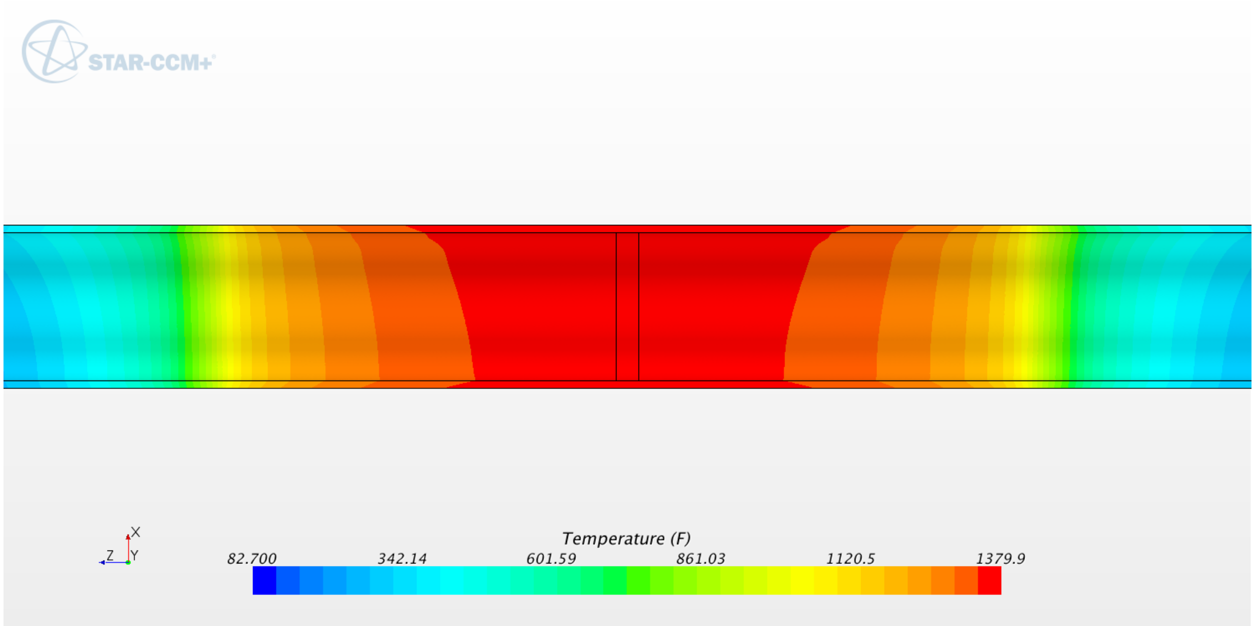

Figure B-101: Temperature contours in SB (°F). 30 inch schedule 80

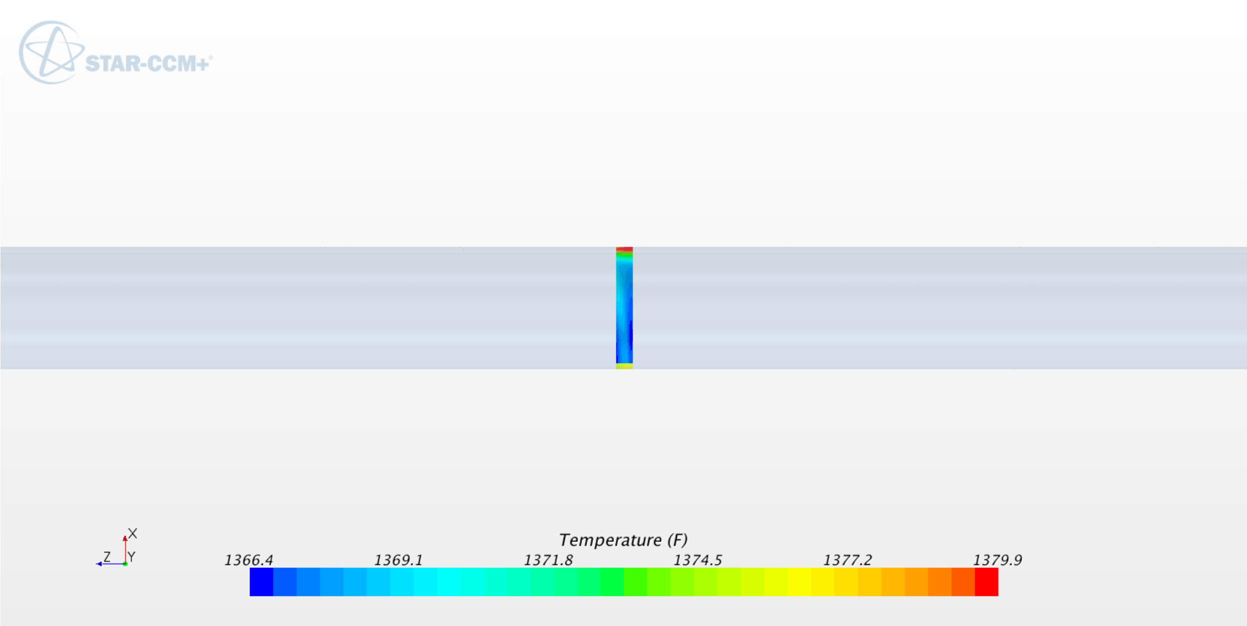

Figure B-102: Temperature contours in SB, isometric view (°F). 30 inch schedule 80

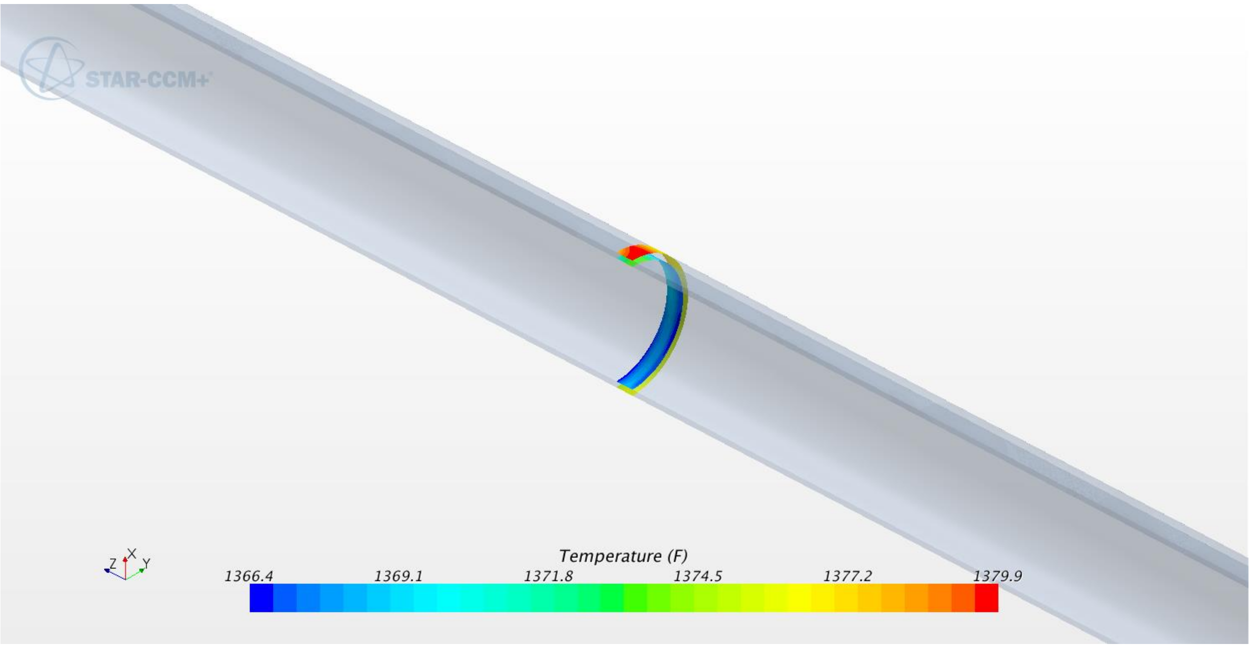

Figure B-103: Velocity contours, cross section of all regions (ft/s). 30 inch schedule 80

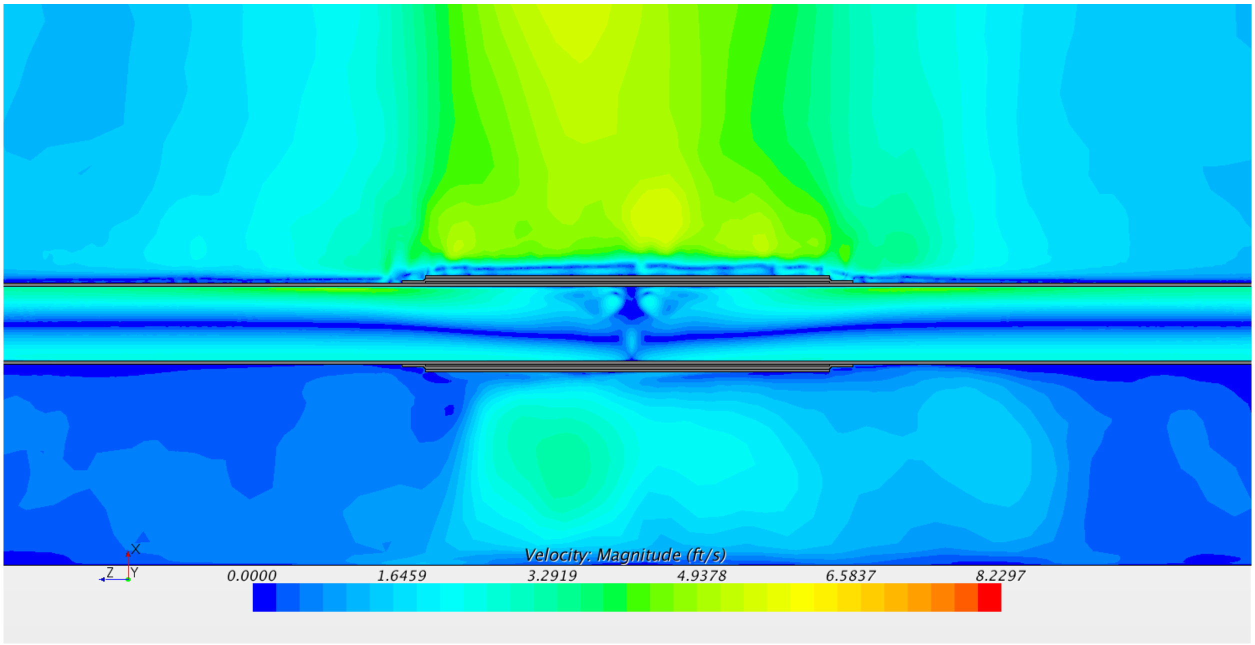

Figure B-104: Velocity contours, cross section of all regions, isometric view (ft/s). 30 inch schedule 80

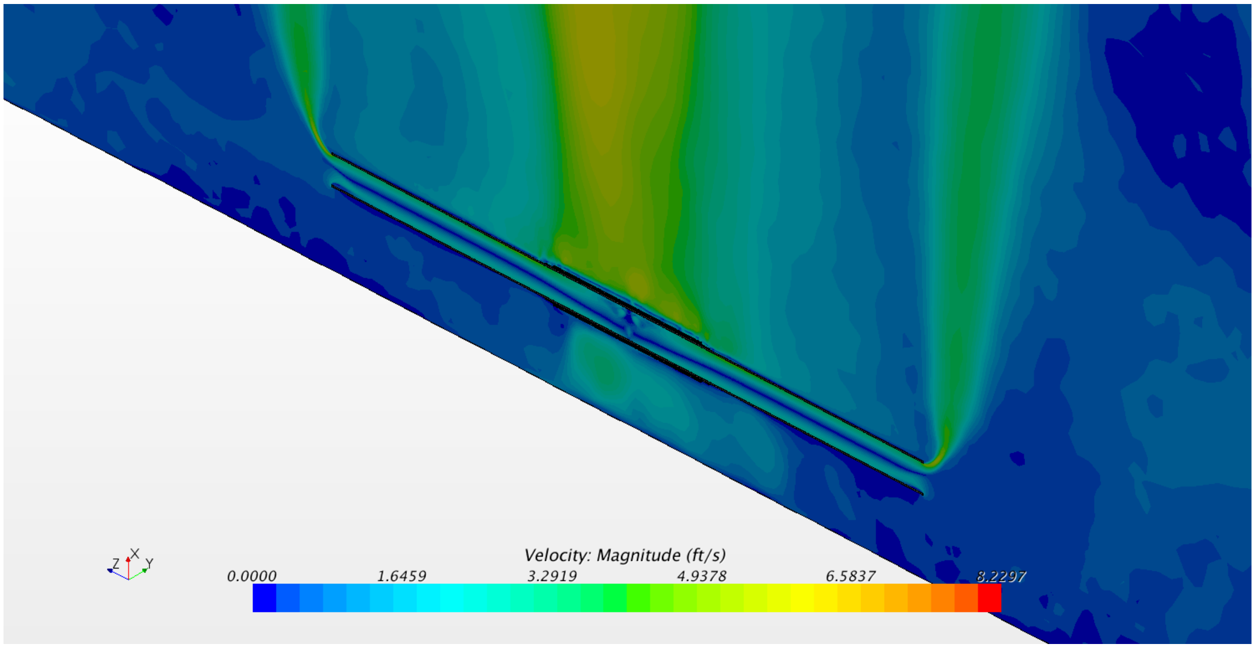

Figure B-105: Temperature contours, cross section of all regions (°F). 30 inch schedule 120

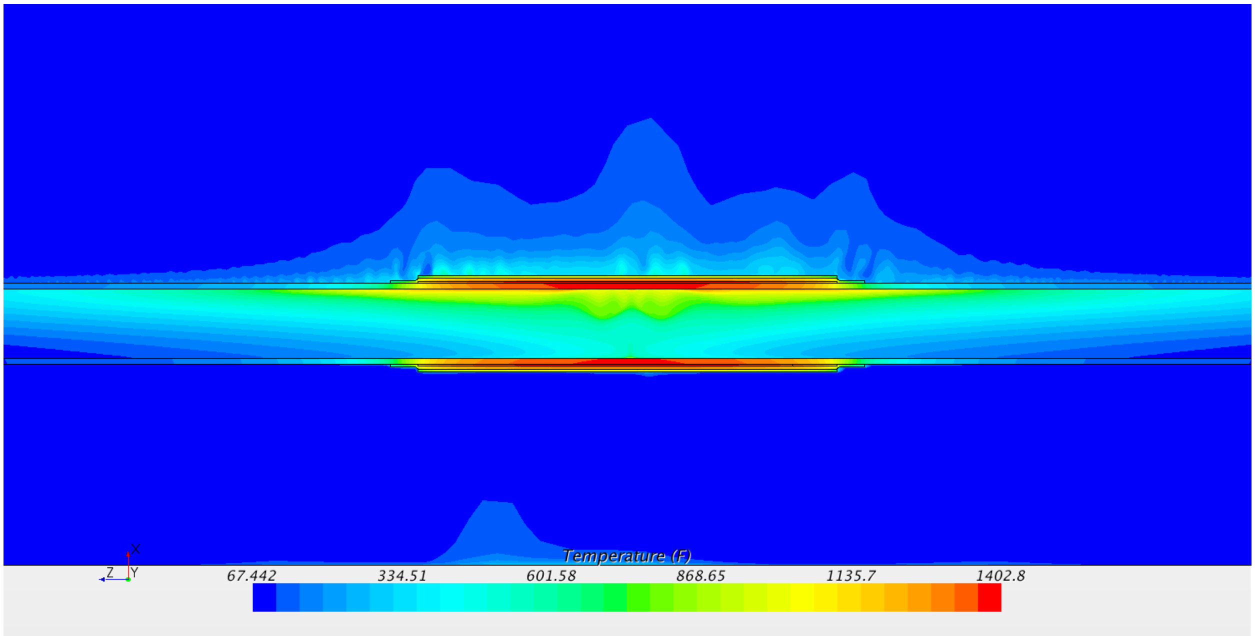

Figure B-106: Temperature contours, cross section of all regions, close-up (°F). 30 inch schedule 120

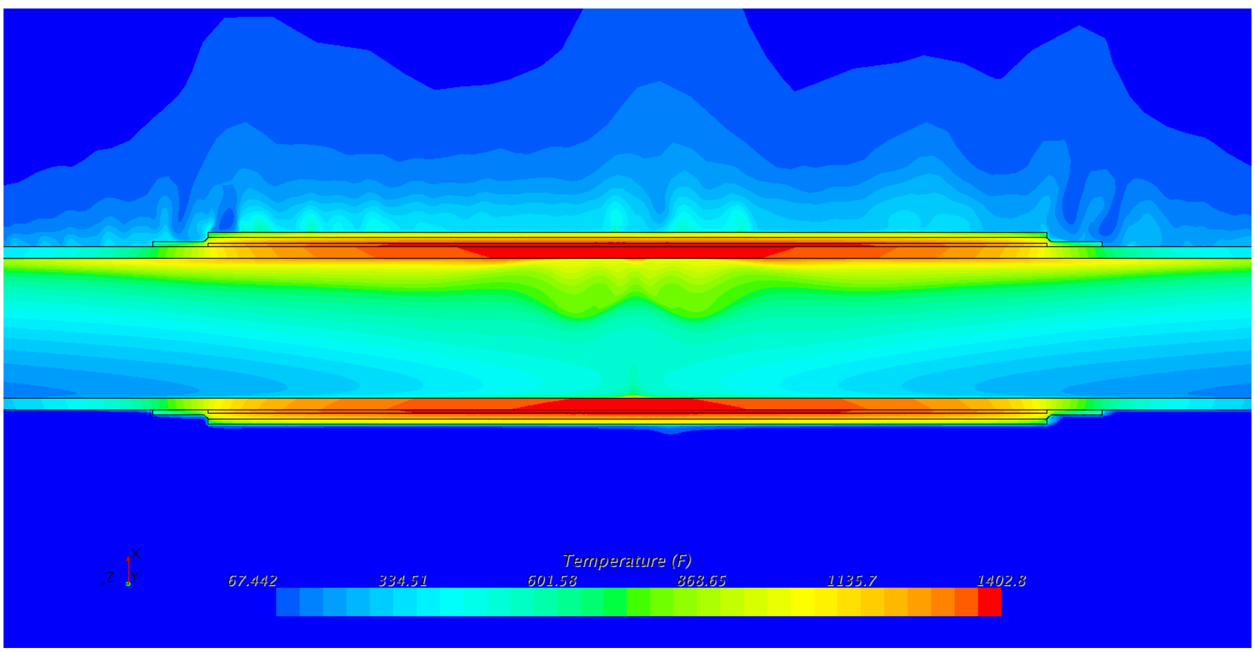

Figure B-107: Temperature contours in pipe wall (°F). 30 inch schedule 120

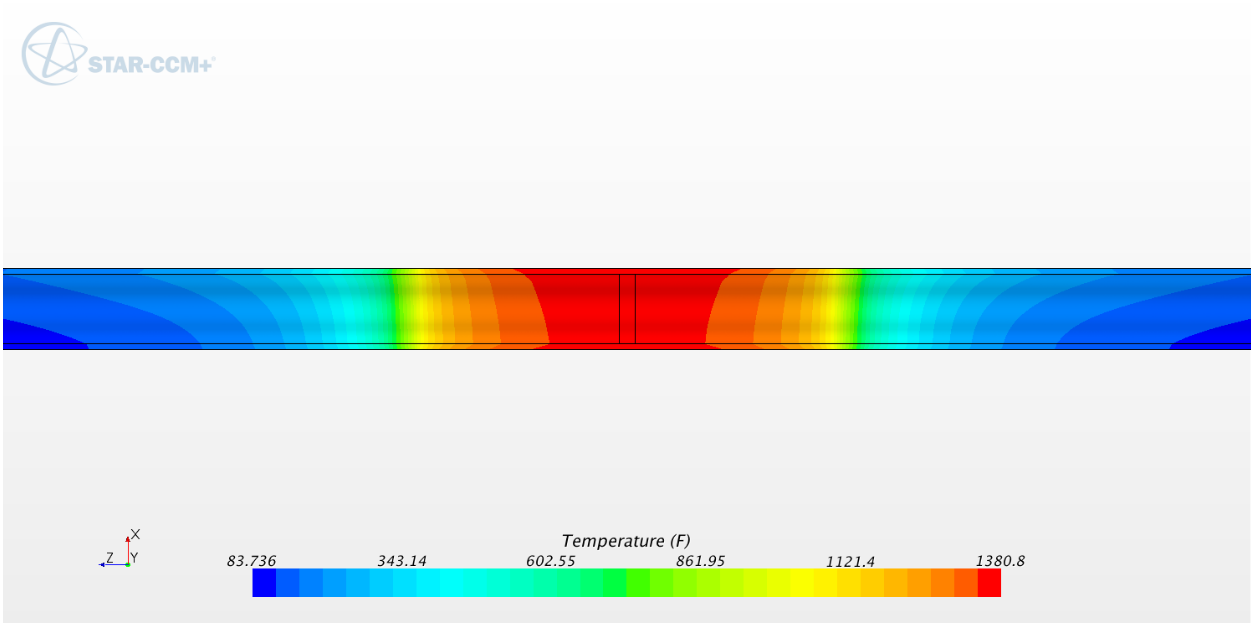

Figure B-108: Temperature contours in pipe wall, close-up (°F). 30 inch schedule 120

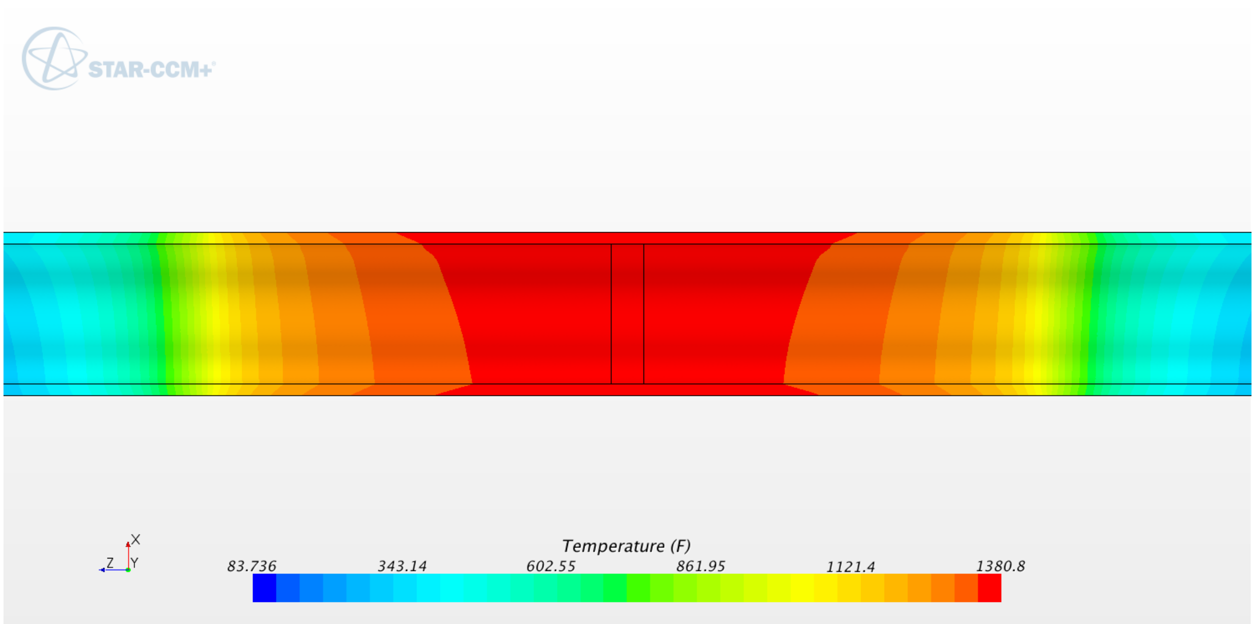

Figure B-109: Temperature contours in SB (°F). 30 inch schedule 120

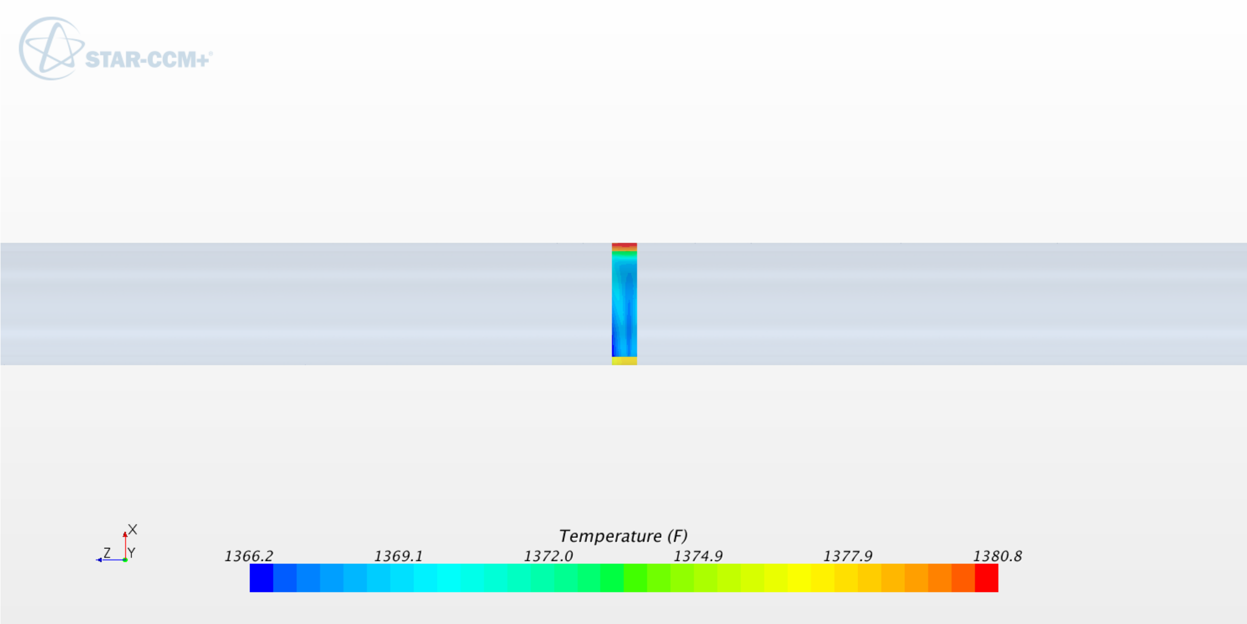

Figure B-110: Temperature contours in SB, isometric view (°F). 30 inch schedule 120

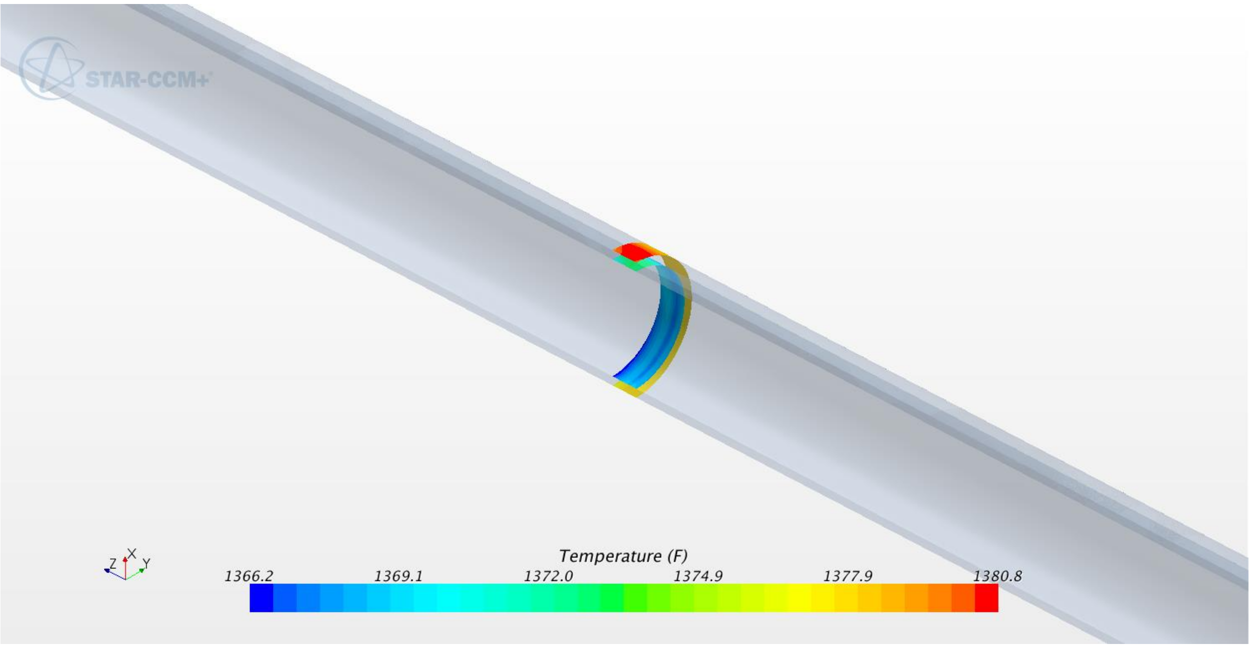

Figure B-111: Velocity contours, cross section of all regions (ft/s). 30 inch schedule 120

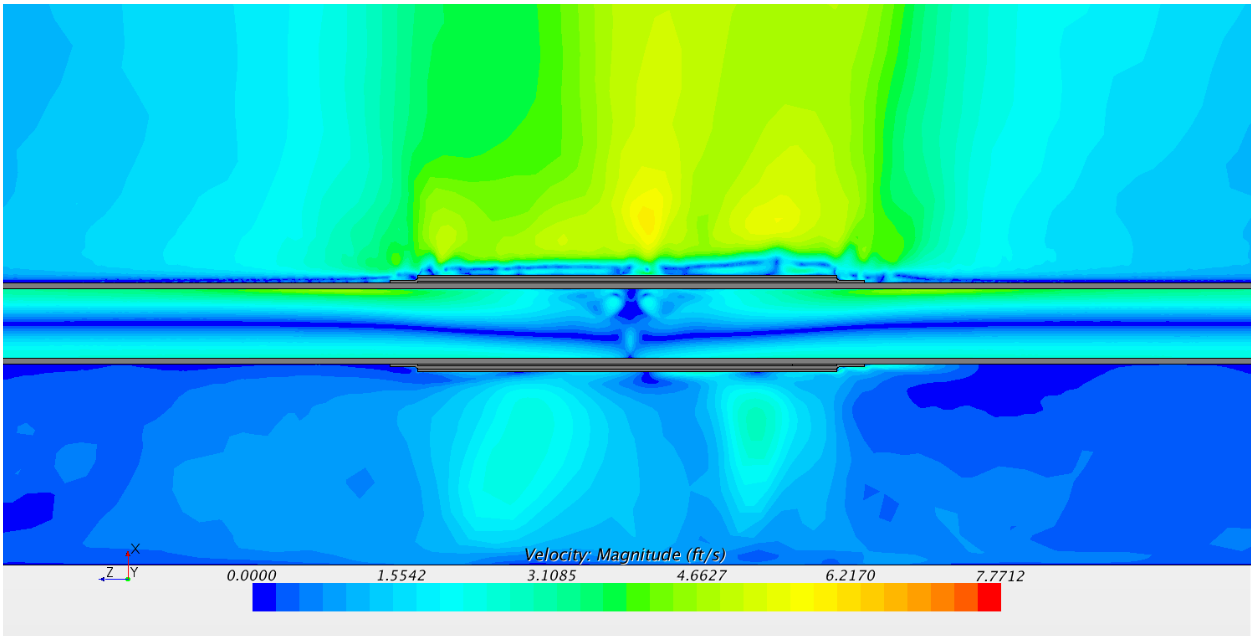

Figure B-112: Velocity contours, cross section of all regions, isometric view (ft/s). 30 inch schedule 120

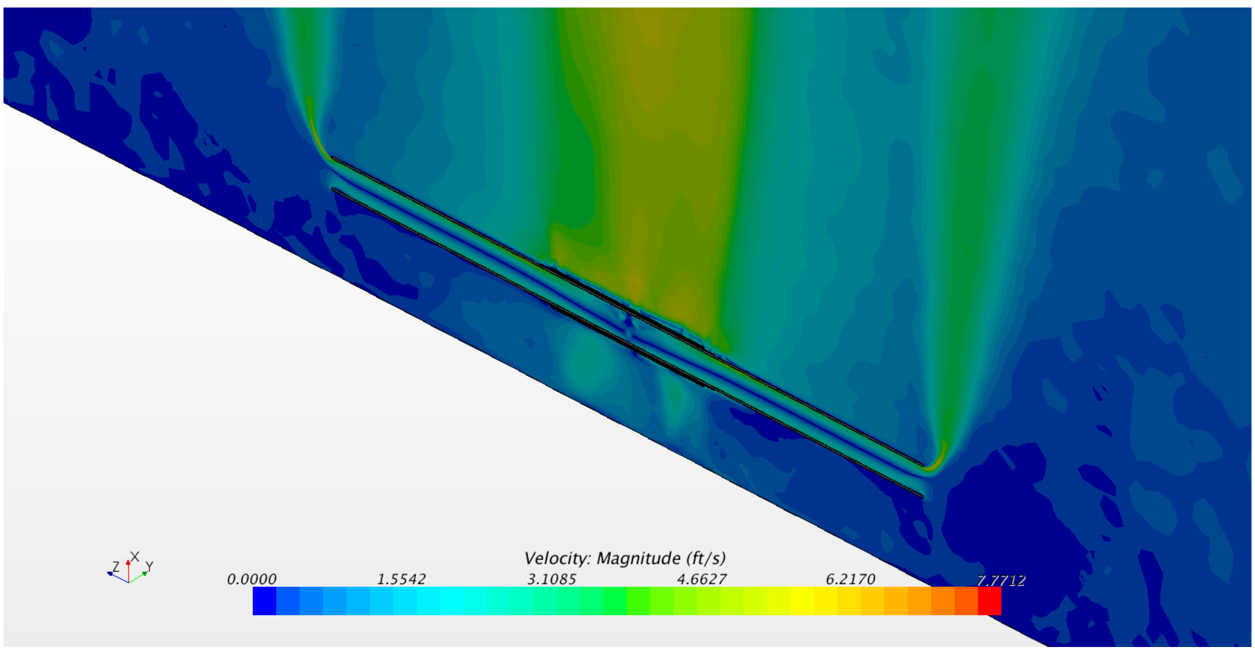

Figure B-113: Temperature contours, cross section of all regions (°F). 30 inch schedule 160

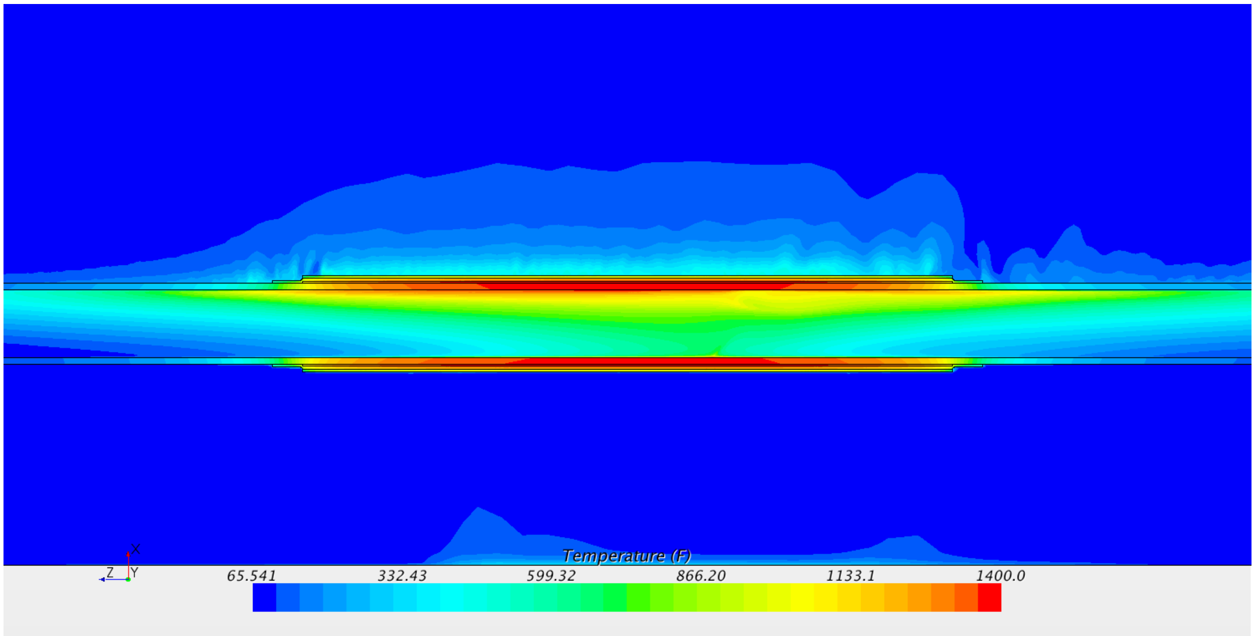

Figure B-114: Temperature contours, cross section of all regions, close-up (°F). 30 inch schedule 160

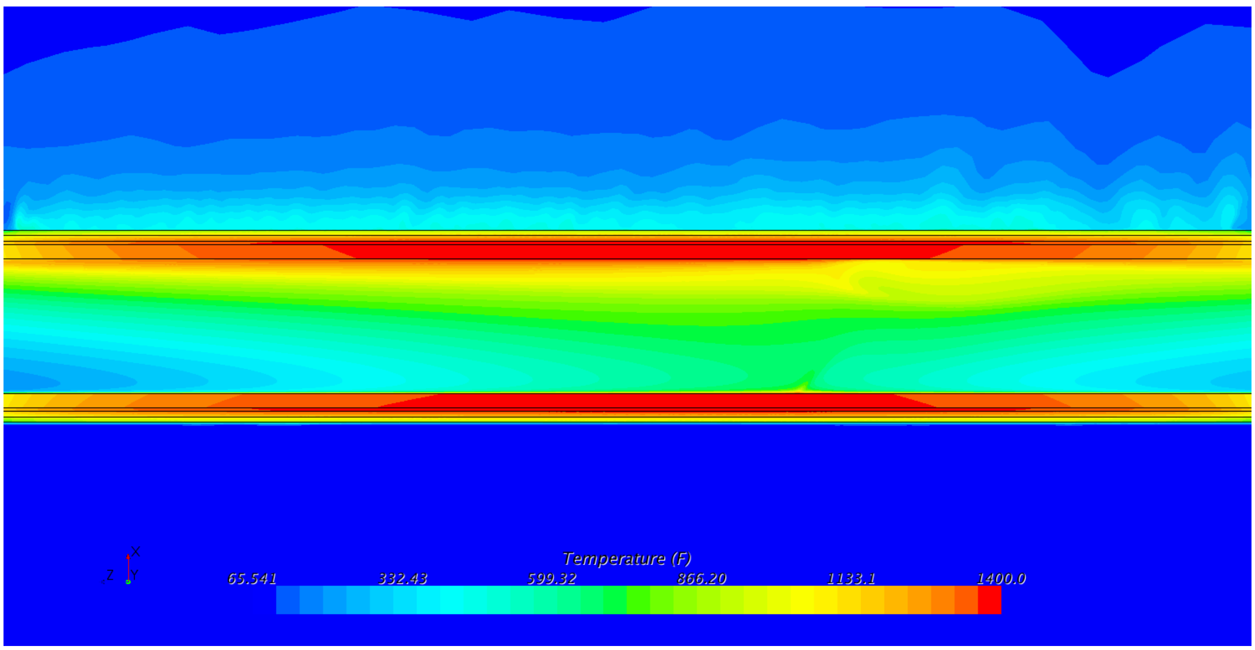

Figure B-115: Temperature contours in pipe wall (°F). 30 inch schedule 160

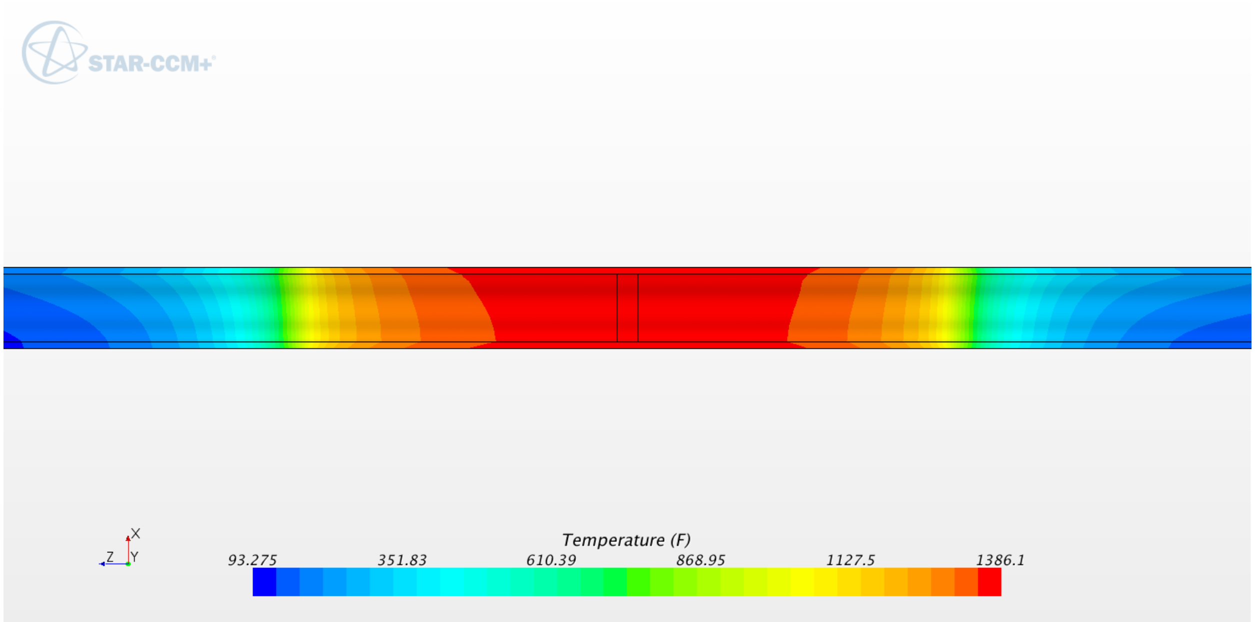

Figure B-116: Temperature contours in pipe wall, close-up (°F). 30 inch schedule 160

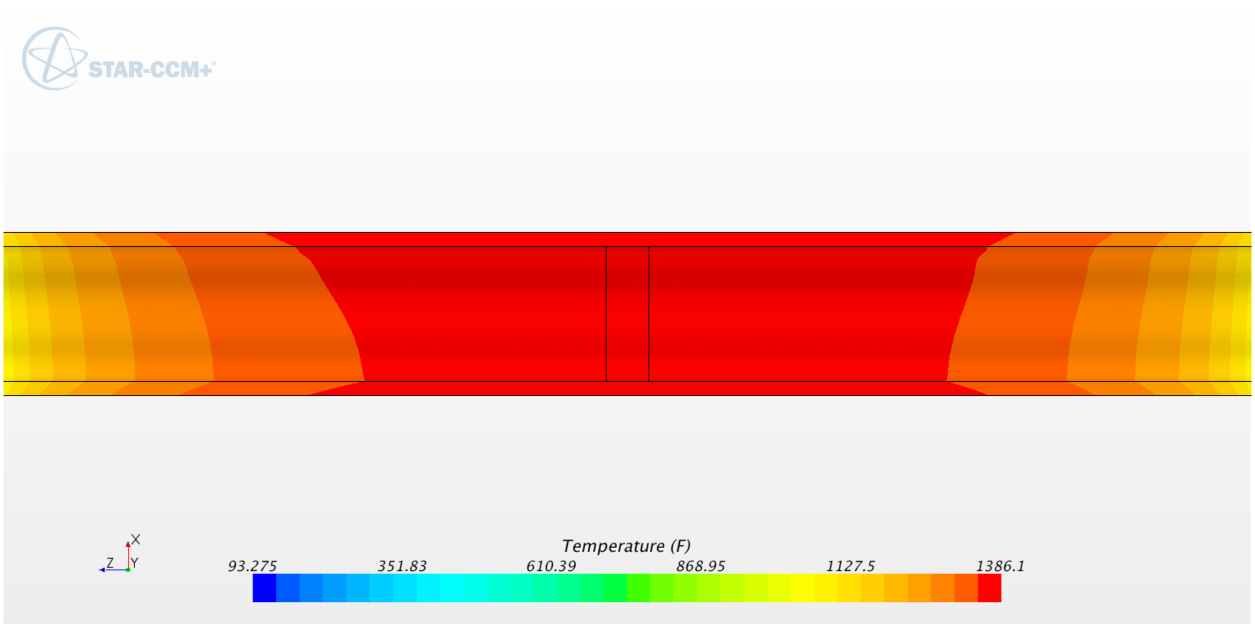

Figure B-117: Temperature contours in SB (°F). 30 inch schedule 160

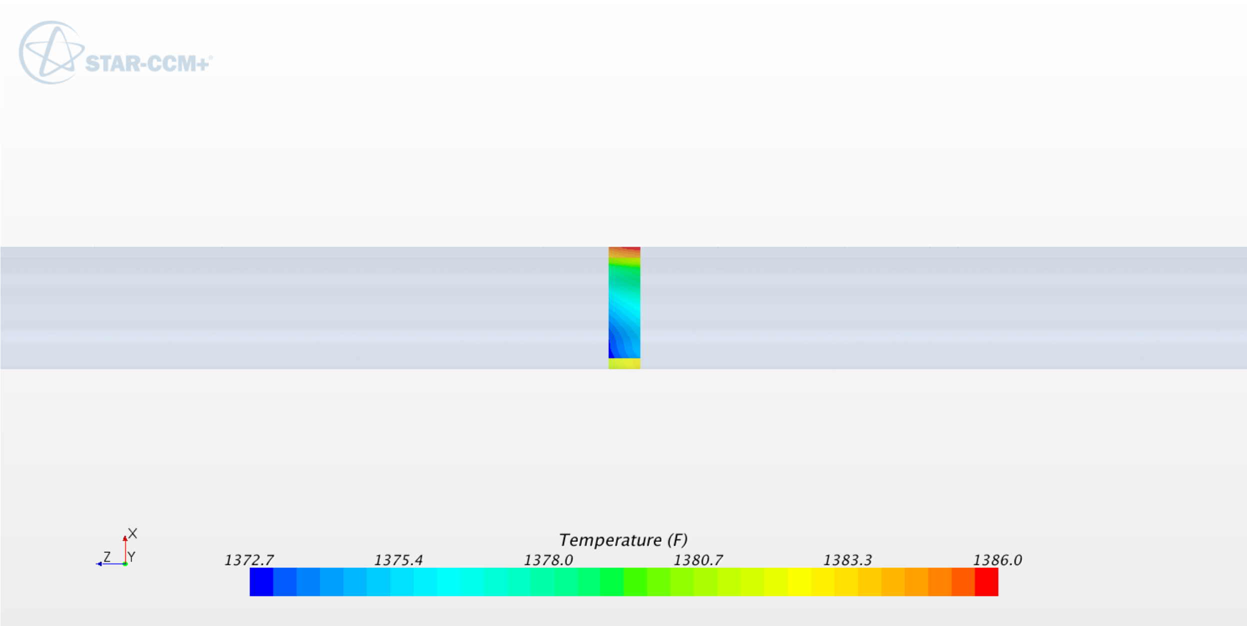

Figure B-118: Temperature contours in SB, isometric view (°F). 30 inch schedule 160

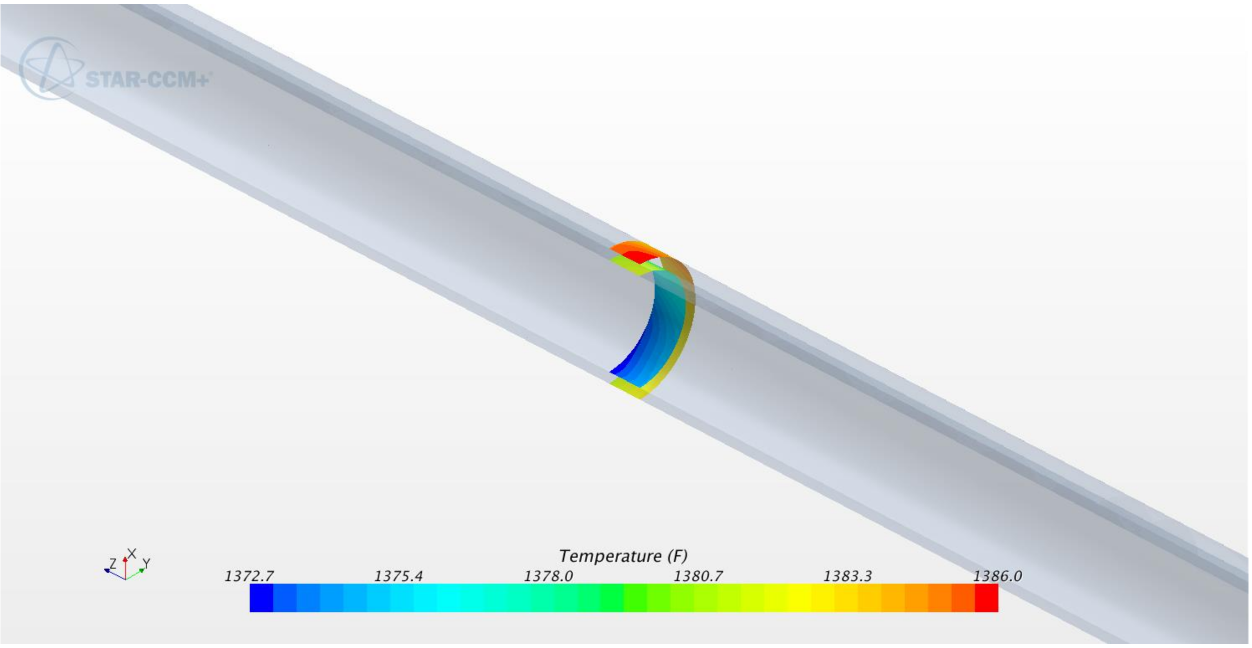

Figure B-119: Velocity contours, cross section of all regions (ft/s). 30 inch schedule 160

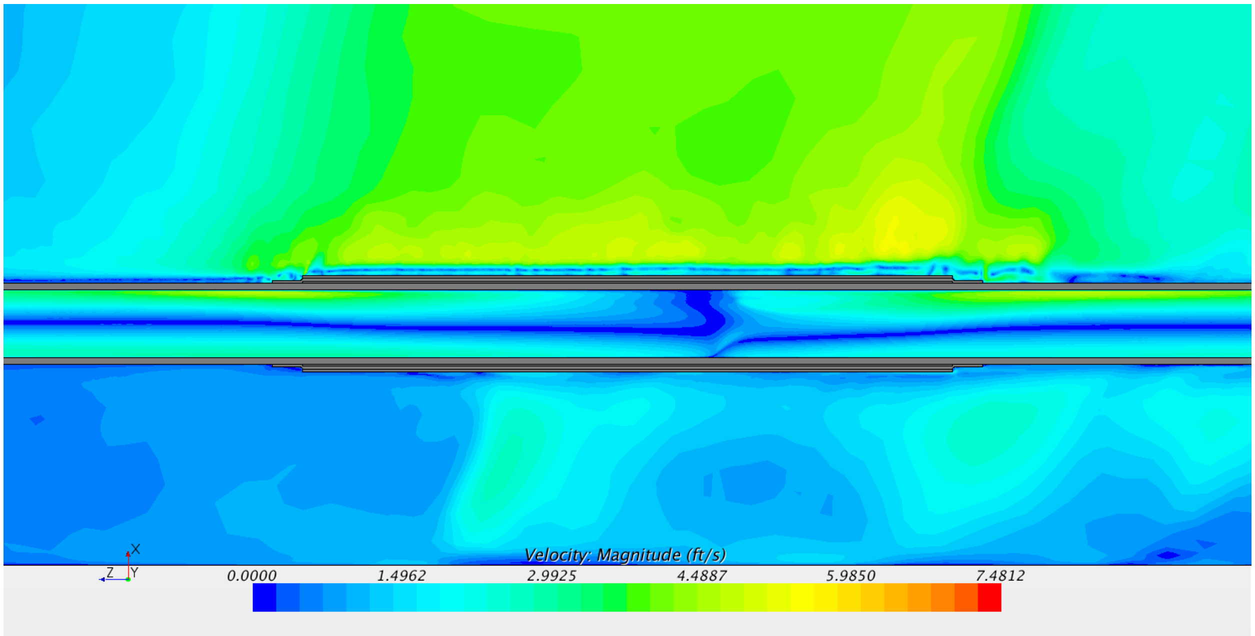

Figure B-120: Velocity contours, cross section of all regions, isometric view (ft/s). 30 inch schedule 160

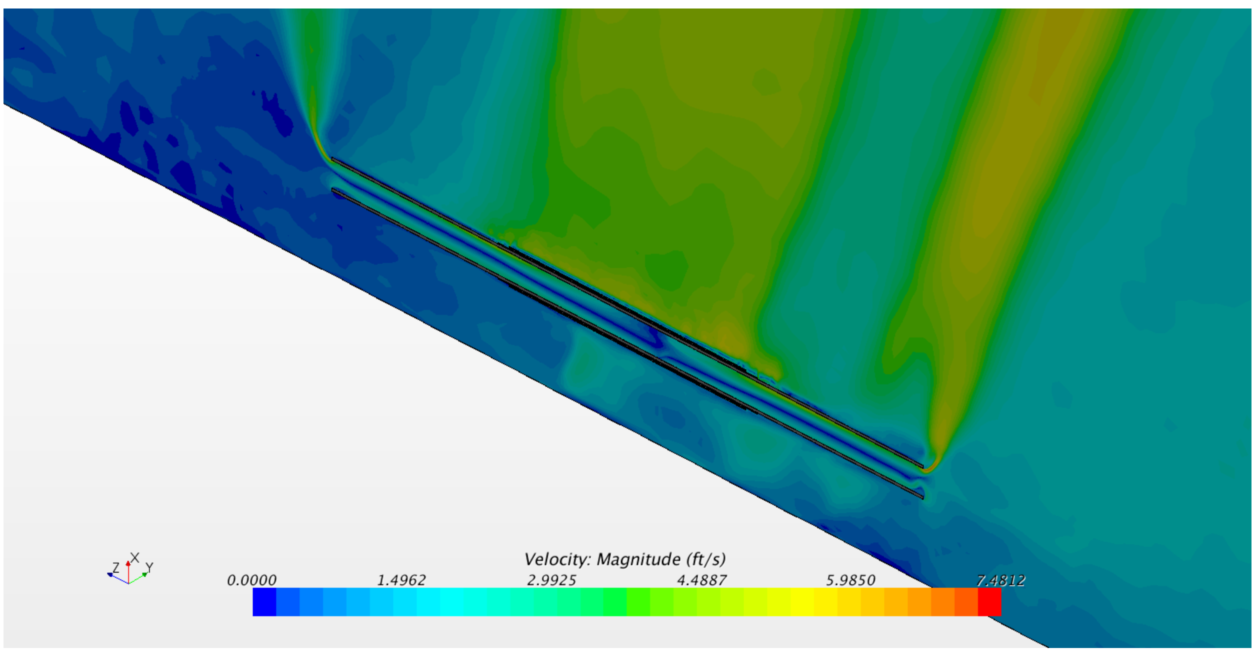

REFERENCES

[1] American Welding Society, D10.10 Recommended Practices for Local Heating of Welds in Piping and Tubing, Miami, FL: American Welding Society, 1999.

[2] CD-adapco, Star-CCM+ 10.02.010, Melville, NY: CD-adapco, 2015.

[3] H. K. Versteeg and W. Malalasekera, An Introduction to Computational Fluid Dynamics: The Finite Volume Method, 2nd ed., Essex: Pearson Education Limited, 2007.

[4] S. B. Pope, Turbulent Flows, New York: Cambridge University Press, 2010.

[5] F. R. Menter, "Review of the Shear-Stress Transport Turbulence Model Experience from and Industrial Perspective," International Journal of Computational Fluid Dynamics, vol. 23, no. 4, pp. 305-316, 2009.

[6] K. Stephan and A. Laesecke, "The Thermal Conductivity of Fluid Air," Journal of Physical Chemical Reference Data, vol. 14, no. 1, pp. 227-234, 1985.

[7] The American Society of Mechanical Engineers, ASME Boiler and Pressure Vessel Code, Section II, Part D, New York, NY: The American Society of Mechanical Engineers, 2013.

[8] Morgan Thermal Ceramics, "Europe Product Data Book," 2014. [Online]. Available: http://www.morganthermalceramics.com/sites/default/files/documents/2014_product_data_book.pdf. [Accessed June 2015].

[9] The American Society of Mechanical Engineers, B36.10M Welded and Seamless Wrought Steel Pipe, New York, NY: The American Society of Mechanical Engineers, 2004.

STP-PT-079

ASME ST-LLC

ISBN 978-0-7918-7125-6

9 780791 871256

A 2 7 4 1 Q